Modelling of Multicomponent Diffusion and Swelling in Protein Gels

A thesis submitted in fulfilment of the requirements of the degree of

Doctor of Philosophy in Chemical and Process Engineering

Kang Lu

Department of Chemical and Process Engineering

University of Canterbury

January 2011

Contents

Abstract

Some protein gels are products of the dairy industry and some are used as pH-sensitive gels for the controlled delivery of biologically active substances. To understand the dynamics of drug delivery it is very important to establish a mathematical model of protein gel swelling. This required the identification and integration of theory and equations from a wide range of topics. The aim of this research was to develop a mathematical model of transport in polyelectrolyte gels (using the example of β-lactoglobulin protein gels).

A complete mathematical model of protein gel swelling was established. The swelling process of protein gels in this thesis involved multicomponent diffusion, chemical ionisation and mechanical deformation. Diffusion of electrolyte solutions through protein gels was modelled using the generalised Maxwell-Stefan (GMS) equation. The swelling pressure as a driving force in the GMS equation was described by rubber elasticity theory. Thermodynamic factors including the charged protein effect were considered in the GMS equation. The model included pH as a variable so it could be applied to both acidic and alkaline cases.

The model yielded a set of partial differential equations with algebraic equations for which COMSOL was selected as the simulation software. Although it was found that COMSOL could not always solve the model equations, numerical solutions were obtained for several cases. The model predicted that the equilibrium swelling degree of the gel decreased with high concentration of salts in the bulk solution. The model also predicted that the non-ideal effects were not always small and they depended on the activity coefficients of the species. Satisfactory solutions could not be obtained for all cases using commercial software such as COMSOL Multiphysics. It was shown that COMSOL did not conserve mass but conservativeness was critical in this application because pH and hence the net protein charge is very sensitive to the mass

of hydrogen present.

In the future, research should be carried out to improve the pressure model in the GMS equation. Theoretical research on Manning condensation theory should be done to modify Manning's model for more robust prediction of activities of water and ions with protein, and experiments should be done to validate the performance of the modified Manning model. Efforts should be made to write the programming code for a finite volume method to solve the system in three dimensions.

Acknowledgments

I am very grateful to Associate Professor Ken R. Morison, my research supervisor, for his constant guidance and help in valuable discussion on difficult parts of the research and for his help with MATLAB programming.

I am also thankful to the members of the Chemical and Process Engineering Department for their support and encouragement.

Thanks also to my family and friends. This journey would not have been complete without their support.

Nomenclature

a_i	The activity of component i
A	Area in Maxwell-Stefan equation derivation
A	Helmholtz free energy in Section 2.3
A	Debye-Hückel coefficient in equation (2.3.12)
A_d	Deformation free energy
A_V	Free energy function per unit volume
A_x	Debye-Hückel parameter on a mole fraction basis
$\mathbf{b}$	Body force
b	Average charge distance in Manning's condensation theory
b_x	The closest approach parameter in Pitzer-Debye-Hückel equation
c_t	Total concentration in moles per volume
c_i	The molar concentration of component i
c_ρ	Molar density
c_{pt}	Total protein concentration
C_i	Two elastic constants in Mooney's function i=1,2
C_{mn}	Elastic constants in Rivlin's formulation
C^ϕ	Interaction parameter in Pitzer's equations
D_{12}	Fick diffusion coefficient
$\mathbb{D}_{ij}$	Maxwell-Stefan diffusion coefficient between species i and j
e	Charge on a proton
E	Young's modulus
$\boldsymbol{F}$	Net force
$\widetilde{\boldsymbol{F}}_i$	Force acting per unit mass of component i
$\boldsymbol{F}_i$	Body force
G	Gibbs free energy
G^{ex}	Excess Gibbs free energy

G	Shear modulus
G'	Modulus in the swollen state
G_0	Modulus in the unswollen state
G_{el}	Shear modulus in the unstrained state
h	The thickness of undeformed sheet
I	Molal ionic strength
$\boldsymbol{j}_i$	The mass diffusion flux of component i
$\boldsymbol{J}_i$	The molar diffusion flux of component i
k	Boltzmann's constant [1.38065×10^{-23} J molecule^{-1} K^{-1}]
K_a	Thermodynamic equilibrium constant
L	The end to end distance of the polyion chain in the state of maximum exension
L_0	The initial longitudinal length of the element
ΔL	The change in length
m_i	The molal concentration of component i
$m_{\pm}$	The molal concentration of the solute
M_s	The molar weight of the solvent
M_w	Molar mass of water
n_i	The number of moles of component i
n_t	Total charged groups in Manning's condensation
n_e	The equivalent number concentration of polyions
n_s	Salt concentration
$\mathbf{n}$	The outward directed unit normal to the surface
$\boldsymbol{n}_i$	The mass flux of species i
$\boldsymbol{n}_t$	The total mass flux of the mixture
$\boldsymbol{n}(\mathbf{x}, t)$	The mass flux at the surface
$\boldsymbol{N}_i$	The molar flux of component i
$\boldsymbol{N}_t$	Total molar flux
N	The number of crosslinked chains in a polymer network structure
N_{ki}	Protein side chain numbers

N_V	The number of crosslinks per unit volume
N_A	Avogadro's number [6.022×10^{23} molecule mol^{-1}]
p_1	The partial pressure of species 1
p	An arbitrary hydrostatic pressure in equation (2.4.21)
P	Pressure
P_{gel}	The pressure inside the gel
P_0	The pressure outside the gel
R	Gas constant
S	Entropy
T	Temperature
$\mathbf{u}$	The displacement vector of the network
u_x	A given displacement in the x direction
u_y	A given displacement in the y direction
$\boldsymbol{u}$	Molar average velocity
$\boldsymbol{u}$	The surface velocity of the control volume moving through the fluid
$\boldsymbol{u}^a$	The velocity relative to an arbitrary reference
$\boldsymbol{u}_i$	The component velocity of component i of the mixture
$\boldsymbol{v}$	The mass average velocity of the mixture
v	Poisson's ratio
$\bar{V}_i$	Partial molar volume of component i
V_0	The volume of the rubber at preparation state
V	The volume of the swollen rubber
W	Work done by deformation
W_w	The mass of water
w_i	The mass fraction of component i.
x_i	The molar fraction of component i
y	Manning's activity coefficients
z_i	The ionic charge of component i
z_p	The charge number of charged groups

Greek Letters

ρ_i	The density of species *i*
ρ_t	Mixture density
ρ_0	Solvent density [g/cm^3]
ξ_{12}	The friction coefficient between the gas 1 and 2
ξ	Manning condensation parameter
μ	Chemical potential
μ_i^0	The chemical potential of component *i* in reference state
μ_w	The chemical potential of the solvent
γ_i	The activity coefficient of component *i* in the mixture on a mole fraction scale
γ_i^m	Molal activity coefficient
$\gamma_\pm$	Mean or average activity coefficient
γ_+	The activity coefficients of cations
γ_-	The activity coefficients of anions
δ_{ij}	Kronecker delta function
$\boldsymbol{\sigma}$	Stress tensor
ϕ	Osmotic coefficient
ϕ_i	The volume fraction of component *i*
$\boldsymbol{\Phi}$	The diffusion flux of the field quantity through external surface
$\Phi_{aa'}$	Interaction parameter in Pitzer's equations
Φ	Strain-energy function
$\mathfrak{F}$	Faraday constant
ϵ	The dielectric constant of water in Debye-Hückel
λ_i	Principle stretches *i*=1,2,3
λ_{ij}	Represents the short-range interaction in the presence of water between ions *i* and *j*
λ^*_{ijk}	Short-range interactions between ions *i*, *j* and *k*
α_T	Thermal expansion parameter

β	The charge density of Manning's condensation
$\beta^{(0)}$	Interaction parameter in Pitzer's equations
$\beta^{(1)}$	Interaction parameter in Pitzer's equations
$\beta^{(2)}$	Interaction parameter in Pitzer's equation
$\psi_{aa'c}$	Interaction parameter in Pitzer's equations
ν_2	The volume fraction of rubber in swollen network
ν_i	The stoichiometric number of moles of ions in one mole of electrolyte *i*.
ν	The stoichiometric number of moles of ions in one mole of salt $\nu=\nu_+ + \nu_-$
ε_i	Strain in *i* direction, *i*=1, 2, 3
ε_x	Strain in the *x* direction
ε_y	Strain in the *y* direction
ε_{xy}	Engineering shear strain

Subscripts

s	Referring to the solvent
p	Referring to the polymer
w	Denotes to water
0	Referring to the initial state
i, j	Component indices
n	The number of components

Mathematical Symbols

∇	Gradient
Δ	Difference operator

Matrix Operations and Notation

( )	Column matrix
[ ]	Square matrix

1 Introduction

Polymers are macromolecules consisting of many small molecules that are linked together to form long chains. There are naturally occurring polymers such as starches, proteins and rubber. Many polymers can be cross linked to form elastic solids. A particular kind of polymers that have attracted a lot of attention in recent years are hydrogels.

1.1 Hydrogels

Hydrogels are water swollen polymers with a tendency to absorb water when placed in an aqueous environment. Hydrogels have attracted research interest over recent years because of the potential for a wide range of applications. They have been successfully used in biomedical fields due to their high water content. Successful examples include soft contact lens, superabsorbents and drug delivery systems (Li and Tanaka, 1992). Hydrogels can be divided into two categories based on the chemical or physical nature of the crosslink junctions. Chemically crosslinked networks have permanent junctions, while physical networks have transient junctions that arise from either polymer chain entanglements or physical interactions such as ionic interactions or hydrogen bonds. Hydrogels can also be classified as neutral or ionic based on the side groups of the polymers. For neutral hydrogels, the degree of swelling only depends on the chemical compositions of the polymers. Ionic hydrogels contain ionic groups, such as carboxylic acid. The swelling of ionic hydrogels depends not only on the chemical composition of the gel but also on the pH of the surrounding medium. Generally speaking anionic hydrogels deprotonate and swell more when the external pH is higher than the pK_a of the ionisable groups on polymer chains while cationic hydrogels protonate and swell more when the external pH is lower than the pK_b of the ionisable groups on polymer chains as shown by Figure 1.1 (Lin and Metters, 2006).

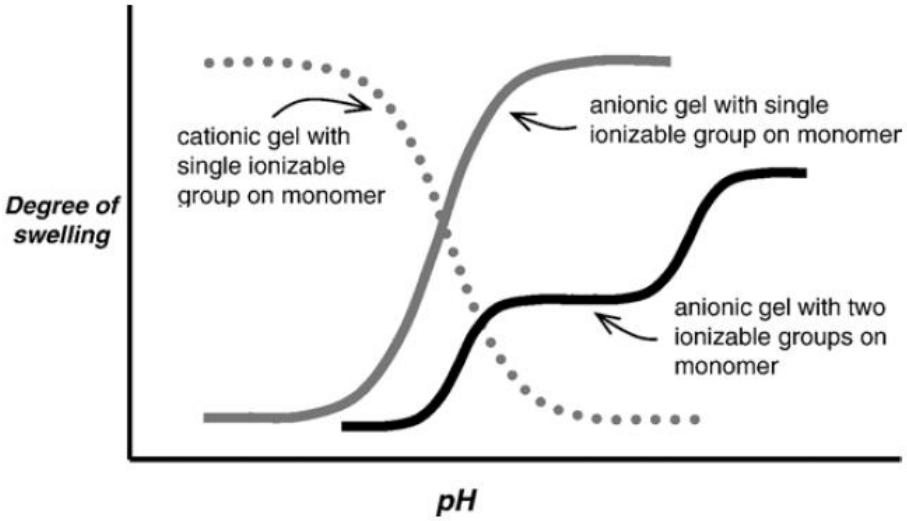

Figure 1.1 Schematic of relative ionic hydrogel swelling as a function of pH adapted from Fig. 2 in Lin and Metters (2006)

1.2 Polyelectrolyte gels

Polyelectrolytes are substances obtained when ionic groups are incorporated in a polymer chain, combining the properties of electrolytes and of polymers. Many natural and synthetic macromolecules are polyelectrolytes. Most tissues of plants and animals contain polyelectrolytes. Except for bones, teeth, nails and the outer layers of skin, most living organisms are largely made of polyelectrolytes (Hong et al., 2010; Osada and Khokhlov, 2002). The DNA, the carrier of genetic code, is also a polyelectrolyte (Manning, 1979). The ionic groups on the polymer chain dissociate when the molecule is in solution generating a long charged chain and large number of small ions of opposite charge. Since the chain units, covered with like charges, repel each other, the chain stretches out. The counter-ions can exist in two different states; some of them are condensed on the molecule chain and others are mobile in solutions (Manning, 1969a; 1969b). Figure 1.2 shows a representation of a polyelectrolyte gel.

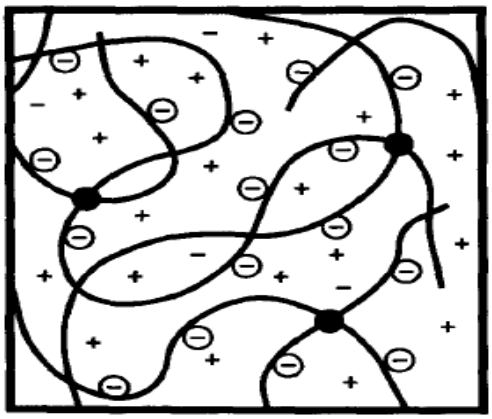

Figure 1.2 A polyelectrolyte gel with distribution of fixed and mobile charged ions (Berkenblit et al., 1995)

A large number of flexible polyelectrolytes can form a three-dimensional network by covalent crosslinks. When immersed in a suitable solvent, often called "a good solvent", small solvent molecules can migrate into the network, forming a gel (Maurer and Prausnitz, 1996). Inside the gel, cross-links prevent the complete mixing of the polymer chains and the solvent by providing an elastic restoring force that counters the expansion of the network. The liquid prevents the network from collapsing (Grimshaw et al., 1990). As a result, the gel swells and shrinks reversibly as the small solvent molecules migrate in and out. The volume of the gel is typically many times the volume of the dry network (Hong et al., 2010).

Polyelectrolyte gels are ionic hydrogels. Like hydrogels, polyelectrolyte gels are also widely used in technologies due to their swelling ability caused by external stimuli such as outside solution concentrations, pH, temperature and applied electrical field. This includes super-absorbent materials (Buchholz and Peppas, 1994), drug delivery (Uhrich et al., 1999) and artificial muscles (Lee and Mooney, 2001). In recent years, polyelectrolyte gels have become increasingly important carriers for the development of drug devices. For example, polyelectrolyte gels with pH-sensitivity are especially suitable as carriers for oral protein delivery systems due to their pH-dependent swelling behaviour. In the acidic environment of the stomach, these gels are in the collapsed state. Therefore, proteins incorporated in the gels are protected, while in the

basic and neutral environments of the intestine, the gels are swollen and proteins are released (Lowman and Peppas, 2000; Siegel, 1990).

The state of swelling is generally characterised by the degree of swelling, Q, which is defined as the quotient of the final volume V_f and the initial or preparation volume V_0. It is the same as the quotient of the volume fractions of the network in the initial and final gel, ϕ_{p0} and ϕ_p, respectively.

$$Q = \frac{V_f}{V_0} = \frac{\phi_{p0}}{\phi_p} \tag{1.2.1}$$

The degree of swelling is limited to a maximum, equilibrium degree of swelling, Q_{eq}. In the 1940's, Flory was the first to establish a theory to predict the equilibrium degree of swelling. His theory is presented in Section 2.5.1.

1.3 Protein gels

The protein molecule consists mainly of amino-acids linked in a linear chain which is folded into a globular form. The principal bond is the peptide link between the carboxyl groups and the amino groups. All amino acids found in proteins have the basic structure shown in Figure 1.3, differing only in the structure of the *R*-group.

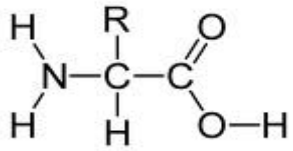

Figure 1.3 Basic structure of an amino acid

Normally the amino acid produces a nearly neutral solution. The different properties of amino acids result from the structures of different *R* groups. The *R* group is often referred to as the amino acid side chain. If there is an extra acid on the side chain, there is a net acid producing effect. If the side chain contains an extra amine group, then the amino acid produces a basic solution. In β-lactoglobulin proteins, acidic amino acids include aspartic (Asp) and glutamic (Glu) and basic side chains include

lysine (Lys), arginine (Arg) and histidine (His).

There can be an internal transfer of a hydrogen ion from the –COOH group to the $–NH_2$ group to leave an ion with both a negative charge and a positive charge. This is called a zwitterion shown in Figure 1.4.

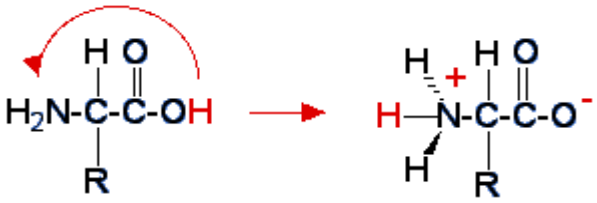

Figure 1.4 The internal transfer of H

Proteins gels can be found in the dairy industry. Milk is composed of water, carbohydrate, fat, protein, minerals and vitamins. Pasteurisation and sterilisation are generally used in milk processing. In pasteurisation, milk receives mild heat treatment to reduce the number of bacteria present. In sterilisation, milk is subjected to severe heat treatment that ensures almost complete destruction of the microbial population. Both result in the fouling deposits on heat transfer equipment surfaces. The deposits consist of proteins, fats, sugars and mineral salt. Among them, whey proteins, and especially *β*-lactoglobulin (βLg) (Mercadé-Prieto et al., 2006, 2007), constitute the bulk of fouling deposits and thus some fouling deposits are considered to be primarily heat-induced protein gels. Whey proteins are also co-products of the cheese industry. Like polyelectrolyte gels, protein gels may be used as pH-sensitive gels for the controlled delivery of biologically active substances and they may also be formed into nanoparticles which entrap drugs or bioactive compounds within but not chemically bound to them (Gunasekaran et al., 2007). This research is focused on modelling transport in polyelectrolyte gels (using the example of *β*-lactoglobulin protein gels). It is important not only for explaining process and geometry dependent material properties but also for predicting dynamic properties such as swelling rates and ion fluxes.

In the author's master of engineering research (Lu, 2007) a simple, yet effective dynamic model of diffusion of electrolytes in gel was established. The dynamics of diffusion of electrolytes in a protein gel were successfully described on the basis of the generalised Maxwell-Stefan description. The model can be applied to several cases including electrolytes only and electrolytes with a gel. The model yielded differential equations solved numerically by discretisation in place and time. The numerical solutions were obtained by using MATLAB® ODE15S. However this was only a good start and can be improved in many aspects. For example, the gel geometry was considered constant. The study of swelling behaviour of a gel should include a moving geometry. More work was required on the thermodynamics of solutions. More research was also required to investigate the swelling of the gel and the effects of ionic forces, the pH and the concentration of the salt.

1.4 Aim of this research

Models to describe swelling of gels that can be found in literature have two major limitations. One is that many models describe equilibrium swelling but not dynamic. The other is that most models describe two-component systems and cannot be extended to multicomponent systems. Even when dealing with multicomponent systems, models are usually based on Fick's law which is not reliable in the case that involves multicomponents and a gel, or use Nernst-Planck equation as a simplified model for multicomponent diffusion. A detailed review on previous modelling of diffusion in polyelectrolye gels will be given in Section 2.1. Table 1.1 presents the summary of those models. None included variable pH.

Protein gels in an aqueous solution are net charged depending on the pH of the surrounding solution. Modelling the swelling of polyelectrolyte gels has always been a difficult and complicated task. Systems can involve numerous coupled partial differential equations and can be complicated or impossible to solve analytically. Numerical methods are frequently used in an attempt to predict the swelling, but these

are usually limited by the numbers of equations involved.

Table 1.1 Models in literature

Authors	Dimensions	Components	Diffusion	Elastics	Pressure	Thermodynamics
Tanaka et al. (1973, 1979)	1	2	Dynamics[0]	Hooke's law	No	Ideal
Hasa et al. (1975)	1	2	Equilibrium swelling[1]	Flory-Huggins	Osmotic	Non-ideal
Grimshaw et al. (1990)	1	3	Nernst-Planck	Hooke's law	Osmotic	Ideal
Bisschops et al. (1998)	1	2	Maxwell-Stefan	Flory-Huggins	No[2]	Ideal
Horkay et al. (2000)	1	2[3]	Equilibrium swelling[1]	Rubber elasticity	Three contributions[4]	Ideal
Zhang et al. (2009)	3	2	Fick	Flory-Rehner	No	Ideal
Wallmersperger et al. (2011)	1	4[5]	Nernst-Planck	Stress-strain relations	Osmotic	Ideal

[0] The equation of the network motion was used.

[1] In equilibrium swelling concentrations were obtained by Donnan equilibrium.

[2] There was no pressure term in the model however a Flory-Huggins polymer-solvent mixing term was used as the driving force for the Maxwell-Stefan diffusion.

[3] Two components were a polyelectrolyte gel and one salt solution and other two components were water and a neutral gel.

[4] The three contributions were the elastic pressure obtained from the theory of rubber elasticity, osmotic pressure due to the mixing of network chains and solvent molecules expressed by the Flory-Huggins and osmotic pressure due to mixing of ions with solvent molecules and interactions between ions, polymer segments, and solvent molecules.

[5]Four components included a polyelectrolyte gel, bound charges in the gel, water and oxonium.

Based on my previous research, the aim of this research was to extend the previous model to any situation (acid and base conditions) involving diffusion, swelling and external forces such as pressure and electrical potential and to be able to set up the dynamic model of protein gel swelling.

The scope of the research was set as follows:

- The model was to be based on the Maxwell-Stefan equations, and therefore take into account the diffusive interaction between all components. The model is

easily extended to multiple ion systems.

- The model was to have as few assumptions as possible without omitting terms. This would be the challenge of the work. For example, thermodynamics would be difficult. Although there are several models to calculate ions and water activities in multi-electrolyte systems, it is very difficult to define the activities in real simulations caused by interactions between ions and the charged polymer.
- The model was to be able to handle both acid and alkali situations.
- As a complete system for standard equations, COMSOL Multiphysics was to be used to obtain simulation results because of its power in solving coupled systems of partial differential equations.
- The model was to apply to a 3-dimensional system.

The rest of the thesis is organised as follows:

Chapter 2 explains all the relevant theories which can be selected to set up the model such as the generalised Maxwell-Stefan theory, rubber elasticity theory, continuity equations and mechanical structure equations. A key feature of this thesis was the selection and interpretation of relevant literature within a wide range of topics and over a time period from the 1940's until now. After that, Chapter 3 is an introduction of COMSOL including some modelling examples. Chapter 4 presents the complete mathematical model for the dynamics of a polyelectrolyte gel system composed of partial differential and algebraic equations (PDAEs). The challenge was to combine the wide range of models of each feature of the system into a single coherent model. Chapter 5 provides simulation results and discussion. Chapter 6 presents the overall discussion, conclusions and recommendations for future work.

2 Literature and model components

Studying the swelling process of polyelectrolyte gels has always been a difficult and complicated task. Systems can involve numerous coupled partial differential equations and can be complicated or impossible to solve analytically. Numerical methods are frequently used in an attempt to predict the swelling response but they are also limited by the numbers of equations involved.

The overall swelling process consists of many different processes that all occur simultaneously. A concentration difference within a gel or between a gel and bulk solution may create a chemical potential across the gel. Under this potential, free ions and water in the gel and bulk solution regions migrate and diffuse through the polymer matrix. The extra water introduced into the gel causes deformation or mechanical swelling. As a result, this deformation leads to a local displacement of the gel network. From this description, it is clear that the swelling process involves theories in different areas: multicomponent diffusion, chemical ionisation and mechanical deformation. Therefore, it is of utmost importance to study all the theories involved before the complete swelling model of a polyelectrolyte gel is set up. In this chapter the theories of equations for each part of the model are drawn from literature and developed for use in this thesis.

2.1 Overview of past research on polyelectrolytes

Because of the wide use of polyelectrolyte including protein gels in many areas, many researchers have interest in this field. For applications as drug carriers or in cleaning of milk fouling, the diffusion of solutes into polymer networks and the resulting swelling of the networks are very important and need to be understood very clearly.

Previous work by researchers in the area of milk fouling has been largely focused on the experimental studies in order to obtain a good understanding of the cleaning

behaviour. A recent review of milk fouling in heat exchangers is given by Bansal and Chen (2006).

Xin et al. (2004) did an important experimental study on the removal of a protein foulant from metal surfaces. They introduced a polymer dissolution concept to describe the complicated protein deposit cleaning process. The essential steps of the cleaning are: the diffusion of the cleaning agent from the bulk solution into the top layer of the deposit, the reaction of the cleaning agent with the deposit, the formation of the swollen gel and finally the diffusion of the disengaged protein from the gel surface into the bulk solution. They proposed a simple mathematical model to estimate the cleaning rate and cleaning time for proteinaceous fouling. The good agreement of experimental results and model predictions supported the modelling concepts used. Although the model in the paper cannot be applied in removing large aggregates, the model provides a good foundation for further studies on the cleaning mechanisms of protein-based milk fouling.

Mercadé-Prieto and Chen (2006) tried to analyse each protein cleaning step proposed by Xin et al. (2004). In their research, they firstly examined the sodium hydroxide solution diffusivity at different pH values at 22 ^{o}C. Then they studied the influence of dissolution pH of proteins. Finally, they considered the influence of temperature on the dissolution process. They found that the diffusivity of NaOH in a protein gel was about two thirds of that in water. They also found that at a low dissolution pH, between 12 and 13, the dissolution rate started from a small value and it reached a constant value after a time. At a high dissolution pH, on the other hand, this rate showed a decreasing trend. They found that at high temperatures, the dissolution rate decreased with time, and the remaining gels became more yellowish.

Mercadé-Prieto et al. did considerable work on the study of heat-induced β-lactoglobulin (βLg) gels. During two years between 2006 and 2007, this research group produced five papers on this field.

Mercadé-Prieto et al. (2006a) investigated the influence of the gel structure on the dissolution rate of heat-induced βLg gels. The dissolution rate profile of βLg gels was found to resemble those reported for whey protein concentrate gels (Mercadé-Prieto and Chen, 2006). The dissolution rate profiles observed at high alkaline pH (>13) were smaller and decreased over time, which was similar to the result reported previously for whey protein concentrate gels (Mercadé-Prieto and Chen, 2006). Therefore they reached the conclusion that βLg can be used successfully as a model of whey protein. They also developed the idea that swelling may be related to the low dissolution observed at high pH. The group found that at high salt concentrations the swelling ratio of βLg gels decreased. The addition of salts greatly reduced the dissolution rate. However, they did not provide accurate swelling rates at high pH owing to the gels undergoing dissolution.

Mercadé-Prieto et al. (2006b) further studied the influence of the gel structure on the dissolution rate of βLg heat-induced gels. The results were similar to the previous findings (Mercadé-Prieto et al., 2006a). They found that the dissolution behaviour was strongly influenced by the condition under which the gel was formed. At low alkaline pH values (<13), the dissolution rate decreased with longer gelation time and higher temperature. In addition, they observed an inverse relationship between the dissolution rate and the amount of covalently cross-linked proteins in the gel.

Mercadé-Prieto et al. (2007a) studied the polyelectrolyte screening effects on the dissolution of whey protein gels at high pH conditions. In this study, they provided strong evidence that the dissolution rate was affected by the equilibrium-swelling ratio in βLg gels. The swelling ratio was reduced in the presence of salts because of the polyelectrolyte screening effect of the cations. At high dissolution pH (>13.3), the high sodium ion concentration reduced swelling in spite of the high surface charge of the protein. They also observed that the final dissolution rate of gels pre-soaked in 1M sodium hydroxide or sodium chloride was similar, even though their pH values were

different. This dissolution rate was much lower than that of untreated gels. The reason for this was that the high sodium ion concentration in the soaked gels hindered swelling, and inhibited the disentanglement of the protein clusters regardless of the high pH.

Mercadé-Prieto et al. (2007b) presented a simple model for the swelling of protein gels including the effect of solvent pH and ionic strength. They developed the model for the swelling equilibrium, which meant the difference between the ionic contributions from the chemical potential inside the gel and in solution equalled the sum of the contributions to the chemical potential of the mixing and elastic forces. Because the model was derived for equilibrium state, it cannot be applied for the study of the dynamic behaviour of the swelling mechanism. However, the paper provided many useful experimental results. Particularly, Figure 7 in the paper (Mercadé-Prieto et al., 2007b) (Figure 2.1 below) showed the effect of the molar electrolyte concentration in solution on the equilibrium swelling ratio for sodium chloride electrolyte.

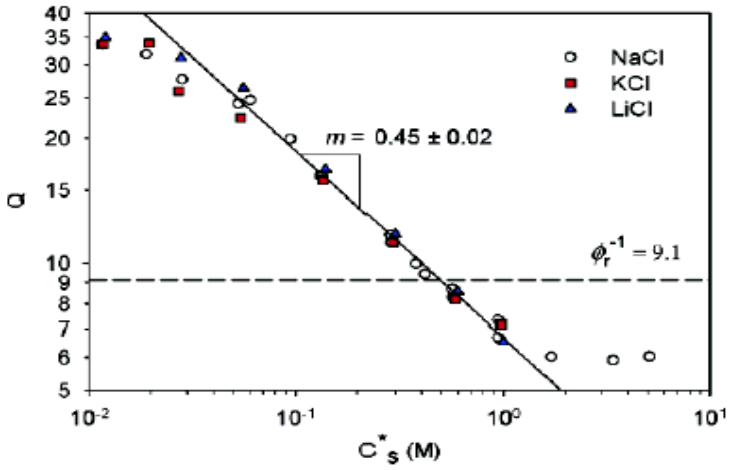

Figure 7. Effect of c_s^* on the equilibrium swelling ratio for NaCl, KCl, and LiCl electrolytes at pH 11.2. The line shows the experimental scaling law found (eq 30). The dashed line shows the Q value of the gels in the relaxed state.

Figure 2.1 Figure 7 from Mercadé-Prieto et al. (2007b)

Mercadé-Prieto et al. (2007c) believed that there was a pH below which the dissolution rate was very low and above which the dissolution rate was high. Thus,

they carried out a series of experiments to confirm and characterise the existence of such pH threshold for the dissolution of heat-induced βLg gels. They did observe a sharp transition in solubility between pH 11 and 12 and this transition shifted to higher pHs for gels formed at higher temperatures and for longer gelling times. They also found the destruction of large aggregates was faster at higher pH and this destruction also showed a transition between pH 11 and 12.

Gunasekaran and co-workers (2007) did experiments to investigate the use of whey proteins as pH-sensitive gels and nanoparticle systems. They used caffeine as a model bioactive, and encapsulated this in a commercial whey protein concentrate. They reported that the gels exhibited a pH-sensitive swelling especially at pH values above their isoelectric point (pI, the point at which the gels are not net electrically charged). They also reported that the release of encapsulated model drug from the gels was slower when the pH was below isoelectric point than when it was above pI.

There have been numerous studies of swelling of polyelectrolyte system in the presence of different stimuli. Some early experiments were carried out by Loeb (1921) who used gelatine in the presence of HCl and any one of NaCl, $NaSO_4$, or $CaCl_2$ and found the swelling, electrical potential and osmotic pressure were affected by the ionic concentration. Katchalsky (1949) and Kuhn (1949) independently reported on chemo-mechanical deformation of collagen fibres, and raised the possibility of using these materials as artificial muscles. They suggested that by varying the pH of a surrounding solvent, the polymers could be chemically contracted or swollen, thus behaving as an artificial muscle. A year later, Kuhn et al. (1950) demonstrated that this suggestion was correct.

Tanaka et al. (1982) demonstrated electrical influence on certain polymers. In their experiment, an acrylamide cylinder was submerged in a 50:50 acetone-water solution under the influence of a 5V DC electric field. It was found that by reversing the polarity of the applied field, the gel could swell to a volume 500 times its original.

Later, this result was confirmed by De Rossi et al. (1986) by experiments on strips of polyvinyl alcohol and polyacrylic acid gels. Grimshaw et al. (1990) demonstrated the electrically induced swelling of a thin poly (methacrylic) acid membrane compressed between two regions with different chemical potentials, thereby introducing the concept of an electrical-chemical interaction. Osasa et al. (1992) extended this work and demonstrated a Grimshaw's example of electrically-driven motility of a polymer gel.

Shahinpoor (1993) performed experimental comparisons between the swelling of polymer gels under the influence of an electric field and under the influence of a pH gradient. They suggested that there are two distinct mechanisms involved in the swelling of charged polymers. The first mechanism produced a quick response to an external electric field. The second one is much slower and also in response to an advancing pH gradient. They suggested that the short-time response is caused by the migration of the unbounded counter-ions, and it is predominantly responsible for the bending of polymer gels under the influence of an electric field.

Li and Tanaka (1990) studied the swelling kinetics of polyacrylamide hydrogels with three different shapes: small disks, large disks and long cylinders. They found that the gel swelling and shrinking processes were not pure diffusion processes and the gel adjusted its shape in order to minimise the total shear energy. They also found that the apparent diffusion coefficient was smaller than the pure diffusion coefficient and that the observed apparent diffusion constant was time independent. Furthermore, they showed that the diffusion constant and relaxation time were geometry dependent. Horkay et al. (2000) studied the equilibrium swelling ratio of sodium polyacrylate gels immersed in different concentrations of alkali metal salts (Li^+ and Na^+) and alkaline earth metal salts (Ca^{2+} and Sr^{2+}) and tried to relate these to the Flory theories (1953). They showed that monovalent counter-ions only had influence on the ionic contribution. Conversely, the divalent counter-ions affected both the ionic and mixing terms in the free energy. The elastic term was not significantly affected by both types

of ions.

Along with these experimental works, theoretical research was carried out trying to find robust models that can predict the experimental results such as swelling rate and gel network movements. Early researches were mainly focus on equilibrium swelling models. In the 1940's Flory was the first to establish a theory predicting the equilibrium degree of swelling as a function of network characteristics and the interaction between solvent and network (Flory, 1969).

Flory's theory for network swelling is based on the postulate that gel swelling can be seen as the mixing of a network with a solvent. The free energy change ΔG_{mix} is composed of an enthalpic part ΔH_{mix} and an entropic part ΔS_{mix}:

$$\Delta G_{mix} = \Delta H_{mix} - T\Delta S_{mix} \tag{2.1.1}$$

in which

$$\begin{aligned} \Delta H_{mix} &= kT\chi_{sp} n_s \phi_p \\ \Delta S_{mix} &= -k\left[n_s \ln\left(1-\phi_p\right) + n_p \ln \phi_p\right] \end{aligned} \tag{2.1.2}$$

where k is the Boltzmann constant, T is the absolute temperature, χ_{sp} is the Flory-Huggins parameter for interactions between solvent and polymer network, n_s and n_p are the number of solvent and polymer molecules respectively and ϕ_p is the final volume fraction of polymer network. ϕ_p is related to n_s and n_p by:

$$\phi_p = \frac{n_p \bar{V}_p}{n_s \bar{V}_s + n_p \bar{V}_p} \tag{2.1.3}$$

where $\bar{V}_s$ and $\bar{V}_p$ represent the molar volumes of solvent and polymer respectively.

Entropy of mixing is always positive as can be seen in equation (2.1.2). The heat of mixing on the other hand may be positive or negative. The sum of both terms determines the sign of ΔG_{mix}. In the particular case where ΔG_{mix}=0 the system is at equilibrium.

The motion of chains in a network is limited because of the presence of crosslinks. When the network swells chains are extended between the network junctions causing an elastic force. This new configuration imposes an entropy change ΔS_{el}. Assuming a Gaussian chain distribution and affine chain deformation during swelling the free energy change caused by chain stretching ΔG_{el} was expressed by (Flory, 1969):

$$\Delta G_{el} = -T\Delta S_{el} = \frac{kT\nu_e}{2}(3\lambda^2 - 3 + \ln\lambda^3) \tag{2.1.4}$$

with ν_e the effective number of chains in the network and λ an expansion factor relative to the reference state which is the relaxed unswollen state V_0 in Flory's theory, $\lambda^3 = V/V_0$.

The equilibrium degree of swelling can be defined by ΔG_{el} minimal. Flory set the initial volume fraction of polymer to unity and the equilibrium degree of swelling was calculated as a function of system parameters by:

$$Q_{eq}^{5/3} \cong \frac{M_c\nu^*}{\bar{V}_s}\left(\frac{1}{2} - \chi_{sp}\right)\left(1 - 2\frac{M_c}{M}\right)^{-1} \tag{2.1.5}$$

with M_c the average molar weight between two junctions in a polymer chain, ν^* the specific volume and M the molar weight of the mixture. Flory gave experimental results that confirmed his theory.

In the case of polyelectrolyte systems, the total change in the free energy is the sum of the free energy of elastic deformation of the network, the free energy of mixing of the network chains and solvent molecules, and the mixing of the network chains with counter-ions. Hasa's swelling model (Hasa et al., 1975) included the electrostatic term of Katchalsky and Lifson (1953), a non-Gaussian elastic term (Smith et al., 1964), Flory-Huggins (Flory, 1953) polymer-solvent mixing and entropic solvent-ion mixing. The elastic term was a series expansion of the inverse Langevin function which is valid for small extensions (Hill, 1986). The swelling pressure was related to the osmotic pressure of the external solution to describe isotropic swelling. Non-ideal Donnan equilibrium was used to describe the ion concentrations. Vasheghani-Farahani

et al. (1990) used Hasa's model with experimental osmotic coefficients (Denbigh, 1981) and obtained good predictions for the swelling of anionic and cationic acrylamide copolymer gels.

More recently, Horkay et al. (2000) studied equilibrium swelling of hydrogels in different salt solutions. They calculated the total swelling pressure of the gel by adding up three terms. The first term was the swelling pressure of the gel network which was obtained from the theory of rubber elasticity (Flory, 1953). The second one was the mixing of network chains and solvent molecules expressed by Flory-Huggins equation. The third was the contribution of mixing of ions with solvent molecules and interactions between ions, polymer chains and solvent molecules, given by the Donnan theory.

However, the gel swelling often involves the motion of the gel network. This is a dynamic process and a dynamic model is much more plausible. The equation of motion of a gel network in a static solvent was first introduced by Tanaka, Hocker and Benedek (1973) to describe the dynamics of thermal fluctuations of gel networks, which are responsible for the dynamic light scatting. The Tanaka-Hocker-Benedek model used linear elasticity and force balances to describe gel network movements. Later Tanaka and Fillmore (1979) developed a model in which the swelling process is described as a balance between a driving force and friction. The driving force is assumed to result from a uniform stress. Tanaka and Fillmore suggested this stress as an osmotic pressure. When the network was transferred into a fluid, this pressure forced the network to expand until the osmotic pressure difference between the gel and solution became zero. Komori and Sakamoto (1989) argued that the driving force for the swelling process was not caused by a stress that was latent in the network before it was contacted with the fluid because the unswollen network was mechanically stable in itself. Apart from this disagreement, the models were limited to two component systems: polymer network and solvent.

Gel swelling processes involve the diffusion of electrolyte solutions such as sodium hydroxide through the gel. Very often more than one single anion and one single cation are present and thus the modelling of such diffusion requires a multicomponent description. In the case of protein gel, the protein gel is charged and is thus an extra ionic component. Grimshaw et al. (1990) investigated a three component model for 1D swelling of a polyelectrolyte membrane under an applied electric field. In this work a Nernst-Planck equation was used to model ion diffusion. De and Aluru (2004) also used this approach. However the Nernst-Planck equation is applicable for dilute solutions only. Thus a generalised method to describe multicomponent diffusion is needed such as the generalised Maxwell-Stefan diffusion approach.

Bisschops et al. (1998) attempted to model the swelling of Dextran gels by using multicomponent diffusion approach. They aimed to demonstrate the potential of the generalised Maxwell-Stefan approach for describing the swelling kinetics of hydrogels. Although, this model only had two components it was still valuable because the model predicted the shrinking-core behaviour whereas other models based on Fickian diffusion did not. More recently Mercadé-Prieto and co-workers (Mercadé-Prieto et al., 2006; 2007) have considered cases where, in addition to charged βLg protein gel, at least three other ions are involved. However, little attention has been paid to the dynamic diffusion modelling of multi-ions from the bulk solution into the gel.

Because of the mathematical difficulties of the coupling equations of ion diffusion and gel network movements, some researchers have tried to use numerical methods. The finite element method was commonly used. Achilleous et al. (2000; 2001) developed a transport model to explain the swelling of polyelectrolyte gels in salt solutions. The model offered a detailed finite element description of the chemical gradients in a gel under the influence of an electric field. Other numerical methods, such as Monte Carlo methods, were also used. Kekare et al. (2000) used a combination of discontinuous molecular dynamics and Monte Carlo techniques to

create a model that described the swelling of athermal gels in an athermal, monomeric solvent. The most remarkable contribution of this work was that it lacked the complexity of similar models developed using other numerical methods, but still provided good agreement with experimental results. This suggests that it is possible to develop a simple model that can describe the complex gel swelling.

2.2 Diffusion theories: Fickian diffusion and Maxwell-Stefan diffusion

Diffusion is a time-dependent process originated by the motion of given entities that are spread in space. The classical description of the diffusion process goes back to Fick. He postulated that the flux goes from high concentration regions to low concentration regions with a magnitude proportional to the concentration gradient. The direct proportionality between flux and concentration gradient provides a reasonable approximation of the diffusion process in many common situations. However, as experimentally observed, this postulate may be sometimes too simplistic. Indeed, there are some situations where the flux goes from regions of low concentration to regions of high concentration. This kind of behaviour has been observed, among other situations, in multicomponent gaseous mixtures (see Krishna and Wesselingh, 1997 for a physical review of this behaviour). The diffusion phenomenon in a multicomponent gaseous mixture was first accurately described by Maxwell (1867) and Stefan (1871). They suggested an explanation of the process based on the binary reciprocal interaction of gas molecules. The result of their analysis is a system of coupled and nonlinear partial differential equations, and the diffusion happens in a much more complex way than the one suggested by Fick. It was later called Maxwell-Stefan diffusion. This chapter will present Fickian diffusion theory and explain the physical derivation of the Maxwell-Stefan equations.

To begin with, it is useful to introduce definitions of fluxes and diffusion fluxes and their relationships.

2.2.1 Fluxes

Most of this section is based on Taylor and Krishna (1993). Consider a mixture with *n* components; let $\boldsymbol{u}_i$ be the component velocity of component *i* of the mixture, defined with respect to a stationary coordinate reference frame. Then the mass flux of species *i*, $\boldsymbol{n}_i$ in [kg/m^2.s] is given by:

$$\boldsymbol{n}_i = \rho_i \boldsymbol{u}_i \tag{2.2.1}$$

where ρ_i is the concentration [kg/m^3] of species *i*. In this thesis fluxes and velocities can be applied in up to three spatial dimensions.

The total mass flux of the mixture, $\boldsymbol{n}_t$, follows from equation (2.2.1):

$$\boldsymbol{n}_t = \sum_{i=1}^{n} \boldsymbol{n}_i = \rho_t \boldsymbol{v} \tag{2.2.2}$$

To derive the above equation we have used the definition that the mass flux is the product of the mixture density ρ_t and the mass average velocity of the mixture $\boldsymbol{v}$. Therefore:

$$\rho_t \boldsymbol{v} = \sum_{i=1}^{n} \rho_i \boldsymbol{u}_i \tag{2.2.3}$$

Dividing the above equation through by ρ_t, the mass average velocity is obtained:

$$\boldsymbol{v} = \sum_{i=1}^{n} \frac{\rho_i}{\rho_t} \boldsymbol{u}_i = \sum_{i=1}^{n} w_i \boldsymbol{u}_i \tag{2.2.4}$$

where $w_i = {}^{\rho_i}/_{\rho_t}$ denotes the mass fraction of component *i*.

The molar flux, $\boldsymbol{N}_i$ [mol/m^2.s], of component *i* is defined by:

$$\boldsymbol{N}_i = c_i \boldsymbol{u}_i = c_t x_i \boldsymbol{u}_i \tag{2.2.5}$$

where c_t is the total concentration in moles per volume and c_i is the molar concentration of component *i*.

The total molar flux, $\boldsymbol{N}_t$, is the sum of the molar flux of all the components:

$$\boldsymbol{N}_t = \sum_{i=1}^{n} \boldsymbol{N}_i = c_t \boldsymbol{u} \tag{2.2.6}$$

The molar average velocity $\boldsymbol{u}$ is defined in the same way as the mass average velocity:

$$\boldsymbol{u} = \sum_{i=1}^{n} \frac{c_i}{c_t} \boldsymbol{u}_i = \sum_{i=1}^{n} x_i \boldsymbol{u}_i \tag{2.2.7}$$

where $x_i = {}^{c_i}/_{c_t}$ denotes the molar fraction of component *i*.

The diffusion flux is normally based on the velocity difference between the individual velocities of components and the reference average velocity. Therefore, different definitions of the diffusion fluxes may be introduced depending on the way of the choice of the reference velocity. For example, if mass average velocity is chosen as the reference velocity the mass diffusion flux can be defined. On the other hand, the molar diffusion flux can be defined with respect to the molar average velocity.

The mass diffusion flux of component *i* denoted by $\boldsymbol{j}_i$ [kg/m^2.s] is defined with respect to the mass average velocity:

$$\boldsymbol{j_i} = \rho_i(\boldsymbol{u}_i - \boldsymbol{v}) \tag{2.2.8}$$

The mass flux can be related to the mass diffusion flux as:

$$\boldsymbol{n}_i = \boldsymbol{j_i} + \rho_i \boldsymbol{v} \tag{2.2.9}$$

Alternatively, the molar diffusion flux of component *i* denoted by $\boldsymbol{J}_i$ [mol/m^2.s] is defined by:

$$\boldsymbol{J}_i = c_i(\boldsymbol{u}_i - \boldsymbol{u}) \tag{2.2.10}$$

The molar flux, $\boldsymbol{N}_i$, can be related to the molar diffusion flux, $\boldsymbol{J}_i$, by

$$\boldsymbol{N}_i = \boldsymbol{J}_i + c_i \boldsymbol{u} \tag{2.2.11}$$

2.2.2 Fickian diffusion theory

Back in 1855, Adolf Fick published his first work on mass transfer “On Liquid Diffusion”, where he showed the analogy between diffusion and heat conduction

(Fick, 1855). The result of his work is now the most commonly used diffusion theory referred as the Fick' law. It defines the connection between the concentration gradient and the diffusion flux, which is caused by the gradient. In this section the Fick's diffusion theory is presented mainly based on Taylor and Krishna (1993).

The form of the Fick's law for binary mixtures is the following:

$$\boldsymbol{J}_1 = -c_t D_{12} \nabla x_1 \tag{2.2.12}$$

Here the gradient of mole fraction ∇x_1 of the diffusing component 1 is the driving force for the diffusion process. D_{12} is the Fickian diffusion coefficient or diffusivity of component 1 in component 2. Diffusion mass transfer tends to distribute the ions and molecules evenly. Thus a component normally diffuses from high concentration regions to low concentration regions, which is indicated by the negative sign in the above equation.

An analogous relation may also be written for component 2.

$$\boldsymbol{J}_2 = -c_t D_{21} \nabla x_2 \tag{2.2.13}$$

There is only one independent concentration gradient in a binary mixture. Also due to the conservation of the total flux in the volume, there is only one independent diffusion flux. As a result the Fick diffusion coefficient in a binary mixture is symmetric:

$$D_{12} = D_{21} \tag{2.2.14}$$

Provided that the concentration gradient of one component is known, only one value of diffusion coefficient is required to estimate the diffusion flux. However, in industrial applications diffusion transfer mainly occurs in mixtures with more than two components.

For the binary systems discussed above Fickian diffusion can be seen as a linear relationship between the independent flux $\boldsymbol{J}_1$ and driving force ∇x_1. For a mixture of *n* components, *n*-1 independent diffusion fluxes exist. The linear relationship needs to be extended and generalised:

$$\boldsymbol{J}_i = -c_t \sum_{k=1}^{n-1} D_{ik} \nabla x_k \quad i = 1, \ldots, n-1 \tag{2.2.15}$$

The flux of component *i* now depends not only on its own concentration gradient but also on the concentration gradients of other components in the mixture.

The matrix form of the above *n*-1 equations is more convenient to use:

$$(\boldsymbol{J}) = -c_t [D](\nabla x) \tag{2.2.16}$$

where (***J***) represents a column matrix of independent molar diffusion fluxes and (∇x) represents a column matrix of independent composition gradients with *n*-1 elements.

The diffusion flux of component *n* is not independent and normally can be evaluated by the relation:

$$\sum_{k=1}^{n} \boldsymbol{J}_k = 0 \tag{2.2.17}$$

The matrix [*D*] of Fickian diffusion coefficients is a square matrix of dimension *n*-1. The diagonal diffusivity D_{ii} connects the fluxes of a component with its own concentration gradient while non-diagonal diffusivities D_{ij} connect the flux of this component with the concentration gradients of other components. The diffusion coefficients D_{ij} in multicomponent mixtures are not binary properties, but are the result of complex interactions between all the species. Therefore the values of diffusivities D_{ij} in a multicomponent mixture are not equal to the D_{ij} in a binary mixture of the components *i* and *j*. This means matrix [*D*] is not symmetrical.

Even when Fick's law is generalised, it does not easily deal with systems with non-idealities or driving forces other than concentration. Plenty of such examples can be found in Wesselingh and Krishna (2000). Therefore the Maxwell-Stefan diffusion theory is introduced.

2.2.3 Maxwell-Stefan diffusion theory

The Maxwell-Stefan equation will be employed as the theoretical base for the diffusion model in this thesis. Thus, it is very important to understand the theory before using it. For that reason its derivation will be presented. Back in 1859, Maxwell published two works on diffusion, based upon the kinetic theory of gases. In 1871 Stefan extended the theory, which is now known as the Maxwell-Stefan (MS) theory for transport phenomena. Later, it was generalised by Taylor and Krishna (1993).

The general idea of the Maxwell-Stefan approach is to consider balance between driving forces and friction forces. Friction occurs between the diffusing components. A driving force can be represented as a gradient of a potential, which is the measurement for the deviation from equilibrium. Depending on the conditions of the mass transfer, many possible sets of driving forces may exist. Examples of possible driving forces are:

- the gradient of the chemical potential of a species,
- the pressure gradient,
- the gradient of the electrical potential,
- external forces, such as gravity, centrifugal, etc.

The basic driving force is the chemical potential, which is related to the variation of the concentration in an ideal mixture, and to the gradient of the corresponding chemical potential in a non-ideal mixture. However, the Maxwell-Stefan formula allows straightforward inclusion of other effects into the driving force.

It is straightforward to derive the Maxwell-Stefan diffusion in binary gas mixtures and then generalise it to a multicomponent system.

Considering a *z*-directional diffusion in an isothermal system, the force balance for the control volume is shown is Figure 2.2.

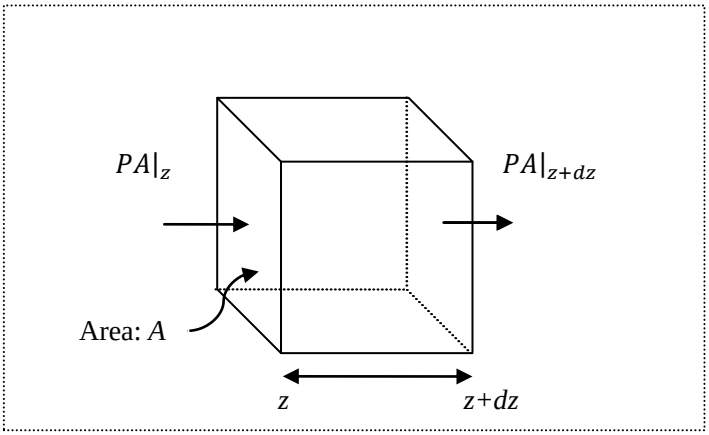

Figure 2.2 A simple force balance on a control volume containing an ideal gas mixture

The net force acting on the left-hand wall is the pressure force *PA* exerted by the molecules outside this box striking this imaginary surface. The force acting on the species 1 molecules alone is the partial pressure of species 1, p_1=Px_1, multiplied by the area *A*.

Therefore, the net force, ***F***, acting on component 1 in direction *z* is given by:

$$Net\ force\ acting\ on\ component\ 1 = Ap_1|_z - Ap_1|_{z+dz} \tag{2.2.18}$$

Dividing by the volume *Adz*:

$$Net\ force\ acting\ on\ component\ 1\ per\ unit\ volume = \frac{p_1|_z - p_1|_{z+dz}}{dz} \tag{2.2.19}$$

Taking the limit as *dz* tends to zero, we find net force acting on component 1 molecules per unit volume to be

$$Net\ force\ per\ unit\ volume = \lim_{dz\to 0} \frac{p_1|_z - p_1|_{z+dz}}{dz} = -\frac{dp_1}{dz} \tag{2.2.20}$$

This force is balanced by the frictional force between diffusing particles of the species as shown in Figure 2.3.

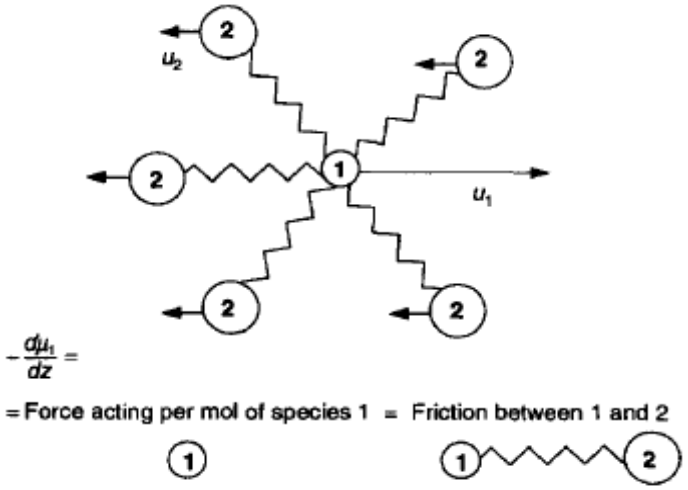

Figure 2.3 Relative motions between species 1 and 2

(Krishna and Wesselingh, 1997)

We expect friction between the two gases to be proportional to the amounts of the two gases in the volume and to their velocity difference. The amounts are proportional to the partial pressures:

$$Friction\ force \propto p_1 p_2(\boldsymbol{u}_1 - \boldsymbol{u}_2) \tag{2.2.21}$$

Therefore:

$$-\frac{dp_1}{dz} \propto p_1 p_2(\boldsymbol{u}_1 - \boldsymbol{u}_2) \tag{2.2.22}$$

They are forces per unit volume. The force per mole is obtained by diving by its concentration. For an ideal gas mixture the concentration of component 1 is:

$$c_1 = \frac{p_1}{RT} \tag{2.2.23}$$

This yields:

$$-\frac{RT}{p_1}\left(\frac{dp_1}{dz}\right) \propto RTp_2(\boldsymbol{u}_1 - \boldsymbol{u}_2) \tag{2.2.24}$$

The left-hand side is the driving force on gas 1:

$$-\frac{RT}{p_1}\left(\frac{dp_1}{dz}\right) \tag{2.2.25}$$

The right-hand side is the friction force exerted by gas 2 on gas 1. Using $x_2 \propto p_2$ we rewrite it as:

$$\xi_{12} x_2 (\boldsymbol{u}_1 - \boldsymbol{u}_2) \tag{2.2.26}$$

in which ξ_{12} is the friction coefficient between the gas 1 and 2.

The friction coefficient is related to the Maxwell-Stefan diffusion coefficient, $Đ_{12}$, by:

$$\xi_{12} = \frac{RT}{Đ_{12}} \tag{2.2.27}$$

The driving force can be expressed in terms of the chemical potential gradient of species 1, at constant temperature and pressure in vector form:

$$-\nabla_{T,P} \mu_1 = -\frac{d\mu_1}{dz} \tag{2.2.28}$$

By equating the expression for the driving force and the friction force we can write the Maxwell-Stefan (MS) equation for diffusion in a binary gas mixture:

$$-\frac{d\mu_1}{dz} = \frac{RT}{Đ_{12}} x_2 (\boldsymbol{u}_1 - \boldsymbol{u}_2) \tag{2.2.29}$$

Multiplying both sides of equation (2.2.29) by $\frac{x_1}{RT}$:

$$-\frac{x_1}{RT}\frac{d\mu_1}{dz} = \frac{x_1}{Đ_{12}} x_2 (\boldsymbol{u}_1 - \boldsymbol{u}_2) \tag{2.2.30}$$

Combined with equation 2.2.5:

$$-\frac{x_1}{RT} \nabla_{T,P} \mu_1 = \frac{x_2 \boldsymbol{N}_1 - x_1 \boldsymbol{N}_2}{c_t Đ_{12}} \tag{2.2.31}$$

This is the form of Maxwell-Stefan equations for binary gas mixtures. It has been derived on the basis of a binary ideal gas in one dimension; the extension to liquids, other phases and three dimensions is relatively simple. For multicomponent systems, the driving force on component 1 is identical to that in binary systems. However, the friction force is much more complicated. For component 1, interactions between species 1 and 3, 1 and 4, and so on up to species 1 and *n* must also be accounted for. All of these frictional interactions will have an effect on the rate of diffusion of component 1. That is:

$$\begin{aligned} -\nabla_{T,P} \mu_1 = \frac{RT}{Đ_{12}} x_2 (\boldsymbol{u}_1 - \boldsymbol{u}_2) + \frac{RT}{Đ_{13}} x_3 (\boldsymbol{u}_1 - \boldsymbol{u}_3) + \cdots \\ + \frac{RT}{Đ_{1n}} x_n (\boldsymbol{u}_1 - \boldsymbol{u}_n) \end{aligned} \tag{2.2.32}$$

For an arbitrary component *i*, the above equation is:

$$-\nabla_{T,P}\mu_i = \sum_{\substack{j=1 \\ j\neq i}}^{n} \frac{RT}{\mathcal{D}_{ij}} x_j \left(\boldsymbol{u}_i - \boldsymbol{u}_j\right) \quad i = 1,2,\dots,n \tag{2.2.33}$$

where $\mu_i = \mu_i^0 + RT\ln(\gamma_i x_i)$ with γ_i the activity coefficient of component *i* in the mixture on a mole fraction basis and μ_i^0 the chemical potential of component *i* in reference state.

Applying a similar procedure as above, we have:

$$-\frac{x_i}{RT}\nabla_{T,P}\mu_i = \sum_{\substack{j=1 \\ j\neq i}}^{n} \frac{x_j \boldsymbol{N}_i - x_i \boldsymbol{N}_j}{c_t \mathcal{D}_{ij}} \quad i = 1,2,\dots,n \tag{2.2.34}$$

Define a quantity $\boldsymbol{d}_i$:

$$\boldsymbol{d}_i = -\frac{x_i}{RT}\nabla_{T,P}\mu_i \tag{2.2.35}$$

Equation (2.2.34) can be written in terms of $\boldsymbol{d}_i$ as:

$$\boldsymbol{d}_i = \sum_{\substack{j=1 \\ j\neq i}}^{n} \frac{x_j \boldsymbol{N}_i - x_i \boldsymbol{N}_j}{c_t \mathcal{D}_{ij}} \quad i = 1,2,\dots,n \tag{2.2.36}$$

For non-ideal fluids, $\boldsymbol{d}_i$ may be expressed in terms of the mole fraction gradients as follows:

$$\begin{aligned} \boldsymbol{d}_i = -\frac{x_i}{RT}\nabla_{T,P}\mu_i &= -\frac{x_i}{RT}\sum_{j=1}^{n-1}\left.\frac{\partial \mu_i}{\partial x_j}\right|_{T,P,\Sigma}\nabla x_j \\ &= -\frac{x_i}{RT}\sum_{j=1}^{n-1} RT\left.\frac{\partial ln(\gamma_i x_i)}{\partial x_j}\right|_{T,P,\Sigma}\nabla x_j \\ &= -x_i\sum_{j=1}^{n-1}\left.\left(\frac{\partial ln\gamma_i}{\partial x_j} + \frac{\partial ln x_i}{\partial x_j}\right)\right|_{T,P,\Sigma}\nabla x_j \\ &= -\sum_{j=1}^{n-1}\left.\left(\delta_{ij} + x_i\frac{\partial ln\gamma_i}{\partial x_j}\right)\right|_{T,P,\Sigma}\nabla x_j = -\sum_{j=1}^{n-1}\Gamma_{ij}\nabla x_j \end{aligned} \tag{2.2.37}$$

where δ_{ij} is the Kronecker delta which have value zero except when $i=j$, when it has value unity.

$$\Gamma_{ij} = \delta_{ij} + x_i \left.\frac{\partial ln\gamma_i}{\partial x_j}\right|_{T,P,\sum} \tag{2.2.38}$$

The symbol $\sum$ indicates that the differentiation of $\ln\gamma_i$ with respect to mole fraction x_j is to be carried out while keeping the mole fraction of all the other species constant except the *n*th because the mole fraction of component *n* must satisfy the fact that the sum of x_i is unity.

It is possible that other effects such as electrical gradients and pressure drops may also have a significant effect on diffusion. Next we want to treat the driving force in a more general sense. We write the force acting per unit volume of the mixture as:

$$c_t RT\boldsymbol{d}_i = -c_i \nabla_{T,P}\mu_i \tag{2.2.39}$$

Under the action of external forces acting on component *i*, the conservation of linear momentum gives:

$$-\frac{1}{\rho_t}\nabla P + \sum_{i=1}^{n} \omega_i \widetilde{\boldsymbol{F}}_i = \frac{d\boldsymbol{v}}{dt} + \nabla \cdot \boldsymbol{\sigma} \tag{2.2.40}$$

where $\widetilde{\boldsymbol{F}}_i$ represents the force acting per unit mass of component *i*, and $\boldsymbol{\sigma}$ is the stress tensor.

In most chemical processes, mechanical equilibrium is achieved long before chemical equilibrium and that for a system at mechanical equilibrium, the right-hand side of the above equation is zero:

$$-\frac{1}{\rho_t}\nabla P + \sum_{i=1}^{n} \omega_i \widetilde{\boldsymbol{F}}_i = 0 \tag{2.2.41}$$

When the system is subject to external body forces the generalised driving force is redefines as:

$$c_t RT\boldsymbol{d}_i = -c_i \nabla_T \mu_i + \rho_i \widetilde{\boldsymbol{F}}_i \tag{2.2.42}$$

Because the left side of equation (2.2.41) is equal to zero, it can be added to right side of the above equation without changing its value:

$$c_t RT\boldsymbol{d}_i = -c_i \nabla_T \mu_i + \rho_i \widetilde{\boldsymbol{F}}_i + \rho_i \left(\frac{1}{\rho_t}\nabla P - \sum_{j=1}^{n} \omega_j \widetilde{\boldsymbol{F}}_j \right) \tag{2.2.43}$$

Expanding the chemical potential term to include the pressure gradients:

$$\nabla_T \mu_i = \nabla_{T,P} \mu_i + \bar{V}_i \nabla P \tag{2.2.44}$$

in which $\bar{V}_i$ is the partial molar volume of component *i*.

Combining equation (2.2.42) with equation (2.2.43):

$$c_t RT \boldsymbol{d}_i = -c_i \nabla_{T,P} \mu_i - c_i \bar{V}_i \nabla P + \rho_i \widetilde{\boldsymbol{F}}_i + \rho_i \left(\frac{1}{\rho_t} \nabla P - \sum_{j=1}^{n} \omega_j \widetilde{\boldsymbol{F}}_j \right) \tag{2.2.45}$$

After some mathematical transformations, the final relation is obtained:

$$c_t RT \boldsymbol{d}_i = -c_i \nabla_{T,P} \mu_i + (\omega_i - c_i \bar{V}_i) \nabla P + \rho_i \left(\widetilde{\boldsymbol{F}}_i - \sum_{j=1}^{n} \omega_j \widetilde{\boldsymbol{F}}_j \right) \tag{2.2.46}$$

Incorporating this $\boldsymbol{d}_i$ in equation (2.2.36), we have the generalised Maxwell-Stefan (GMS) equations:

$$\begin{aligned} \boldsymbol{d}_i &= -\frac{x_i}{RT} \nabla_{T,P} \mu_i + \frac{(\omega_i - c_i \bar{V}_i)}{c_t RT} \nabla P + \frac{\rho_i}{c_t RT} \left(\widetilde{\boldsymbol{F}}_i - \sum_{j=1}^{n} \omega_j \widetilde{\boldsymbol{F}}_j \right) \\ &= \sum_{\substack{j=1 \\ j \neq i}}^{n} \frac{x_j \boldsymbol{N}_i - x_i \boldsymbol{N}_j}{c_t \mathcal{D}_{ij}} \quad i = 1,2,\dots,n \end{aligned} \tag{2.2.47}$$

2.3 GMS in electrolyte systems

The generalised driving force has been identified by equation (2.2.46). For electrolyte systems it is convenient to express it in terms of the external body force exerted per mole of component *i*; the corresponding equations are:

$$c_t RT \boldsymbol{d}_i = -c_i \nabla_{T,P} \mu_i + (\omega_i - c_i \bar{V}_i) \nabla P + \left(c_i \boldsymbol{F}_i - \omega_i \sum_{j=1}^{n} c_j \boldsymbol{F}_j \right) \tag{2.3.1}$$

The quantity $c_i \bar{V}_i$ represents the volume fraction ϕ_i of component *i*.

For isothermal transport in electrolyte systems, the body force $\boldsymbol{F}_i$ is the electrical force caused by the electrostatic potential gradient $\nabla\varphi$

$$\boldsymbol{F}_i = -z_i \mathfrak{F} \nabla \varphi \tag{2.3.2}$$

where z_i is the ionic charge of component *i* and $\mathfrak{F}$ is the Faraday constant.

Equation (2.3.1) becomes:

$$c_t RT\boldsymbol{d}_i = -c_i \nabla_{T,P}\mu_i + (\omega_i - c_i\bar{V}_i)\nabla P - \left(c_i z_i - \omega_i \sum_{j=1}^{n} c_j z_j\right)\Im\nabla\varphi \quad (2.3.3)$$

The condition of electroneutrality is everywhere:

$$\sum_{i=1}^{n} c_i z_i = 0 \quad (2.3.4)$$

Therefore, the generalised driving force in electrolyte systems simplifies to:

$$c_t RT\boldsymbol{d}_i = -c_i \nabla_{T,P}\mu_i + (\omega_i - c_i\bar{V}_i)\nabla P - c_i z_i\Im\nabla\varphi \quad (2.3.5)$$

Thus, the generalised Maxwell-Stefan equation can be written for each of the *n* components as:

$$\begin{aligned}\boldsymbol{d}_i &= -\frac{x_i}{RT}\nabla_{T,P}\mu_i - \frac{(c_i\bar{V}_i - \omega_i)}{c_t RT}\nabla P - \frac{x_i z_i}{RT}\Im\nabla\varphi \\ &= \sum_{\substack{j=1 \\ j\neq i}}^{n} \frac{x_j\boldsymbol{N}_i - x_i\boldsymbol{N}_j}{c_t \text{Đ}_{ij}} \quad i = 1,2,\dots,n\end{aligned} \quad (2.3.6)$$

An important property of the multicomponent Maxwell-Stefan diffusion coefficients is their symmetry.

$$\text{Đ}_{ij} = \text{Đ}_{ji} \quad (2.3.7)$$

There is only one independent GMS diffusion coefficient for a pair of components. This significantly reduces the number of the independent diffusion coefficients for multicomponent mixtures: $n\times(n\text{-}1)/2$ for an *n*-component mixture.

Another important property of the GMS multicomponent diffusion coefficients applies to ideal gases. In ideal gases multicomponent Maxwell-Stefan diffusion coefficients are equal to the binary coefficients and are almost independent of the mixture composition. In liquids, the third party influence on interaction between two species contributes to the values of the diffusion coefficients. As a result, the GMS diffusivities in a multicomponent mixture are no longer equal to the binary diffusion

coefficients.

It can be seen that the definition of the generalised driving force makes it possible to account for a variety of different conditions under which the mass transfer occurs.

For non-ionic systems it is usual to use diffusion fluxes $\boldsymbol{J}_i$ with respect to a reference velocity. For diffusion in electrolyte systems the most commonly used reference velocity is the velocity $\boldsymbol{u}_n$ of the solvent.

$$\boldsymbol{J}_i^n = \boldsymbol{N}_i - c_i \boldsymbol{u_n} \tag{2.3.8}$$

With this choice the flux of species *n* is zero:

$$\boldsymbol{J}_n^n = 0 \tag{2.3.9}$$

The GMS equations can be written in terms of these diffusion fluxes:

$$\begin{aligned} \boldsymbol{d}_i &= -\frac{x_i}{RT}\nabla_{T,P}\mu_i - \frac{(c_i\bar{V}_i - \omega_i)}{c_t RT}\nabla P - \frac{x_i z_i}{RT}\Im\nabla\varphi \\ &= \sum_{\substack{j=1 \\ j\neq i}}^{n} \frac{x_j \boldsymbol{J}_i^n - x_i \boldsymbol{J}_j^n}{c_t \mathcal{D}_{ij}} \quad i = 1,2,\dots,n \end{aligned} \tag{2.3.10}$$

The next step is to rearrange these equations into a form which can be solved numerically. By applying standard linear algebra techniques, these equations can be worked into the following *n*-1 dimensional form:

$$\frac{1}{RT}\mathrm{x}\cdot\nabla_{T,P}\mu + \frac{(\mathrm{c}\cdot\bar{\mathrm{V}} - \omega)}{c_t RT}\nabla P + \frac{\mathrm{x}\cdot\mathrm{z}}{RT}\Im\nabla\varphi = -\frac{1}{c_t}\mathrm{B}\mathbf{J}^n \tag{2.3.11}$$

where B is a *n*-1 square matrix with elements

$$B_{ii} = \sum_{\substack{k=1 \\ k\neq i}}^{n} \frac{x_k}{\mathcal{D}_{ik}} \quad i = 1,2,\dots,n-1 \tag{2.3.12}$$

$$B_{ij} = -\frac{x_i}{\mathcal{D}_{ij}} \quad i \neq j = 1,2,\dots,n-1 \tag{2.3.13}$$

By applying the non-ideal equation (2.2.37), the first term in equation (2.3.11) can be written as

$$\frac{1}{RT}\mathrm{x}\cdot\nabla_{T,P}\mu = \Gamma\nabla\mathrm{x} \tag{2.3.14}$$

Thus equation (2.3.11) can be written for *n*-1 components in matrix form as equation (2.3.15) which is a convenient form for solution

$$\Gamma\nabla \mathrm{x} + \frac{(\mathrm{c}\cdot\overline{\mathrm{V}} - \omega)}{c_t RT}\nabla P + \frac{\mathrm{x}\cdot\mathrm{z}}{RT}\Im\nabla\varphi = -\frac{1}{c_t}\mathrm{B}\mathbf{J}^n \tag{2.3.15}$$

In the case of an ideal solution, the activity coefficients are unity and $\mathbf{\Gamma}$ is the identity matrix.

In electrolyte systems, when individual ions are considered as components, the diffusion of one or more of the ions will result in a local electrical potential difference (diffusion potential) that will drag a counter ion in the same direction (Wesselingh and Krishna, 2000). When there is a single pair of ions, e.g., NaCl in water, there is no need to involve the electrical potential as both ions move together to maintain electroneutrality. However, diffusion potential is important when there are more than one species of either anion or cation. The difficulty here is that diffusion potential is not explicitly defined.

It can be assumed that initially, at time t_0, a system is electrically neutral everywhere

$$\sum_{i=1}^{n} z_i x_i(t_0) = 0 \tag{2.3.16}$$

And to retain neutrality there must be no net current:

$$\sum_{i=1}^{n} z_i \boldsymbol{J}_i^n = 0 \tag{2.3.17}$$

Krishna (1987) showed that equations (2.3.15) and (2.3.17) can be combined to give an augmented matrix:

$$\begin{bmatrix} -c_t\left(\Gamma\nabla \mathrm{x} + \dfrac{(\mathrm{c}\cdot\overline{\mathrm{V}} - \omega)}{c_t RT}\nabla P\right) \\ \cdots\cdots\cdots\cdots\cdots\cdots\cdots\cdots\cdots\cdots\cdots\cdots \\ 0 \end{bmatrix} = \begin{bmatrix} [\mathrm{B}] & \vdots & [\mathrm{c}\cdot\mathrm{z}] \\ \cdots\cdots\cdots & \vdots & \cdots\cdots\cdots \\ [\mathrm{z}] & \vdots & 0 \end{bmatrix} \begin{bmatrix} [\mathbf{J}^n] \\ \cdots\cdots \\ \dfrac{\Im}{RT}\nabla\varphi \end{bmatrix} \tag{2.3.18}$$

From which $\boldsymbol{J}_i^n$ and $\nabla\varphi$ could be determined. The profile of φ through a matrix can be determined by numerical integration of $\nabla\varphi$ with an external boundary condition of zero.

2.4 Thermodynamics

One of the most important advantages by using GMS equation is to consider the system as a non-ideal solution. In the system containing electrolytes and gels, it is necessary to define the activity coefficients of all combinations: activity coefficients of ions, solvent and the gel. It is also important to consider the effect of polymer network on the activities.

Firstly, it is important to know some thermodynamic basics. For an open system, when a chemical substance is added to or removed, the thermodynamic properties of the system are altered. These properties include the energy, enthalpy and free energy associated with each substance added. For a system with a given composition, one can construct a thermodynamic function from which all the thermodynamic properties can be calculated. Two well known such functions are the Gibbs free energy *G* and the Helmholtz free energy *A*.

The Gibbs free energy function is useful if the pressure and the temperature of the system are defined.

$$dG = -SdT + VdP + \sum_i \mu_i dn_i \tag{2.4.1}$$

in which *S* is the entropy and n_i denotes the number of moles of component *i* added to the phase.

The Helmholtz free energy function is useful if the volume and temperature of the system are defined.

$$dA = -SdT - PdV + \sum_i \mu_i dn_i \tag{2.4.2}$$

For liquids at not too high pressures at constant temperatures, the pressure and volume terms in the above equations are unimportant. The Gibbs and Helmholtz free energies are then identical.

Recall in Section 2.2.3, we used the following chemical potential equation defined for equation (2.2.33):

$$\mu_i = \mu_i^0 + RT \ln(\gamma_i x_i) \tag{2.4.3}$$

in which μ_i^0 is the chemical potential of component *i* in reference state and γ_i is actually the activity coefficient of component *i* on a mole fraction scale.

It is more convenient in aqueous solution thermodynamics to describe the chemical potential of a species *i* in terms of its activity a_i.

$$\mu_i = \mu_i^0 + RT \ln(a_i) \tag{2.4.4}$$

From the above equation one can see that the activity is a measure of the difference between the component's chemical potential at the state of interest and at its reference state. As the chemical potential of component *i* approaches the chemical potential at its reference state, the activity of component *i* reaches unity.

The basic definition of the activity coefficient is given by Zemaitis et al. (1986). For aqueous solutions in which the composition of the solution is expressed in terms of molality, the chosen reference state is the ideal solution of unit molality at the system temperature and pressure. The activity coefficient on a molal scale is defined as:

$$\gamma_i^m = \frac{a_i(m) m_i^0}{m_i} \tag{2.4.5}$$

in which γ_i^m denotes the molal activity coefficient, $a_i(m)$ is the activity on molal basis and m_i is the molal concentration of component *i* defined by:

$$m_i = \frac{moles\ of\ solute\ i}{mass\ of\ solvent\ in\ kg} \tag{2.4.6}$$

m_i^0 is the unity molality and for convenience it is omitted when writing equations with the understanding that the activity and the activity coefficient are dimensionless.

The activity coefficient on a mole fraction scale is given by:

$$\gamma_i = \frac{a_i(x)}{x_i} \tag{2.4.7}$$

This is the activity coefficient used in the Maxwell-Stefan diffusion non-ideality

calculation.

The activity and activity coefficient of a component *i* have been defined. However, in electrolytes a solution always contains cations and anions and thus a mean or average activity coefficient $\gamma_{\pm}$ is needed:

$$\gamma_{\pm} = (\gamma_{+}{}^{\nu_{+}}\gamma_{-}{}^{\nu_{-}})^{1/\nu} \tag{2.4.8}$$

where γ_{+} and γ_{-} are the activity coefficients of cations and anions respectively, $\nu = \nu_{+} + \nu_{-}$ is the stoichiometric number of moles of ions in one mole of salt.

Most activity coefficient calculation models are based on molality but activity coefficients of interest are based on mole fraction. Therefore activity coefficients may be converted a molal basis to a mole fraction basis via the following relationships given by Robinson and Stokes (1959):

$$\gamma_{\pm} = (1 + M_s \nu m_{\pm})\gamma_{\pm}^{m} \tag{2.4.9}$$

where M_s is the molar mass of the solvent in [kg/mol] and $m_{\pm}$ is the molal concentration of the solute.

2.4.1 Activity coefficients of the Debye-Hückel limiting law

Knowing the basic concepts of activity and activity coefficients in solutions we first look at activities of aqueous solutions of single strong electrolytes. Strong electrolytes are fully dissociated in solution and this results in high mutual attraction between oppositely charged ions. Based on the assumption of each ion being surrounded by an ionic atmosphere consisting of ions of the opposite charge, the Debye-Hückel limiting law for electrolyte solutions was formulated by Debye and Hückel (1923). The Debye-Hückel limiting law describes the non-ideal behaviour caused by electrostatic forces in extremely dilute electrolyte solutions:

$$\log_{10} \gamma_{\pm}{}^{m} = -A|z_{+}z_{-}|\sqrt{I} \tag{2.4.10}$$

in which z_{+} and z_{-} are the charge number of cations and anions.

Molal ionic strength *I* is defined by:

$$I = \frac{1}{2}\sum_i m_i z_i^2 \tag{2.4.11}$$

The coefficient *A* is defined by:

$$A = \frac{1}{2.303}\left(\frac{e}{\sqrt{\epsilon kT}}\right)^3 \sqrt{\frac{2\pi\rho_0 N_A}{1000}} \tag{2.4.12}$$

in which *e* is the charge on a proton, ϵ is the dielectric constant of water, *k* is the Boltzmann's constant, *T* is the absolute temperature, ρ_0 is the solvent density in g/cm^3 and N_A is the Avogadro's number. The factor of 1000 in the equation is used for density unit conversion from g/cm^3 to kg/m^3. *A* is a constant that depends on the solvent (water). An experimental value for *A* is 0.509 mol$^{-1/2}$ kg$^{1/2}$.

The Debye-Hückel limiting law provides an accurate representation of the limiting behaviour of the activity coefficients for very dilute solutions of ionic strength 0.001 molal or less. Recognising this, Debye and Hückel added a correction term to the limiting law. This extended form of the Debye-Hückel limiting is expressed as:

$$\log_{10} {\gamma_\pm}^m = -\frac{A|z_+ z_-|\sqrt{I}}{1 + \beta a\sqrt{I}} \tag{2.4.13}$$

where:

$$\beta = \sqrt{\frac{8\pi e^2 \rho_0 N_A}{1000\epsilon kT}} \tag{2.4.14}$$

The distance *a* is assumed to be the same for all ions in the system. Problems arise as this parameter is not measurable, but by choosing values close to the hydrated radius, often in the range of 3.5 to 6.2 Å suggested by Robinson and Stokes (1959), reasonable results can be obtained. Güntelberg (Zemaitis et al., 1986) suggested that setting a standard value for $a = 3.04\text{Å}$ so that the βa quantity becomes unity. The extended Debye-Hückel equation holds quite well up to an ionic strength of 0.1 molal.

In the following figures, the mean activity coefficient of HCl in water calculated with the Debye-Hückel limiting law and the extended Debye-Hückel law are compared to experimental values.

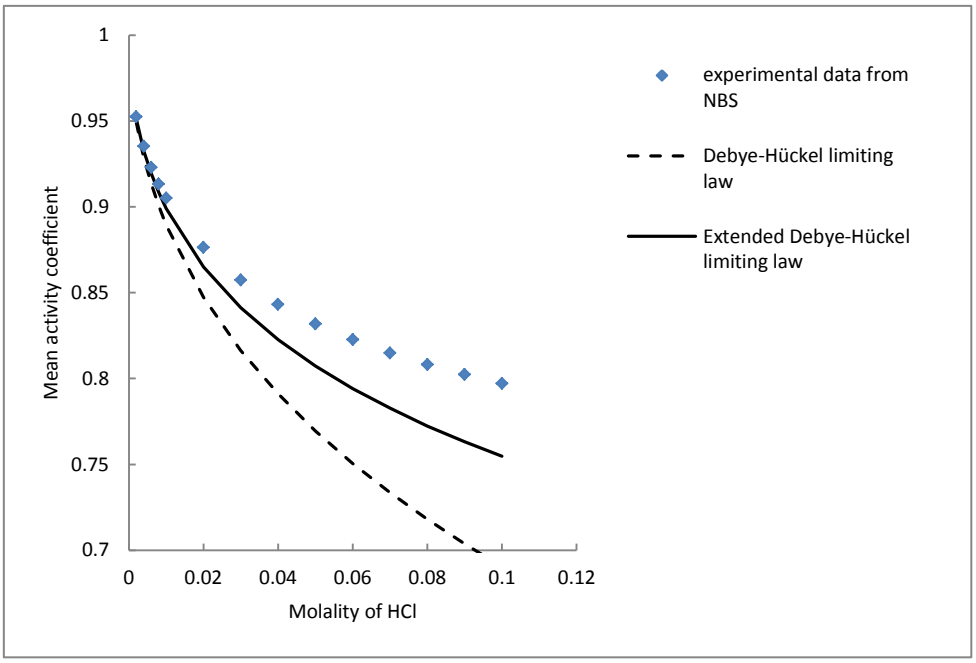

Figure 2.4 Mean molal activity coefficient of dilute aqueous HCl at 25°C calculated by the Debye-Hückel limiting law and the extended Debye-Hückel law compared with experimental values of NBS (Zemaitis et al., 1986)

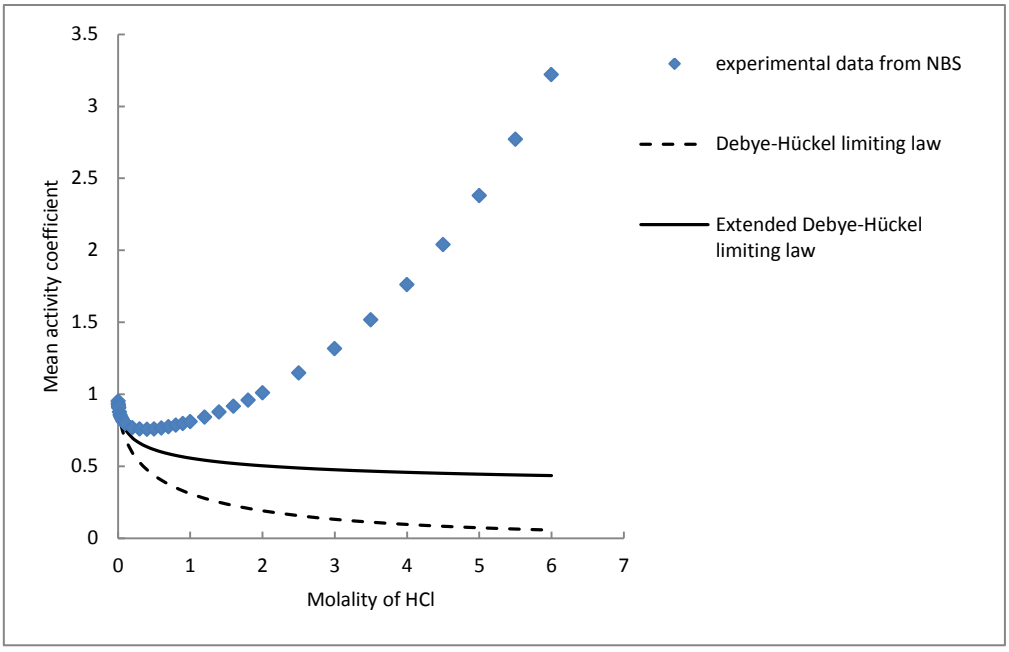

Figure 2.5 Mean molal activity coefficient of aqueous HCl at 25 °C calculated by the Debye-Hückel limiting law and the extended Debye-Hückel law compared with experimental values of NBS (Zemaitis et al., 1986)

The Debye-Hückel limiting law and the extended Debye-Hückel law describe the activity coefficients of very dilute ionic solutions. These equations are therefore often used for extrapolating the properties of electrolyte solutions to infinite dilution. As it

appears from Figure 2.4 and 2.5, however, the Debye-Hückel law is not suitable for describing the properties of real electrolyte solutions.

2.4.2 Activity coefficients of Pitzer's equations

The unsuccessful prediction of ion activities by Debye and Hückel is caused by an approximation which omits all of the direct effects of short-range forces.

Recall the Gibbs free energy *G* is:

$$dG = -SdT + VdP + \sum_i \mu_i dn_i \tag{2.4.15}$$

Recall certain basics relationships for solution thermodynamics in the molality system:

$$\mu_i = \mu_i^0 + RT \ln a_i \tag{2.4.16}$$

$$a_i = m_i \gamma_i^m \tag{2.4.17}$$

For the solvent (water), the chemical potential, μ_w, is:

$$\mu_w = \mu_w^0 + RT \ln a_w \tag{2.4.18}$$

With the superscript 0 indicates the standard or the reference state and the subscript *w* indicates water.

The water activity is commonly expressed by the osmotic coefficient ϕ:

$$\phi = -\frac{1000}{M_w \sum_i v_i m_i} \ln a_w \tag{2.4.19}$$

with M_w is the molar mass of water and v_i is the stoichiometric number of moles of ions in one mole of electrolyte *i*.

The change of the total Gibbs energy of mixing from its standard state is:

$$\begin{aligned} \Delta_{mix} G &= n_w(\mu_w - \mu_w^0) + \sum_i n_i(\mu_i - \mu_i^0) \\ &= RT\left(n_w \ln a_w + \sum_i n_i \ln a_i\right) \end{aligned} \tag{2.4.20}$$

One can substitute equations (2.4.17) and (2.4.19) for the activities:

$$\Delta_{mix}G = RT\sum_i n_i[-\phi + \ln(m_i\gamma_i^m)] \tag{2.4.21}$$

It is separated into two parts: one dependent on composition and a second part with terms of γ_i^m or (1-ϕ):

$$\Delta_{mix}G = RT\sum_i n_i(\ln m_i - 1) + RT\sum_i n_i[1 - \phi + \ln\gamma_i^m] \tag{2.4.22}$$

This second part is called the excess Gibbs free energy:

$$G^{ex} = RT\sum_i n_i[1 - \phi + \ln\gamma_i^m] \tag{2.4.23}$$

If the excess Gibbs energy is written as suggested by Pitzer (1991):

$$\frac{G^{ex}}{W_w RT} = \mathrm{f}(I) + \sum_i\sum_j m_i m_j \lambda_{ij}(I) + \sum_i\sum_j\sum_k m_i m_j m_k \lambda^*_{ijk} + \cdots \tag{2.4.24}$$

where W_w is the mass of water and I is also the molal ionic strength.

The first term includes the Debye-Hückel limiting law only depending on the ionic strength. The binary interaction parameter $\lambda_{ij}(I)$ represents the short-range interaction in the presence of water between ions i and j. It is dependent on the ionic strength. The triple interaction parameter λ^*_{ijk} represents the short-range interaction between ions i, j and k.

Using this excess Gibbs energy equation one can obtain the activity coefficient and osmotic coefficient by differentiation of $\frac{G^{ex}}{W_w RT}$:

$$\ln \gamma_i^m = \left.\frac{\partial\left(\frac{G^{ex}}{W_w RT}\right)}{\partial m_i}\right|_{n_w}$$
$$= \left(\frac{z_i^2}{2}\right)\mathrm{f}' + 2\sum_j \lambda_{ij} m_j + \frac{z_i^2}{2}\sum_j\sum_k \lambda'_{jk} m_j m_k \qquad (2.4.25)$$
$$+ 3\sum_j\sum_k \lambda^*_{ijk} m_j m_k + \cdots$$

and

$$\phi - 1 = \left(\sum_i m_i\right)^{-1}\left[(I\mathrm{f}' - \mathrm{f}) + \sum_i\sum_j \left(\lambda_{ij} + I\lambda'_{ij}\right) m_i m_j\right.$$
$$\left. + 2\sum_i\sum_j\sum_k \lambda^*{}_{ijk} m_i m_j m_k + \cdots\right] \qquad (2.4.26)$$

The variables f$'$ and λ'_{ijk} are the ionic strength derivatives of f and λ. The sums cover all ion species.

The above two equations are the general equations of Pitzer's activity coefficients.

For m molal pure electrolytes MX with v_M positive ions of charge z_M and v_X negative ions of charge z_X, the osmotic coefficient given by Pitzer is:

$$\phi - 1 = |z_M z_X|\mathrm{f}^\gamma + m\left(\frac{2v_M v_X}{v}\right)B^\phi_{MX} + m^2\left[\frac{2(v_M v_X)^{\frac{3}{2}}}{v}\right]C^\phi_{MX} \qquad (2.4.27)$$

with

$$v = v_M + v_X \qquad (2.4.28)$$

Pitzer measured the osmotic coefficients of 1-1, 2-1 and 1-2 types of salt at 25^{o}C and found that the best results were obtained for the forms:

$$\mathrm{f}^\phi = -A_\phi \frac{I^{1/2}}{1 + bI^{1/2}} \qquad (2.4.29)$$

$$B^\phi_{MX} = \beta^{(0)}_{MX} + \beta^{(1)}_{MX} e^{(-\alpha I^{1/2})} \qquad (2.4.30)$$

b with the value of 1.2 kg$^{1/2}$.mol$^{-1/2}$ and α with the value of 2.0 kg$^{1/2}$.mol$^{-1/2}$ gave the best fit with experiment results. A_ϕ is the Debye-Hückel parameter in Pitzer's

equations:

$$A_\phi = \frac{1}{3}\left(\frac{e}{\sqrt{DkT}}\right)^3 \sqrt{\frac{2\pi\rho_0 N_A}{1000}} \tag{2.4.31}$$

Compared the above equation with that defined in the Debye-Hückel limiting law the difference is the value 3 used in the equation instead of 2.303. The value of A_ϕ is 0.3915 $kg^{1/2}$ $mol^{-1/2}$ at 25°C. The parameter $\beta_{MX}^{(0)}$ and $\beta_{MX}^{(1)}$ are dependent on the salt *MX*.

The mean activity coefficient for the salt *MX* is defined as:

$$\ln \gamma_\pm^m = |z_M z_X| \mathrm{f}^\gamma + m\left(\frac{2v_M v_X}{v}\right) B_{MX}^\gamma + m^2 \left[\frac{2(v_M v_X)^{\frac{3}{2}}}{v}\right] C_{MX}^\gamma \tag{2.4.32}$$

With the following definitions:

$$\mathrm{f}^\gamma = -A_\phi \left[\frac{I^{1/2}}{1 + bI^{1/2}} + \frac{2}{b}\ln\left(1 + b^{1/2}\right)\right] \tag{2.4.33}$$

$$B_{MX}^\gamma = B_{MX} + B_{MX}^\phi \tag{2.4.34}$$

$$C_{MX}^\gamma = \frac{3C_{MX}^\phi}{2} \tag{2.4.35}$$

B_{MX} is defined by:

$$B_{MX} = \beta_{MX}^{(0)} + \beta_{MX}^{(1)} \mathrm{g}\left(\alpha_1 I^{1/2}\right) + \beta_{MX}^{(2)} \mathrm{g}\left(\alpha_2 I^{1/2}\right) \tag{2.4.36}$$

in which function g is:

$$\mathrm{g}(x) = \frac{2[1 - (1 + x)exp(-x)]}{x^2} \tag{2.4.37}$$

For mixed electrolytes, the Pitzer equations for the activity coefficient of a cation *M* (γ_M^m), the activity coefficient of an anion *X* (γ_X^m) and the osmotic coefficient ϕ, are as follows:

$$ln(\gamma_M^m) = z_M^2 F + \sum_a m_a(2B_{Ma} + ZC_{Ma}) + \sum_c m_c\left(2\Phi_{Mc} + \sum_a m_a\psi_{Mca}\right) + \sum_a\sum_{a'} m_a m_{a'}\psi_{Maa'} + z_M\sum_c\sum_a m_c m_a C_{ca} \quad (2.4.38)$$

$$ln(\gamma_X^m) = z_X^2 F + \sum_c m_c(2B_{cX} + ZC_{cX}) + \sum_a m_a\left(2\Phi_{Xa} + \sum_c m_c\psi_{cXa}\right) + \sum_c\sum_{c'} m_c m_{c'}\psi_{cc'X} + |z_X|\sum_c\sum_a m_c m_a C_{ca} \quad (2.4.39)$$

$$\phi - 1 = \frac{2}{\sum_i m_i}\left[\frac{-A_\phi I^{\frac{3}{2}}}{\left(1 + bI^{\frac{1}{2}}\right)} + \sum_c\sum_a m_c m_a\left(B_{ca}^\phi + ZC_{ca}\right) + \sum_c\sum_{c'} m_c m_{c'}\left(\Phi_{cc'}^\phi + \sum_a m_a\psi_{cc'a}\right) + \sum_a\sum_{a'} m_a m_{a'}\left(\Phi_{aa'}^\phi + \sum_c m_c\psi_{caa'}\right)\right] \quad (2.4.40)$$

The summations in equations over *c* and *a* respectively are summations over the cations and the anions present in the solution. The various terms in equations are defined as follows:

$$Z = \sum_i m_i|z_i| \quad (2.4.41)$$

$$F = f^{\gamma} + \sum_{c}\sum_{a} m_c m_a B'_{ca} + \sum_{c}\sum_{c'} m_c m_{c'} \Phi'_{cc'} + \sum_{a}\sum_{a'} m_a m_{a'} \Phi'_{aa'} \tag{2.4.42}$$

$$B'_{MX} = \frac{\left[\beta^{(1)}_{MX} \mathrm{g}'\left(\alpha_1 I^{1/2}\right) + \beta^{(2)}_{MX} \mathrm{g}'\left(\alpha_2 I^{1/2}\right)\right]}{I} \tag{2.4.43}$$

$$\mathrm{g}'(x) = \frac{-2\left[1 - \left(1 + x + \frac{x^2}{2}\right)e^{-x}\right]}{x^2} \tag{2.4.44}$$

$$C_{MX} = \frac{C^{\phi}}{2|z_M z_X|^{1/2}} \tag{2.4.45}$$

$$\Phi^{\phi}_{cc'} = \Phi_{cc'} + I\Phi'_{cc'} \tag{2.4.46}$$

$$\Phi^{\phi}_{aa'} = \Phi_{aa'} + I\Phi'_{aa'} \tag{2.4.47}$$

In the analysis of experimental data for mixed electrolytes with the use of the equations of Pitzer, it was found that the principal effects on mixing electrolytes arise from differences in the pure electrolyte parameters $\beta^{(0)}$, $\beta^{(1)}$, $\beta^{(2)}$ and C^{ϕ} and that the parameters Φ and ψ have only a small effect. So far a few parameters in Pitzer's equations above have not been found.

For the solvent water, the activity of the pure water is unity. In dilute solutions of electrolytes, the activity is very close to unity. The water activity is found by rearranging equation (2.4.19):

$$\ln a_w = -\frac{M_w \sum_i v_i m_i}{1000}\phi \tag{2.4.48}$$

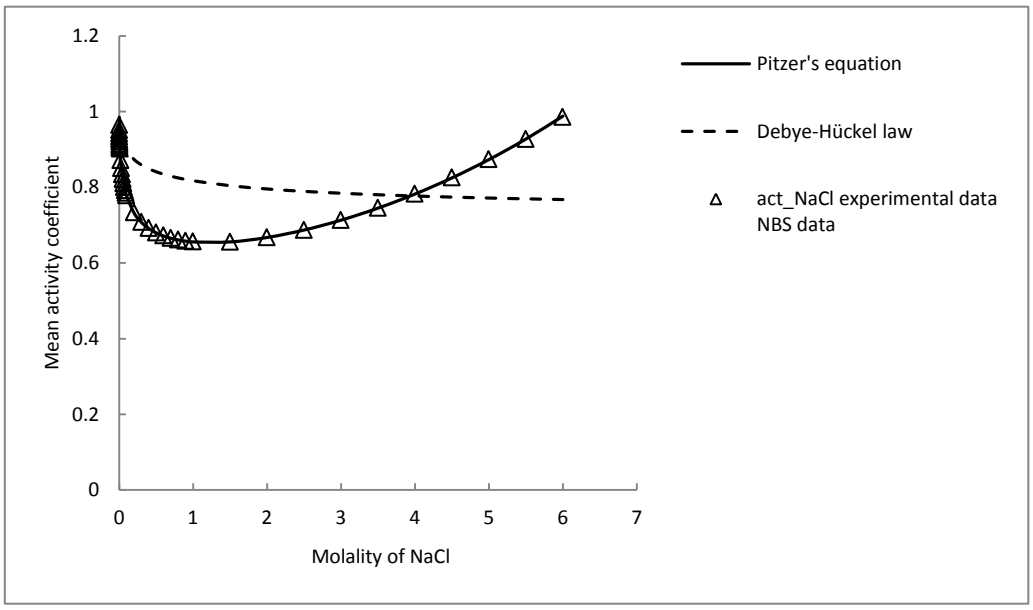

Figure 2.6 Mean molal activity coefficient of aqueous NaCl at 25 ^{o}C calculated by the Debye-Hückel limiting law and the Pitzer's equation compared with experimental values of NBS (Zemaitis et al., 1986)

From the results in Figure 2.6, it can be concluded that the Pitzer model predicts the mean activity coefficients of single salts dissolved in water very well. For the prediction of the mean activity coefficients of an electrolyte in mixtures of electrolytes the Pitzer model can also be applied, which is illustrated in Figure 2.7 and Figure 2.8 for the NaCl and NaOH mixture.

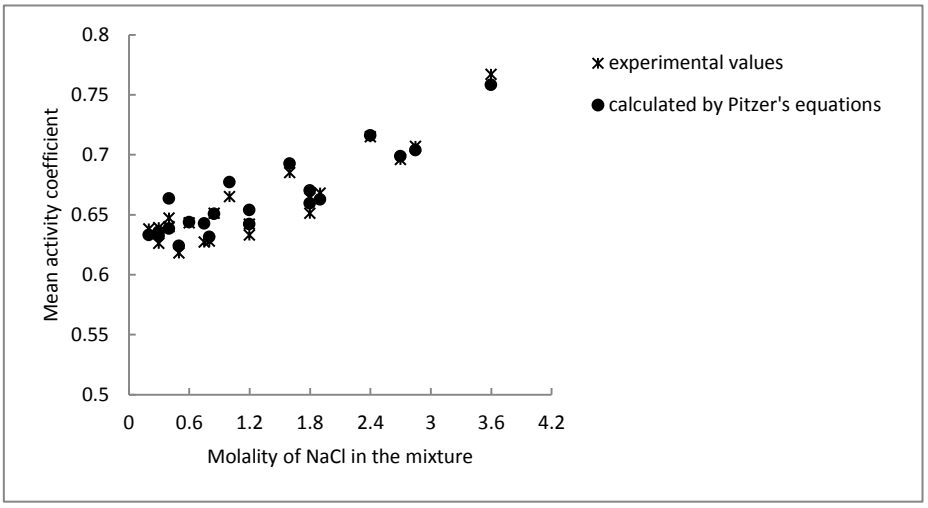

Figure 2.7 Mean molal activity coefficient of aqueous NaCl in NaCl and NaOH mixture calculated by the Pitzer's equation compared with experimental values (Falciola et al., 2003)

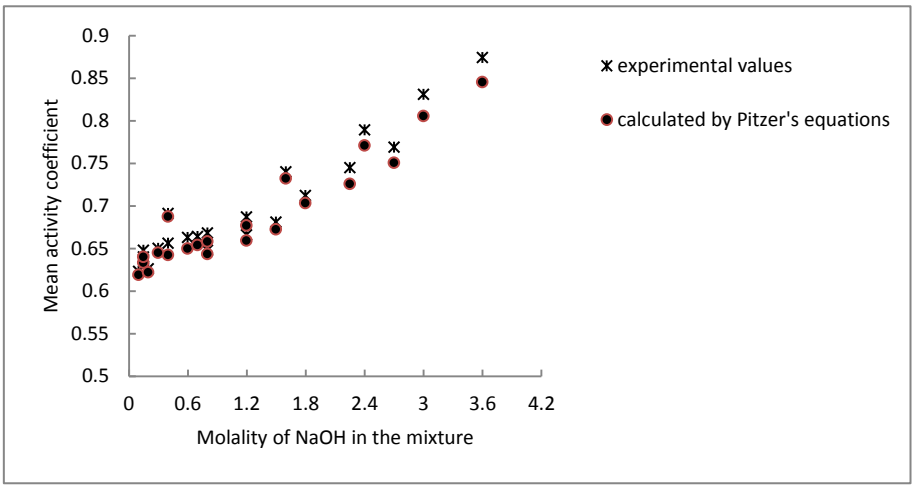

Figure 2.8 Mean molal activity coefficient of aqueous NaOH in NaCl and NaOH mixture calculated by the Pitzer's equation compared with experimental values (Falciola et al., 2003)

The parameters used to calculate activity coefficients of NaCl and NaOH mixture are summarised in the following tables. For many systems the interaction parameters have been tabulated in Pitzer (1991).

Table 2.1 interaction parameters $\beta^{(0)}$, $\beta^{(1)}$, $\beta^{(2)}$ and C^{ϕ}

	$\beta^{(0)}$	$\beta^{(1)}$	$\beta^{(2)}$	C^{ϕ}
Na^+/Cl^-	0.0765	0.2664	0	0.00127
Na^+/OH^-	0.0864	0.253	0	0.0044

Table 2.2 interaction parameter $\Phi_{aa'}$ and $\psi_{aa'c}$

$\Phi_{aa'}$ (Cl^-/OH^-)	-0.050
$\psi_{aa'c}$ ($Na^+/Cl^-/OH^-$)	-0.006

2.4.3 Activity coefficients in polyelectrolytes: Manning's condensation theory

Polyelectrolytes become charged by dissociation of certain functional groups releasing ions into the surrounding solution. For example, proteins can be negatively charged by releasing hydrogen ions into the alkaline surrounding solution. For such a polyelectrolyte system, the system can be seen composed of small ions of electrolytes, polyions of the gel and solvent. The electrostatic interactions between polyions and small ions often exert a significant effect on polyelectrolyte's thermodynamic

properties. Extensive efforts have been made to develop theories and models for these systems. Among them the counter-ion condensation theory developed by Manning (Manning, 1969a, 1969b, 1979) is of interest. The Manning condensation model involves the following assumptions:

- the real polyelectrolyte chain is considered as an infinite line charge with a uniform linear charge density, β;
- the interactions between two or more polyions are neglected;
- the dielectric constant, ϵ, is assumed to be that of the pure bulk solvent;
- for dilute solutions, a sufficient number of counter-ions will condense onto the polyion until the charged density between neighbouring monomer charges along the polyion chain is reduced below a certain critical value called ξ.
- the mobile ions are treated by the Debye-Hückel approximation.

If the end to end distance of the polyion chain in the state of maximum extension is L and the chain have n_t charged groups of valence z_p, the charge density β is given by:

$$\beta = \frac{z_p e}{b} \tag{2.4.49}$$

with

$$b = \frac{L}{n_t} \tag{2.4.50}$$

The physical meaning of b is the average charge distance in the fully stretched configuration. From the assumption the real polyelectrolyte chain is replaced by an infinite line charge with density β given by equation (2.4.49).

Ions, either condensed or mobile, are determined by an observation of Onsager (Manning, 1969a) about the configurational integral of the system. By "condensed" the Manning theory assumes zero mobility. Consider the contribution to this integral from the region of phase space where the mobile ion z_i is sufficiently close to the line charge (say, $l \leq l_0$, where l is the distance from the line charge) to have an unscreened Coulomb interaction with it, and all the other ions are further from the line. The other ions contribute a finite factor $f(l_0)$ to the configurational integral and the entire contribution from this region is given by:

$$A_i(l_0) = f(l_0)\int_0^{l_0} \exp\left(-\frac{u_{ip}(l)}{kT}\right) 2\pi L dl \tag{2.4.51}$$

in which A_i stands for the Onsager configurational integral.

u_{ip} is the polyion-ion interaction obtained by:

$$u_{ip} = -z_i e\left(\frac{2\beta}{\epsilon}\right)\ln l \tag{2.4.52}$$

Thus

$$A_i(l_0) = 2\pi f(l_0)\int_0^{l_0} l^{(1+2z_i z_p \xi)} dl \tag{2.4.53}$$

where the Manning parameter ξ is defined as:

$$\xi = \frac{e^2}{\epsilon kTb} \tag{2.4.54}$$

For a counter-ion i, $z_i z_p$ is negative, the integral in equation (2.4.53) diverges at the lower limit for all ξ such that:

$$\xi \geq \frac{1}{|z_i z_p|} \tag{2.4.55}$$

Mobile ions and charged groups are treated as monovalent, so the condition becomes:

$$\xi \geq 1 \tag{2.4.56}$$

The physical meaning of the divergence of the phase integral for values of ξ greater than unity is that systems with ξ greater than unity are unstable. Therefore many counter-ions will condense on the line charge to reduce the charge density parameter ξ to the value of unity. The uncondensed mobile ions are still subject to electrostatic interactions with the line charge since the charge density of the line after condensation is not zero. In other words if the value of ξ is greater than unity, condensation will happen and after condensation it is equal to unity. If the value of ξ is less than unity, no condensation will occur and all mobile ions are treated in the Debye-Hückel approximation.

For the activity coefficients calculation with ξ less than unity, because there is no condensation and all mobile ions are treated by the Debye-Hückel limiting law, the polyion can be seen as an additional ion component to the electrolyte system and

activity coefficients can be obtained by the Pitzer's equations. The problem here is to find the interaction parameters between electrolyte ions and the polyion. Therefore the activity coefficients are still calculated by using the Debye-Hückel approximation given by:

$$\ln y_i = -\frac{1}{2}\xi X(X+2)^{-1} \;\; i = counter, co;\; \xi < 1 \tag{2.4.57}$$

with

$$X = \frac{n_e}{n_s} \tag{2.4.58}$$

where y_i is the Manning activity coefficient, n_e is the equivalent concentration of polyions and n_s is the salt concentration added to the polyelectrolytes solution.

The osmotic pressure coefficient is given by:

$$\phi = 1 - \frac{1}{2}\xi X(X+2)^{-1} \tag{2.4.59}$$

For ξ larger than unity, a fraction of $(1-\xi^{-1})$ of counter-ions condenses on the polyion reducing its charge and rendering ξ=1. The rest of the counter-ions (a fraction of ξ^{-1}) may then be treated in the Debye-Hückel approximation. The activity coefficient of the counter-ion is:

$$y_{counter} = \frac{(\xi^{-1}X+1)}{X+1}\exp\left(\frac{-\frac{1}{2}\xi^{-1}X}{\xi^{-1}X+2}\right) \tag{2.4.60}$$

The activity coefficient of the co-ion is:

$$y_{co} = \exp\left(\frac{-\frac{1}{2}\xi^{-1}X}{\xi^{-1}X+2}\right) \tag{2.4.61}$$

The osmotic coefficient is:

$$\phi = \frac{-\frac{1}{2}\xi^{-1}X+2}{X+2} \tag{2.4.62}$$

Manning's condensation theory works well for very dilute solutions. Experimental validation had been carried out for the systems in which the polyelectrolyte and the added simple salt had a common counter ion, such as sodium polyvinylsulfonate

(NaPVS)/NaCl, potassium pyrophosphate (KPP)/KBr and sodium polystyrenesulfonate (NaPSS)/NaCl. Alexandrowicz (Manning, 1969a) published extensive data for the osmotic coefficient ϕ and the mean activity coefficients $\gamma_{\pm}$ of the mobile ions. The system is sodium polymethacrylate (NaPMA) with various degrees of neutralisation and with added NaBr in a concentration range from 1.4×10^{-3} N to 0.17 N. It was found that the theory was in excellent agreement with the value of experiments in the more dilute region.

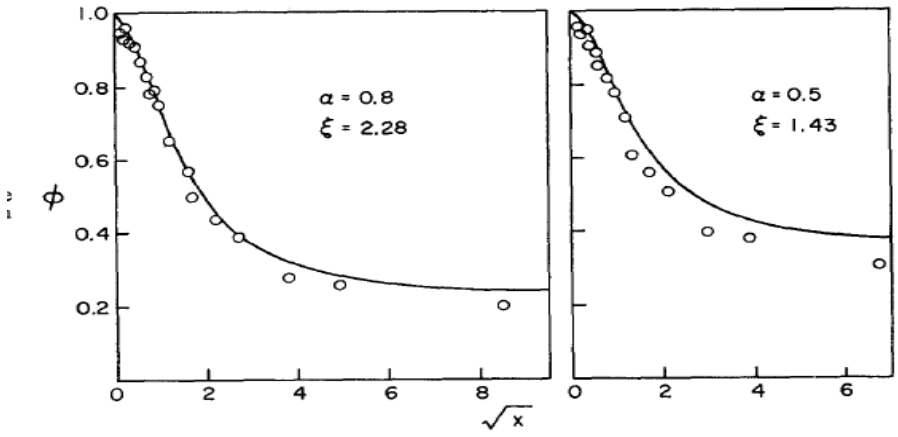

Figure 2.9 Comparison of Manning theory for the osmotic coefficient ϕ (solid lines) with experimental data from Alexandrowicz. (Manning, 1969a)

In less dilute regions the Manning condensation theory did not perform well because the short range interactions between polyelectrolyte ion and counter-ions are ignored. Therefore, this theory may not necessarily be accurate in condensed polyelectrolyte solutions. For real polyelectrolyte solutions, how to incorporate short range interaction into Manning's condensation theory needs to be solved.

Based on the Manning's condensation theory, Iwasa et al. (Iwasa and Kwak, 1977; Iwasa, et al., 1978) found that the higher order cluster terms due to the polyelectrolyte ion-small ion interaction indicated a considerable difference between the counter-ion and co-ion activity coefficients even at ξ=1, where no condensation takes place. Thus, a new limiting law was derived by taking into account a high-order cluster term in the excess free energy. If the high order term in the excess free energy was dropped it reduced to the Manning limiting law.

For $\xi \leq 1$, the activity coefficients are:

$$y_{counter} = \exp\left\{\left(-0.5 + 0.3906\xi\left(\frac{X}{X+2} - 1\right)\right)\left(\frac{\xi X}{X+2}\right)\right\} \quad (2.4.63)$$

$$y_{counter} = \exp\left\{\left(-0.5 + 0.3906\xi\left(\frac{X}{X+2} + 1\right)\right)\left(\frac{\xi X}{X+2}\right)\right\} \quad (2.4.64)$$

For $\xi > 1$, the activity coefficients are:

$$y_{counter} = \frac{(\xi^{-1}X + 1)}{X+1}\exp\left\{\left(\frac{\xi^{-1}X}{\xi^{-1}X+2}\right)\left(-0.5 + 0.3906\left(\frac{\xi^{-1}X}{\xi^{-1}X+2} - 1\right)\right)\right\} \quad (2.4.65)$$

and

$$y_{counter} = \exp\left\{\left(\frac{\xi^{-1}X}{\xi^{-1}X+2}\right)\left(-0.5 + 0.3906\left(\frac{\xi^{-1}X}{\xi^{-1}X+2} + 1\right)\right)\right\} \quad (2.4.66)$$

Kowblansky et al. (1978) measured mean activity coefficients of chloride and sodium ions in aqueous mixtures of sodium chloride with sodium dextran sulfate solutions. For the experiments, 0.001, 0.005 and 0.01M sodium chloride concentrations were used. Their data show that Manning's and Iwasa's predicted results are identical for very low X values but diverge for $X>2$ with Iwasa's results giving more accurate prediction at higher NaCl concentrations (Figure 2.10).

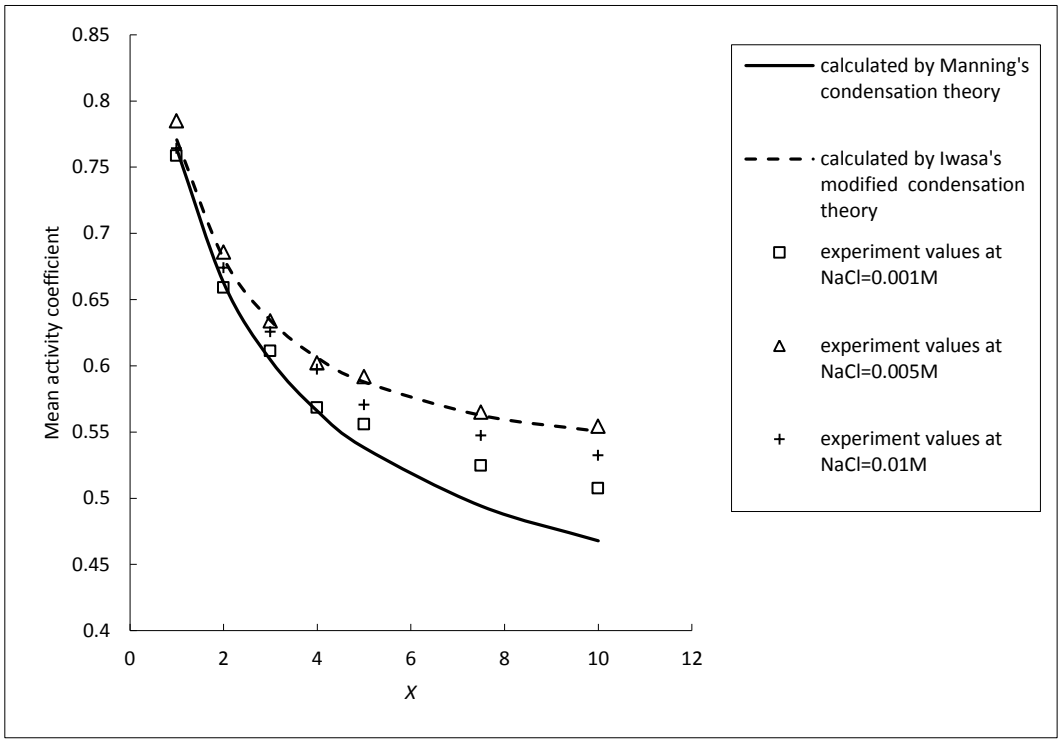

Figure 2.10 $y_{\pm}$ against X for NaDS solutions containing NaCl experimental data from Kowblansky et al. (1978)

When they compared experimental data with activity coefficients calculated by Manning's theory, Wells and Kwak (Wells, 1973; Kwak et al., 1975) found that experimental data should be corrected by activity coefficients in pure electrolytes. The correction procedure can be stated mathematically by:

$$y_{\pm}^{c} = \frac{y_{\pm}^{ex}}{y_{\pm}^{0}} \tag{2.4.67}$$

where $y_{\pm}^{c}$ is the activity coefficients calculated by Manning's theory

$y_{\pm}^{ex}$ is the activity coefficients observed by experiments

$y_{\pm}^{0}$ is the activity coefficient of added salts in pure electrolyte solutions

Therefore, the mean ion activity coefficient of the simple salt can be calculated by the modified form of the Manning theory (Wells, 1973):

$$y_{\pm} = y_{\pm}^{p.m} y_{\pm}^{m.m} \tag{2.4.68}$$

In the above equation the first term in the right hand equation is Manning's contribution and the second term is the activity coefficient in pure electrolytes.

Similarly the osmotic coefficient is given by

$$\phi = \phi^{p.m} + \phi^{m.m} - 1 \approx \phi^{p.m}\phi^{m.m} \tag{2.4.69}$$

Manning's activity coefficients are based on molar concentration while models of activity coefficients in pure electrolytes are calculated based on molality. Therefore it is necessary to keep the activity coefficients on the same basis. The conversion between the two activity coefficients can be achieved by using equation (2.4.9).

2.5 Swelling mechanics

2.5.1 Rubber elasticity

The ability to swell is an important characteristic of a gel. Hydrogels are polymers with a three-dimensional network (De and Aluru, 2004) that can absorb or release water as a response to stimuli of various kinds to reach an equilibrium state. Polyelectrolyte gels are charged gels that can swell and shrink in a reversible way as a reaction to external stimuli such as chemical interactions pH, solvent and solutes. In this thesis, a model of polyelectrolyte gel swelling is to be established. To do this we must know how to describe the swelling mechanics. In numerical simulations or uniaxial and biaxial mechanical deformation tests, polymer gels are often modelled successfully using rubber elasticity theory at large strains and linear elasticity theory at small strains (Lin and Metters, 2008). This is also applicable to swelling which is a kind of deformation caused by diffusion. In this study, the rubber elasticity theory and linear elasticity theory will be examined and then the suitable one will be used to describe the mechanical structure equations in the swelling model.

Firstly it is necessary to know two elastic deformation models in rubber elasticity theory: affine and phantom (Caykara et al., 2004). Under applied stress, the elastic behaviour of gels falls between two idealised limits. In the affine model, it is assumed that chain segments of the network deform independently and on a microscopic scale in the same way as the whole sample (macroscopic scale). The crosslinks are assumed

to be fixed in space at positions exactly defined by the specimen deformation ratio. However, in the phantom model, chains are considered immaterial or phantom and can freely cross each other. Figure 2.11 shows schematically the difference between the affine network model and the phantom network model. The points marked with an *A* indicate the position of the crosslinks assuming affine deformation.

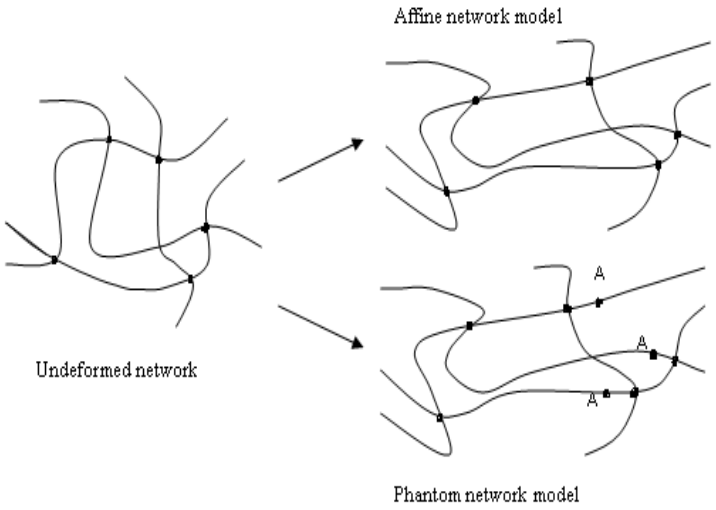

Figure 2.11 Affine network and phantom network (Allen et al., 1996)

There are two approaches to the study of rubber elasticity. Firstly the statistical theory attempts to derive stress-strain relationships of rubber from some idealised model of its structure such as a Gaussian network (Treloar, 2005) when rubber is under extension. Thermodynamics is fundamental to the development of this theory as it postulates that the deformation is accompanied by a reduction of entropy but without change in internal energy. Secondly the phenomenological theory treats the problem from the point view of continuum mechanics. This theory is to construct a mathematical framework to describe rubbery behaviour without the reference to thermodynamics concepts. It can deal with large deformations while the statistical theory assumes that all deformations are small. The first approach, or the classical theory of elasticity, often assumes that all deformations are small. In phenomenological theory, this small deformation assumption is relaxed and the study of large elastic deformations is often called finite elasticity theory.

- **Network theory of rubber elasticity**

The network theory of rubber elasticity is based on the concept that a vulcanised rubber is an assembly of long-chain molecules together to form an irregular three-dimensional network. Firstly, it is required to calculate the entropy of the network, and from this to derive the free energy or work of deformation. From the work of deformation corresponding to a given state of strain the associated stresses are then readily derived by the application of mechanics. The study of rubber networks began with the very early work of Kuhn (1936). Then, explicit forms of stress-strain relations were developed by Wall (1942a; 1942b), Flory and Rehner (1943), James and Guth (1943), and Treloar (1943). These later theories led to results which are substantially similar.

The theories followed the assumption that the material is isotropic and incompressible. Kuhn, Wall and Flory assumed that the deformation is affine.

In rubber elasticity most researchers are concerned with the case of a simple extension. This is defined by three principal extension ratios along three perpendicular axes. These extension ratios may be either greater than unity corresponding to a stretch, or less than unity, corresponding to a compression (Treloar, 2005). With the incompressible assumption, there is a relation between the three principal extension ratios:

$$\lambda_1\lambda_2\lambda_3 = 1 \tag{2.5.1}$$

where λ_1, λ_2 and λ_3 are the principle extension ratios.

1. James-Guth network

James-Guth (1943) network is also called phantom network. Its deformational free energy is:

$$A_d = \frac{NkT}{2}\left[\frac{\langle r_m\rangle^2}{\langle r^2\rangle_0}(\lambda_1^2+\lambda_2^2+\lambda_3^2)-3\right] \tag{2.5.2}$$

where A_d denotes the deformation free energy, and N is the number of crosslinked chains in a polymer network structure. λ_1, λ_2 and λ_3 are the principle extension ratios, and $\langle r_m\rangle^2$ is the mean chain displacement, which is proportional to the cube root of the unstretched volume at temperature T. k is the Boltzmann's constant. The quantity $\langle r^2\rangle_0$ is the mean-square unperturbed end-to-end displacement of the molecule. It is independent of material volume, V, and displacement, r.

2. Kuhn, Wall and Flory network

Others like Kuhn, Wall and Flory proposed for an affine network that the deformational free energy is:

$$A_d = \frac{NkT}{2}\left[\frac{\langle r^2\rangle_i}{\langle r^2\rangle_0}(\lambda_1^2+\lambda_2^2+\lambda_3^2)-3\right] - NkT\ln(\lambda_1\lambda_2\lambda_3) - \frac{3}{2}NkT\ln\frac{\langle r^2\rangle_i}{\langle r^2\rangle_0} \tag{2.5.3}$$

The quantity $\langle r^2\rangle_i$ is the mean-square displacement of the chains in the unstretched network and $\langle r^2\rangle_0$ has the same meaning as that in the James-Guth network.

Flory (1953) quickly modified the above equation by adding to it a free energy of crosslinking because he found it was valid only for a system of 'restrained' but unconnected chains and not for a genuine network. He calculated the deformed free energy of the network as

$$A_d = \frac{NkT}{2}\left[\frac{\langle r^2\rangle_i}{\langle r^2\rangle_0}(\lambda_1^2+\lambda_2^2+\lambda_3^2)-3\right] - \frac{1}{2}NkT\ln(\lambda_1\lambda_2\lambda_3) - \frac{3}{4}NkT\ln\frac{\langle r^2\rangle_i}{\langle r^2\rangle_0} \tag{2.5.4}$$

Smith (Allen et al., 1996) discussed the above deformation energy equations. Both equations (2.5.2) and (2.5.4) are proved to be wrong because they do not obey Edwards' principle that a network theory of elasticity must obey (Allen et al., 1996):

$$\lim_{\lambda_1 \to 1} \left(\frac{\partial A_d}{\partial \lambda_1}\right)_{\lambda_2, \lambda_3} = 0 \tag{2.5.5}$$

It is obvious that equation (2.5.2) fails this test; and equation (2.5.4) yields

$$\frac{\langle r^2 \rangle_i}{\langle r^2 \rangle_0} - \frac{1}{2} = 0 \tag{2.5.6}$$

This is wrong; it is generally close to one and not to one-half.

For equation (2.5.3), the Edwards condition yields:

$$\frac{\langle r^2 \rangle_i}{\langle r^2 \rangle_0} - 1 = 0 \tag{2.5.7}$$

and thus it is satisfied.

The force along the displacement *r* is defined as:

$$\boldsymbol{f} = \left(\frac{\partial A_d}{\partial r}\right)_{T,V} \tag{2.5.8}$$

From the James-Guth equation, the contractile force of uniaxial deformation along the *x* axis with $\lambda_1=\lambda$ is given by:

$$\boldsymbol{f} = NkT \frac{\langle r_m \rangle^2}{\langle r^2 \rangle_0} \left(\lambda - \frac{1}{\lambda^2}\right) \tag{2.5.9}$$

From Kuhn, Wall and Flory

$$\boldsymbol{f} = NkT \frac{\langle r^2 \rangle_i}{\langle r^2 \rangle_0} \left(\lambda - \frac{1}{\lambda^2}\right) \tag{2.5.10}$$

For a given crosslinking, the force predicted by Kuhn, Wall and Flory is about twice that of James-Guth. That means the contractile force of uniaxial deformation of affine model is about twice that of phantom model. However, the experimental force and deformation relation follows neither but is in the middle.

In the mid-1970s researchers realised that elastomeric behaviour varied from the affine network at low deformations to the phantom model at large deformations. Then in 1975 Ronca and Allegra (Allen et al., 1996) put forth a new version of elasticity theory:

$$A_d = \frac{NkT}{8}\left[\frac{\langle r^2 \rangle_i}{\langle r^2 \rangle_0} f^* - 2 + \frac{6}{\lambda_1^2 + \lambda_2^2 + \lambda_3^2} \ln(\lambda_1^2 + \lambda_2^2 + \lambda_3^2)\right](\lambda_1^2 + \lambda_2^2 + \lambda_3^2) - \frac{1}{2} NkT \ln(\lambda_1 \lambda_2 \lambda_3) \tag{2.5.11}$$

where f^* is the junction functionality.

Reconsider a uniaxial deformation of $\lambda_1=\lambda$:

$$A_d = \frac{NkT}{8}\left[\frac{\langle r^2\rangle_i}{\langle r^2\rangle_0} f^* - 2\right]\left(\lambda^2 + \frac{2}{\lambda}\right) + \frac{3}{4}NkT\ln\left(\lambda^2 + \frac{2}{\lambda}\right) \qquad (2.5.12)$$

which gives

$$\boldsymbol{f} = \frac{NkT}{4}\left[\frac{\langle r^2\rangle_i}{\langle r^2\rangle_0} f^* - 2 + \frac{6\lambda}{\lambda^3+2}\right]\left(\lambda - \frac{1}{\lambda^2}\right) \qquad (2.5.13)$$

At low deformation, $\lambda\approx1$, equation (2.5.13) reduces to the affine network of equation (2.5.9); at large deformation, $\lambda>>1$, the phantom network of James-Guth is obtained. The deformational free energy of Ronca and Allegra smoothly transforms from that of the affine network at low deformations to that of the phantom network at large deformations, and the force behaves in accord with observed behaviour.

Flory (1953) was the first to study the thermodynamics of rubber swelling. He described the Helmholtz free energy of a swelling rubber by:

$$A = \frac{1}{2}NkT\left[3\left(\frac{V}{V_0}\right)^{2/3} - 3 - \ln\left(\frac{V}{V_0}\right)\right] \qquad (2.5.14)$$

or in terms of the volume fraction of rubber in swollen network:

$$A = \frac{1}{2}NkT\left[3\nu_2^{-2/3} - 3 - \ln(\nu_2^{-1})\right] \qquad (2.5.15)$$

in which

V and V_0 are the volume of the swollen rubber and the volume of the rubber at preparation respectively.

ν_2 is the volume fraction of rubber in swollen network $\nu_2 = \frac{V_0}{V}$.

N is the number of crosslinked chains in a polymer network structure.

Treloar (1975) provided an alternative formulation for the Helmholtz free energy change of deformation for a swollen rubber:

$$A = \frac{1}{2}NkT\left[3\nu_2^{-2/3} - 3\right] \qquad (2.5.16)$$

Maurer and Prausnitz (1996) used the concept that the pressure difference between the gel and its surroundings is caused by the elastic properties of the network. This can be

written as:

$$P_{gel} - P_0 = \left(\frac{\partial A}{\partial V}\right)\Big|_T \tag{2.5.17}$$

in which P_{gel} is the pressure inside the gel and P_0 is the pressure outside the gel.

If the deformation free energy of equation (2.5.15) is used, an explicit description of pressure is given by:

$$P_{gel} - P_0 = \frac{1}{2} NkT \frac{\nu_2}{V_0}\left[2\nu_2^{-2/3} - 1\right] \tag{2.5.18}$$

- **Phenomenological theory of rubber elasticity**

In phenomenological theory, it is assumed that a strain-energy function has always existed. A material which is isotropic and incompressible can be classified as rubber-like material. Based on these assumptions, many researchers have attempted to construct a strain-energy function which is not only accurate enough to represent the mechanical response of rubber-like material but also simple enough to be amenable to mathematical analysis. Treloar (1944) carried out a series of experiments to study the mechanical properties of vulcanised natural rubber in simple tension, pure shear and uniform equibiaxial tension. Consequently Treloar's data have been used as the basis for comparison with theories.

The strain-energy function denoted by Φ and measured as energy per unit volume, depends only on the final states of strain through the principal extension ratios λ_1, λ_2 and λ_3. All strains are measured from the chosen ground state. The strain-energy function is usually written as a function of two independent invariants. Those commonly used are defined by:

$$I_1 = \lambda_1^2 + \lambda_2^2 + \lambda_3^2 \tag{2.5.19}$$

$$I_2 = \lambda_2^2\lambda_3^2 + \lambda_3^2\lambda_1^2 + \lambda_1^2\lambda_2^2 = \lambda_1^{-2} + \lambda_2^{-2} + \lambda_3^{-2} \tag{2.5.20}$$

From the strain-energy function the principal Cauchy stresses σ_1, σ_2 and σ_3 are obtained:

$$\sigma_i = \lambda_i \frac{\partial \Phi}{\partial \lambda_i} - p \quad i = 1,2,3 \tag{2.5.21}$$

where p is an arbitrary hydrostatic pressure introduced because of the incompressibility constraint.

Therefore the question is to construct an appropriate equation to describe the strain-energy relation. During the past years, different forms of strain-energy functions were introduced. Among them, Mooney, Rivlin, neo-Hookean, and more recently Ogden are the most popular ones.

1. Mooney's formulation

The first phenomenological theory of large elastic deformations was developed by Mooney (1940) and the strain-energy formulation is:

$$\begin{aligned} \Phi &= C_1(\lambda_1^2 + \lambda_2^2 + \lambda_3^2 - 3) + C_2(\lambda_1^{-2} + \lambda_2^{-2} + \lambda_3^{-2} - 3) \\ &= C_1(I_1 - 3) + C_2(I_2 - 3) \end{aligned} \tag{2.5.22}$$

in which C_1, C_2 are two elastic constants.

2. Rivlin's formulation

Rivlin (1948) suggested that the strain-energy function may be expressed as an infinite series in terms of I_1 and I_2:

$$\Phi = \sum_{m,n=0}^{\infty} C_{mn}(I_1 - 3)^m (I_2 - 3)^n \quad C_{00} = 0 \tag{2.5.23}$$

where C_{mn}s are elastic constants.

From mathematical simplicity one might reasonably expect that the first two terms would predominate, i.e.

$$\Phi = C_{10}(I_1 - 3) + C_{01}(I_2 - 3) \tag{2.5.24}$$

Compared with equation (2.5.24) and (2.5.22), it is clear that the Mooney equation is a special case of Rivilin's equation.

3. Neo-Hookean's formulation

Treloar (1943) formulated the neo-Hookean form of the strain energy function:

$$\Phi = \frac{1}{2} G_{el}(I_1 - 3) \tag{2.5.25}$$

in which G_{el} is the shear modulus in the unstrained state in Pa.

Also, this is a special case of Rivlin's formulation equivalent to the first term of equation (2.5.24).

4. Ogden's formulation

More recently, Ogden (1972) proposed an alternative strain-energy function:

$$\Phi = \sum_{r=1}^{n} \frac{G_{elr}}{\alpha_r} \left(\lambda_1^{\alpha_r} + \lambda_2^{\alpha_r} + \lambda_3^{\alpha_r} - 3\right) \tag{2.5.26}$$

In the Ogden formulation, the indices α_r need not be integers.

If n=1, α_1=2 equation (2.5.26) becomes:

$$\Phi = \frac{1}{2} G_{el}(I_1 - 3) \tag{2.5.27}$$

It is the neo-Hookean's model.

If n=2, α_1=2 and α_2=-2:

$$\Phi = \frac{G_{el1}}{2}(I_1 - 3) + \frac{G_{el2}}{-2}(I_2 - 3) \tag{2.5.28}$$

which gives the Mooney model if $G_{el1} = 2C_1$ and $G_{el2} = -2C_2$.

Using the stress-strain data reported by Treloar (1944a), Ogden obtained a material model with the coefficients

$$\alpha_1 = 1.3 \;\; \alpha_2 = 5.0 \;\; \alpha_3 = -2.0 \tag{2.5.29}$$

and

$$G_{el1} = 0.618 \;\; G_{el2} = 0.00118 \;\; G_{el3} = -0.00981 \;\; \text{MPa} \tag{2.5.30}$$

It was found that for simple extension and pure shear a two-term formula was effective, but for the representation of all three types of strain three terms were required. The agreement with the Treloar's data was very satisfactory.

Ogden (1972) considered the inflation of a circular membrane into a spherical shape by using a phenomenological description. He suggested that equibiaxial tension can

be used to effectively describe the stress field in the region of the pole of a spheroid provided the skin thickness is very much less than the radius of curvature at the pole.

In equibiaxial tension, let h be the thickness of undeformed skin and $\boldsymbol{T}_{tension}$ be the surface tension acting on a section of unit length of the sheet. In the deformed state

$$\frac{\boldsymbol{T}_{tension}}{h} = G_{elr}\left[\lambda^{\alpha_r - 2} - \lambda^{-(2+2\alpha_r)}\right] \tag{2.5.31}$$

The pressure of inflation P can approximately be related to the surface tension $\boldsymbol{T}_{tension}$ by:

$$P = 2\frac{\boldsymbol{T}_{tension}}{r} \tag{2.5.32}$$

In a thin rubber balloon, the undeformed thickness of the skin is h and the incompressibility assumption implies that the actual volume, V, of the rubber material remains constant during inflation. Let r be the radius when the pressure is P. When λ is the extension ratio in the surface of the balloon the thickness is $h\lambda^{-2}$. Therefore in the strained state the volume of the balloon membrane is approximately:

$$V = 4\pi r^2 h\lambda^{-2} \tag{2.5.33}$$

Thus

$$r_0 = \frac{r}{\lambda} = \left(\frac{V}{4\pi h}\right)^{\frac{1}{2}} \tag{2.5.34}$$

where r_0 is the radius of the balloon in its initial state.

The general form of the pressure-extension ratio relation for the inflation of a spherical membrane is (Hart-Smith, 1966):

$$P = \frac{4h}{r_0}\frac{\partial \Phi}{\partial I_1}\left(\frac{1}{\lambda} - \frac{1}{\lambda^7}\right)\left(1 + \lambda^2\frac{\frac{\partial \Phi}{\partial I_2}}{\frac{\partial \Phi}{\partial I_1}}\right) \tag{2.5.35}$$

And by equation (2.5.31), (2.5.32) and (2.5.34) the Ogden's pressure in the balloon undergoing inflation gives:

$$\frac{Pr_0}{2h} = G_{elr}\left[\lambda^{\alpha_r - 3} - \lambda^{-(2\alpha_r+3)}\right] \tag{2.5.36}$$

With the particular values of the α_r and G_{elr} given by equation (2.5.29) and (2.5.30) which are related specifically to the rubber of Treloar's experiments, a good

prediction of pressure inside the balloon can be obtained.

Another form of inflation pressure in terms of Mooney formulation of strain energy was given by Green and Adkins (1960):

$$\frac{Pr_0}{8h} = (C_1 + \lambda^2 C_2)\frac{1}{\lambda}\left(1 - \frac{1}{\lambda^6}\right) \tag{2.5.37}$$

- **Compare free energy function with strain energy function**

In a reversible isothermal process the change in Helmholtz free energy is equal to the work done on the system by the applied force (Treloar, 2005).

$$dA = dW \tag{2.5.38}$$

W represents the work of deformation. The work of deformation per unit volume also called the elastically stored free energy per unit volume of the rubber can be referred to as the strain energy function by Φ in J/m^3.

The Treloar and Flory free energy function of incompressible rubber can be written as:

$$A = \frac{NkT}{2}[(\lambda_1^2 + \lambda_2^2 + \lambda_3^2) - 3] \tag{2.5.39}$$

Or it can be written in terms of free energy per unit volume as:

$$A_V = \frac{N_V kT}{2}[(\lambda_1^2 + \lambda_2^2 + \lambda_3^2) - 3] = \frac{N_V kT}{2}[I_1 - 3] \tag{2.5.40}$$

where A_V is the free energy function per unit volume in J/m^3 and consequently N_V is the number of crosslinks per unit volume in 1/m^3.

Compared with equation (2.5.22), it is clear that the first term in equation (2.5.22) corresponds identically to the form derived from network theory with

$$2C_1 = N_V kT \tag{2.5.41}$$

The network theory is thus the particular case of the Mooney theory with C_2=0.

The right hand side of the above equation is actually the shear modulus (Treloar, 2005):

$$G_{el} = N_V kT \tag{2.5.42}$$

This gives:

$$C_1 = \frac{N_V kT}{2} = \frac{1}{2} G_{el} \tag{2.5.43}$$

It is consistent with equation (2.5.25).

N_V can be written in terms of Avogadro's number (N_A) and molar density (c_ρ):

$$N_V = c_\rho N_A \tag{2.5.44}$$

Then

$$G_{el} = c_\rho N_A kT \tag{2.5.45}$$

which is:

$$G_{el} = c_\rho RT \tag{2.5.46}$$

If it is expressed in terms of the number average chain molecular weight M_c then the relationship is:

$$G_{el} = c_\rho RT = \frac{\rho RT}{M_c} \tag{2.5.47}$$

Here ρ is the density of the rubber (kg/m^3) and R is the gas constant (8.314 JK^{-1}mol^{-1}). Therefore, these two approaches to the study of rubber elasticity are actually related to each other in some way via comparison. By adjusting the elastic constants in strain energy functions of phenomenological theory, deformation free energy of network theory can be obtained. Pressure in a swollen membrane can also be calculated from those two theories. The following is the list of the pressure equations calculated by using different energy functions:

$$P_{Kuhn-Wall-Flory} = N_V kT \nu_2 \left[\nu_2^{-2/3} - 1\right] \tag{2.5.48}$$

$$P_{Treloar} = N_V kT \nu_2^{1/3} \tag{2.5.49}$$

$$P_{Ogden} = G_{elr} \left[\nu_2^{-\frac{1}{3}(\alpha_r - 3)} - \nu_2^{\frac{1}{3}(2\alpha_r + 3)}\right] \tag{2.5.50}$$

$$P_{Mooney} = C_1\left(\nu_2^{\frac{1}{3}} - \nu_2^{\frac{7}{3}}\right)\left(1 + \frac{C_2}{C_1}\nu_2^{-\frac{2}{3}}\right) \tag{2.5.51}$$

Figure 2.12 shows the comparison between different pressure models described by the above equations.

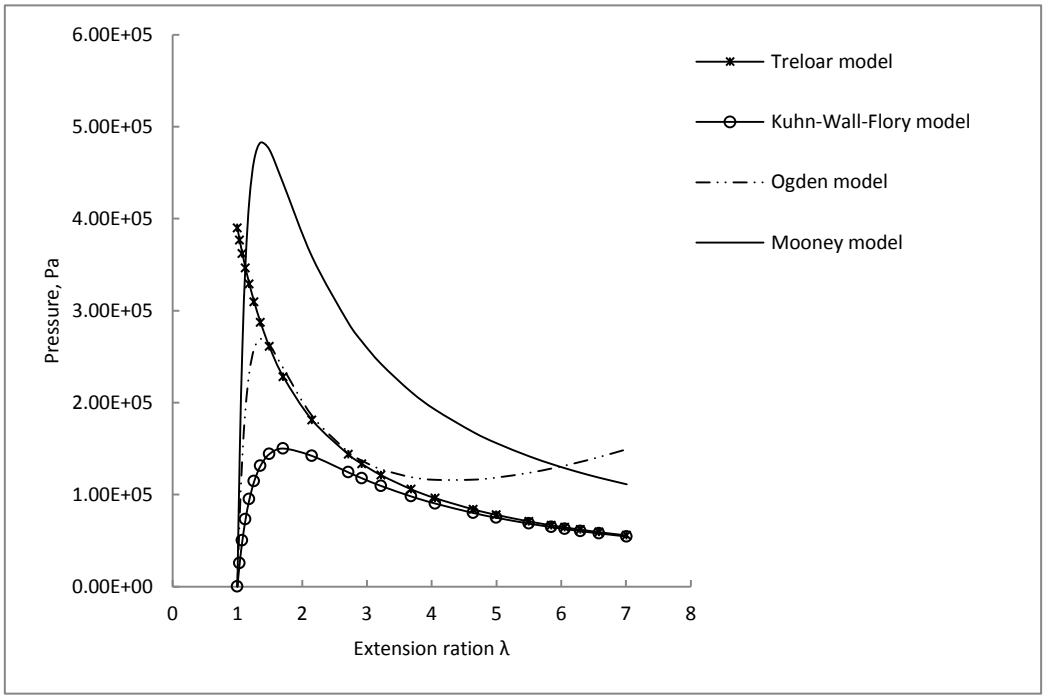

Figure 2.12 Different pressure models of a swollen rubber membrane with parameters: N_vkT=3.9×10^{5}Pa; C_1=1.95×10^{5}Pa, C_2=0; G_{elr} and α_r given by equations (2.5.29) and (2.5.30)

It is found that all the models give zero pressure at initial state except Treloar which gives its highest value at initial state. Kuhn-Wall-Flory and Mooney models show that the pressure quickly increases to a peek and then starts to decrease. The Ogden model is the only one that shows a slowly increase following the pressure decrease. Hart-Smith (1966) measured the pressure and volume of a balloon during inflation and found that after dropping to lower values the inflating pressure started to rise at very large deformations (Figure 2.13).

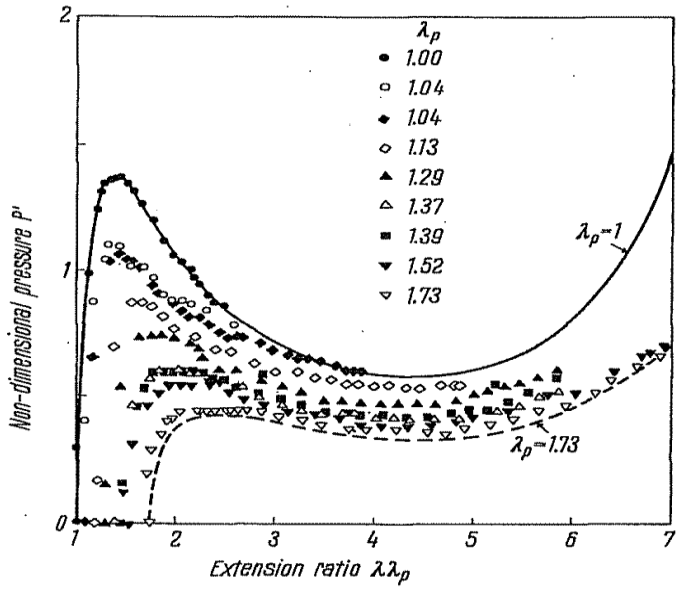

Figure 2.13 Experiment results for the repeated inflation of a spherical balloon (Hart-Smith, 1966)

Compared with Figure 2.12 and Figure 2.13, it can be seen that although the Ogden model shows a pressure increase after the pressure decrease this increase is much smaller than the experiment findings. For instance, at λ=7 the pressure of the balloon is higher than the peak value at λ=1.5 as shown in Figure 2.13. However, the Ogden pressure is only about the half of its peak value as shown in Figure 2.12.

2.5.2 Mechanical structure equations

Another way to describe swelling mechanics is to use the classic linear elasticity theory, the Hooke's law. Tanaka and Fillmore (1979) used the linear elasticity theory to model the swelling of polyacrylamide spheres in water and De and Aluru (2004) used it to model the swelling of pH-sensitive hydrogel.

It is assumed that the polyelectrolyte gel material obeys linear elasticity relationships and the elasticity of the gel is uniform and time invariant. The gravitational and frictional forces experienced by the gel are assumed to be negligible. The mechanical module takes as its input a force vector and returns a nodal displacement vector as output. Hence it is necessary to derive a governing equation to describe the motion of

an elastic body under the influence of an external force.

From the fundamental definitions of elasticity, the engineering strain is defined in terms of displacements by the equation:

$$\varepsilon_i = \frac{\Delta L}{L_0} \tag{2.5.52}$$

where the change in length ΔL is taken in the i^{th} direction and L_0 is the initial longitudinal length of the element.

From equation (2.5.52) for a given displacement of u_x and u_y in the x- and y-directions, the two-dimensional strain vector can be written as:

$$\begin{bmatrix} \varepsilon_x \\ \varepsilon_y \\ \varepsilon_{xy} \end{bmatrix} = \begin{bmatrix} \dfrac{\partial u_x}{\partial x} \\ \dfrac{\partial u_y}{\partial y} \\ \dfrac{\partial u_x}{\partial y} + \dfrac{\partial u_y}{\partial x} \end{bmatrix} \tag{2.5.53}$$

in which ε_x and ε_y are the strains in the x and y directions and ε_{xy} is the engineering shear strain.

For the simplification of plane stress in an isotropic material, where the stresses in the z direction are considered to be negligible, $\sigma_{zx} = \sigma_{zy} = \sigma_{zz} = 0$, the strains in equation (2.5.53) are related to their 2-dimensional stresses via Hooke's law:

$$\sigma_{xx} = \frac{E}{1-\nu^2}\left[\varepsilon_x + \nu\varepsilon_y\right] \tag{2.5.54}$$

$$\sigma_{yy} = \frac{E}{1-\nu^2}\left[\varepsilon_y + \nu\varepsilon_x\right] \tag{2.5.55}$$

$$\sigma_{xy} = \sigma_{yx} = G\varepsilon_{xy} \tag{2.5.56}$$

The shear modulus G is related to the Young's modulus E and the Poisson's ratio v via:

$$G = \frac{E}{2(1+\nu)} \tag{2.5.57}$$

For the case of plane strain, where the strains in the z direction are considered to be

negligible, $\varepsilon_{zz} = \varepsilon_{yz} = \varepsilon_{xz} = 0$, the stress-strain relationships are:

$$\sigma_{xx} = \frac{E}{(1+\nu)(1-2\nu)}\left[(1-\nu)\varepsilon_x + \nu\varepsilon_y\right] \tag{2.5.58}$$

$$\sigma_{yy} = \frac{E}{(1+\nu)(1-2\nu)}\left[(1-\nu)\varepsilon_y + \nu\varepsilon_x\right] \tag{2.5.59}$$

$$\sigma_{xy} = \sigma_{yx} = G\varepsilon_{xy} \tag{2.5.60}$$

The equation of the gel network motion is given by:

$$\rho\frac{\partial^2\mathbf{u}}{\partial t^2} + f\frac{\partial\mathbf{u}}{\partial t} = \nabla\cdot\boldsymbol{\sigma} + \rho\mathbf{b} \tag{2.5.61}$$

where ρ is the effective density of the gel, **u** is the displacement vector of the network, f is the friction coefficient between the network and the solvent, and **b** is body forces. The stress tensor **σ** of a 2-dimensional system can be plane stress or plane strain described by equation (2.5.54) to (2.5.56) or equation (2.5.58) to (2.5.60) respectively.

There are no body forces and the friction is assumed to be negligible, thus equation (2.5.61) becomes:

$$\rho\frac{\partial^2\mathbf{u}}{\partial t^2} = \nabla\cdot\boldsymbol{\sigma} \tag{2.5.62}$$

If the inertial terms are not dominant, then the equation of gel motion becomes:

$$\nabla\cdot\boldsymbol{\sigma} = 0 \tag{2.5.63}$$

Considering the case of thermal expansion, the thermally induced strains can be superimposed to those induced by stresses. In terms of strains, the equations of plane stress are:

$$\sigma_{xx} = \frac{E}{1-\nu^2}\left[\varepsilon_x + \nu\varepsilon_y\right] - \frac{E\alpha_T T}{1-\nu} \tag{2.5.64}$$

$$\sigma_{yy} = \frac{E}{1-\nu^2}\left[\varepsilon_y + \nu\varepsilon_x\right] - \frac{E\alpha_T T}{1-\nu} \tag{2.5.65}$$

$$\sigma_{xy} = \sigma_{yx} = G\varepsilon_{xy} \tag{2.5.66}$$

where α_T is the thermal expansion parameter.

By analogy, the stresses in the motion equation include two parts. One is the stress of the polymer network described by Hooke's law and the other is the stress transmitted by the solvent pressure *P*.

$$\sigma_{ij}^{tot} = \sigma_{ij} - P\delta_{ij} \tag{2.5.67}$$

This idea was used by De and Aluru (2004). They used the osmotic pressure to describe the pressure difference between the gel and outside solution and for a plane strain problem, the stresses are given by:

$$\sigma_{xx} = \frac{E}{(1+\nu)(1-2\nu)}\left[(1-\nu)\varepsilon_x + \nu\varepsilon_y\right] - P_{osmotic} \tag{2.5.68}$$

$$\sigma_{yy} = \frac{E}{(1+\nu)(1-2\nu)}\left[(1-\nu)\varepsilon_y + \nu\varepsilon_x\right] - P_{osmotic} \tag{2.5.69}$$

And

$$\sigma_{xy} = \sigma_{yx} = G\varepsilon_{xy} \tag{2.5.70}$$

However it is questionable that the osmotic pressure can be used in stress equations since the osmotic pressure only describes the equilibrium state. It is also questionable that the shear modulus here is constant as it is not the case in rubber swelling. If *G'* and G_0 are the respective moduli in the swollen and unswollen states, their relation is (Treloar, 2005):

$$G' = G_0 v_2^{\frac{1}{3}} \tag{2.5.71}$$

2.5.3 Swelling mechanics summary

From the discussions in Section 2.5.1 and 2.5.2, it can be summarised that Hooke's law of elasticity is an approximation that the amount by which a material body is deformed (the strain) is linearly related to the force causing the deformation (the stress). The moduli are material independent and keep constant during swelling. Materials for which the Hooke's law holds are known as linear elastic or "Hookean" materials. However, rubber-like materials are nonlinear. The modulus of a rubber is material dependent shown by equation (2.5.47). Equation (2.5.71) also suggests that the modulus of a swollen rubber decreases as the rubber swelling ratio increases.

Therefore, mechanical structure equations cannot be used in this thesis.

The only choice left for swelling mechanics is to use the rubber elasticity theory to describe the pressure inside a polyelectrolyte gel. This choice is not very satisfactory. In Section 2.5.1, several pressure models were presented. When compared those models with experimental results of the inflation of a spherical rubber balloon, divergence was found in regions with large swelling ratios as suggested in Figure 2.12 and 2.13. However, the rubber elasticity theory is still chosen to describe swelling mechanics since there is no evidence that the pressure models can be improved by rubber elasticity theory. To improve the pressure models, a significant amount of new research needs to be carried out.

2.6 Protein charge

Proteins are natural polymer molecules consisting of amino acid units. The number of amino acids in proteins may range differently. Each amino acid has at least one basic amine group $–NH_2$ and one acidic functional group –COOH shown in Figure 2.14.

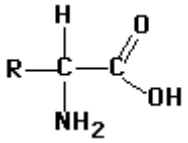

Figure 2.14 The simplest amino acid

where *R* stands for a variety of side chains.

As mentioned before there is an internal transfer of a hydrogen ion from the –COOH group to the $–NH_2$ group to leave an ion with both a negative charge and a positive charge. This is called a zwitterion as shown in Figure 2.15.

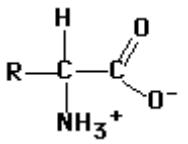

Figure 2.15 A zwitterion

Normally the amino acid produces a nearly neutral solution. The different properties of amino acids result from the structures of different *R* groups. The *R* group is often referred to as the amino acid side chain. If there is an extra acid on the side chain, there is a net acid producing effect. If the side chain contains an extra amine group, then the amino acid produces a basic solution. In β-lactoglobulin proteins, acidic amino acids include aspartic (Asp) and glutamic (Glu) and basic side chains include lysine (Lys), arginine (Arg) and histidine (His).

Most of the following section is based on Fessenden and Fessenden (1986) and Segel (1968).

When an amino acid dissolves in water, the zwitterion interacts with water molecules acting as both an acid and a base. As an acid:

$$NH_3^+RCHCOO^- + H_2O \leftrightarrow NH_2RCHCOO^- + H_3O^+ \qquad (2.6.1)$$

The $-NH_3^+$ group is a weak acid and donates a hydrogen ion to a water molecule. Because it is only a weak acid, the position of equilibrium will lie to the left.

As a base:

$$NH_3^+RCHCOO^- + H_2O \leftrightarrow NH_3^+RCHCOOH + OH^- \qquad (2.6.2)$$

The $-COO^-$ group is a weak base and takes a hydrogen ion from a water molecule. Again the equilibrium lies to the left.

Therefore, in an aqueous solution of an amino acid the above two acid-base dissociation equilibria take place simultaneously. All the species involved in these reactions appear to be electrically charged, except for the neutral zwitterions ($NH_3^+RCHCOO^-$). Each of the above equilibria may be characterised by a thermodynamic equilibrium constant (K_a).

From a standard point of view, for a simple acid/base system we have an equilibrium as:

$$\text{un-ionised acid} \leftrightarrow \text{anion} + H^+ \tag{2.6.3}$$

The pH of a solution is defined as:

$$pH = -log_{10}[H^+] \tag{2.6.4}$$

The equilibrium constant, $K_{a,}$ is defined for acids as:

$$K_a = \frac{[H^+][\text{anion}]}{[\text{un-ionised acid}]} \tag{2.6.5}$$

The pK_a is then obtained:

$$pK_a = -log_{10}(K_a) \tag{2.6.6}$$

Equation (2.6.6) is combined with equation (2.7.4) and (2.7.5) to give:

$$pH = pK_a + log_{10}\frac{[\text{anion}]}{[\text{un-ionised acid}]} \tag{2.6.7}$$

which is also called Henderson-Hasselbach equation.

Similarly for bases we can define pK_b as:

$$K_b = \frac{[OH^-][\text{cation}]}{[\text{un-ionised base}]} \tag{2.6.8}$$

And hence

$$pK_b = -log_{10}(K_b) \tag{2.6.9}$$

Bringing it to equation (2.6.8):

$$pK_b = -(log_{10}[OH^-] + log_{10}[\text{cation}] - log_{10}[\text{un-ionised base}]) \tag{2.6.10}$$

Also we have water dissociation equilibrium:

$$K_w = [H^+][OH^-] \tag{2.6.11}$$

At 25 °C, pK_w is 13.9965 (often 14 is used).

$$log_{10}[H^+] + log_{10}[OH^-] = -14 \tag{2.6.12}$$

Coming back to equation (2.6.10) we have:

$$pK_b = 14 - pH + log_{10}\frac{[\text{cation}]}{[\text{un-ionised base}]} \tag{2.6.13}$$

So

$$-K_b = \frac{[\text{cation}]}{[\text{un-ionised base}]}10^{14-pH} \tag{2.6.14}$$

However, this standard acid/base view is limited when we come to consider amino acids and proteins. A more general view of the equilibrium can be:

$$\text{protonated form} \leftrightarrow \text{unprotonated form} + H^+ \tag{2.6.15}$$

And

$$\text{proton donor} \leftrightarrow \text{proton acceptor} + H^+ \tag{2.6.16}$$

For example:

$$HCl + H_2O \leftrightarrow Cl^- + H_3O^+ \tag{2.6.17}$$

But the presence of water is normally ignored because of the H_2O, OH^- and H^+ equilibrium, so the equivalent form is often written as:

$$HCl \leftrightarrow Cl^- + H^+ \tag{2.6.18}$$

Also we can view the reverse dissociation of a base a giving a proton:

$$Na^+ + H_2O \leftrightarrow NaOH + H^+ \tag{2.6.19}$$

which we might also write as

$$NaOH \leftrightarrow Na^+ + OH^- \tag{2.6.20}$$

The NaOH equilibrium can be written:

$$K_a = \frac{[NaOH][H^+]}{[Na^+]} \tag{2.6.21}$$

Or

$$K_b = \frac{[Na^+][OH^-]}{[NaOH]} \tag{2.6.22}$$

If the above two are multiplied together:

$$K_a K_b = [H^+][OH^-] = K_w \tag{2.6.23}$$

The amino group and the carboxyl group of the amino acid have pKa's of about 9.6 and 2.3 respectively. Thus, the amino acid can exist in three general forms. At low pH the amino and carboxyl groups will be protonated and the molecules will be in the acid form in Figure 2.16.

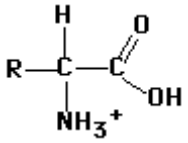

Figure 2.16 Acid form of an amino acid

As the pH increases towards neutrality, the amino acids become zwitterions having both negative and positive charges (Figure 2.15). As the pH increases further, the molecules become basic (Figure 2.17):

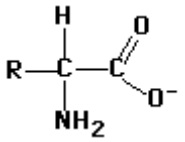

Figure 2.17 Basic form of an amino acid

Proteins are composed of many amino acids. In the context of amino acids (and subsequently proteins) it is best to consider the two protonated forms. The pH dependent equilibrium (using alanine as an example) can be written as:

$$\begin{aligned} NH_3^+CHCH_3COOH &\leftrightarrow NH_3^+CHCH_3COO^- + H^+ \\ &\leftrightarrow NH_2CHCH_3COO^- + 2H^+ \end{aligned} \tag{2.6.24}$$

There are two equilibria and hence two pK_a constants (2.35 and 9.69).

$$K_{a1} = \frac{[H^+][NH_3^+CHCH_3COO^-]}{[NH_3^+CHCH_3COOH]} \tag{2.6.25}$$

with pK_{a1} = 2.35.

and

$$K_{a2} = \frac{[H^+][NH_2CHCH_3COO^-]}{[NH_3^+CHCH_3COO^-]} \tag{2.6.26}$$

with pK_{a2} = 9.69.

From (2.6.25) we have:

$$pH = pK_{a1} + log_{10}\frac{[NH_3^+CHCH_3COO^-]}{[NH_3^+CHCH_3COOH]} \tag{2.6.27}$$

Similarly from equation (2.6.27):

$$pH = pK_{a2} + log_{10}\frac{[NH_2CHCH_3COO^-]}{[NH_3^+CHCH_3COO^-]} \tag{2.6.28}$$

The total concentration can be calculated by:

$$\begin{aligned} [NH_3^+CHCH_3COOH] + [NH_3^+CHCH_3COO^-] \\ + [NH_2CHCH_3COO^-] = total\ concentration \end{aligned} \tag{2.6.29}$$

which will be abbreviated as $c_1 + c_2 + c_3 = c_{total}$

For a given pH, three concentrations can be calculated by using equation (2.6.27), (2.6.28) and (2.6.29). By using equation (2.6.27):

$$c_2 = 10^{(pH - pK_{a1})}c_1 \tag{2.6.30}$$

and from equation (2.6.28):

$$c_3 = 10^{(pH-pK_{a2})}c_2 \tag{2.6.31}$$

So

$$c_3 = 10^{(pH-pK_{a2})}10^{(pH-pK_{a1})}c_1 \tag{2.6.32}$$

Thus c_1 can be found from:

$$c_1\left(1 + 10^{(pH-pK_{a1})} + 10^{(pH-pK_{a2})}10^{(pH-pK_{a1})}\right) = c_{total} \tag{2.6.33}$$

and sequentially the other concentrations can be found.

Let us now consider pH titration from 0 to 14. When the amino acid is dissolved in water, a simple solution contains three forms. If the pH is increased by adding hydroxide ions, the hydrogen ion is removed from the $–NH_3^+$ group.

$$NH_3^+CHCH_3COO^- + OH^- \rightarrow NH_2CHCH_3COO^- + H_2O \tag{2.6.34}$$

The amino acid now exists as a negative ion.

If the pH is decreased by adding an acid to the amino acid, the $–COO^-$ part of the zwitterions picks up a hydrogen ion.

$$NH_3^+CHCH_3COO^- + H^+ \rightarrow NH_3^+CHCH_3COOH \tag{2.6.35}$$

Suppose we start with the ions we have just produced under acidic conditions and slowly add alkali to it. That ion contains two acidic hydrogens: the one in the –COOH group and the one in the $–NH_3^+$ group. The more acidic of these is the one in the –COOH, and so that is removed first and we get back to the zwitterion.

$$NH_3^+CHCH_3COOH + OH^- \rightarrow NH_3^+CHCH_3COO^- + H_2O \tag{2.6.36}$$

So when we have added just the right amount of alkali, the amino acid no longer has a net positive or negative charge. If we go on adding hydroxide ions, we will get the reaction in which a hydrogen ion is removed from the $–NH_3^+$ group.

$$NH_3^+CHCH_3COO^- + OH^- \rightarrow NH_2CHCH_3COO^- + H_2O \tag{2.6.37}$$

The amount of H^+ produced by the shift in equilibrium from 100% c_1 is $c_2 + 2c_3$ and hence the amount of $OH^–$ is the amount required to neutralise the H^+ produced. The titration with $OH^–$ is shown by Figure 2.18.

At this point the equations from Segel (1968) need to be applied to the protein system of interest in this research. The remainder of this section is the application of Segel's calculation methods to the current research.

Each protein molecule has in its amino acid sequence many different residues with potential hydrogen ion equilibria. At any given pH, these residues will be in various protonation states depending on their individual hydrogen ion dissociation constant *i.e.* pK_as. Thus the protein will have a net charge which varies with pH. With knowledge of all the individual pK_as of all the possible hydrogen ion equilibria found in a protein, it is possible to calculate the absolute net charge of a protein as a function of pH.

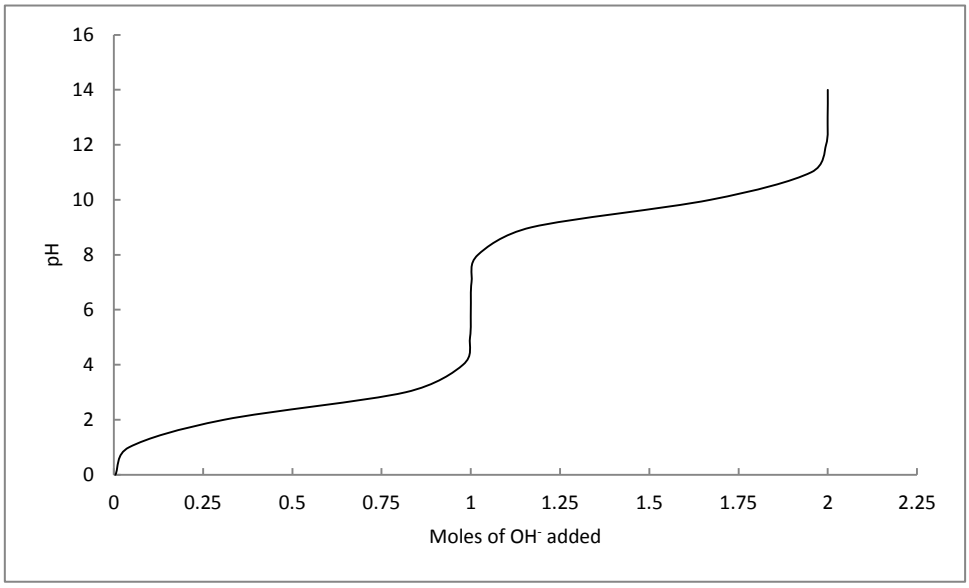

Figure 2.18 The titration of an amino acid

In every protein molecule there are N_{ki} acid/base equilibria of type *i*, each described by a hydrogen ion dissociation constant K_{ai} such that:

$$HA_i^{+/0} \overset{K_{ai}}{\leftrightarrow} H^+ + A_i^{0/-} \tag{2.6.38}$$

The superscript of +/0 indicates that the protein molecule can be positive or neutral and 0/- indicates that the protein molecule can be neutral or negative.

With

$$K_{ai} = \frac{[H^+]\left[A^{0/-}\right]_i}{[HA^{+/0}]_i} \tag{2.6.39}$$

These equilibria occur on the side chains of acidic or basic residues and at the amino

and carboxyl termini of the amino acid chain in the protein. Taking the logarithm of equation (2.6.39) yields the Henderson-Hasselbach equation already mentioned before:

$$pH - pK_{ai} = log_{10} \frac{\left[A^{0/-}\right]_i}{\left[HA^{+/0}\right]_i} \tag{2.6.40}$$

A mass balance on titratable sites of type *i* dictates that the total concentration of sites must equal the sum of the concentrations of unprotonated and protonated sites of type *i*:

$$[S]_i = \left[A^{0/-}\right]_i + \left[HA^{+/0}\right]_i \tag{2.6.41}$$

Here

$$[S]_i = N_{ki} \cdot [P] \tag{2.6.42}$$

where $[P]$ is the total protein concentration denoted by c_{pt} in calculation.

Combining equations (2.6.40) to (2.6.42) yields expressions for the molar concentrations of protonated and unprotonated sites of type *i* in terms of the quantities pH, pK_{ai} and n_i:

$$\left[A^{0/-}\right]_i = [P] \frac{N_{k,i} 10^{(pH - pK_{ai})}}{10^{(pH - pK_{ai})} + 1} \tag{2.6.43}$$

and

$$\left[HA^{+/0}\right]_i = [P] \frac{N_{k,i} 10^{(pK_{ai} - pH)}}{10^{(pK_{ai} - pH)} + 1} \tag{2.6.44}$$

The parameters ($N_{k,i}$ and pK_{ai}) of amino acids found experimentally in β-lactoglobulin protein are given by Table 2.3 (Mercadé-Prieto et al., 2007b).

Table 2.3 Parameters for β-lactoglobulin amino acid groups (Mercadé-Prieto et al., 2007b)

	Amino acid						
	Asp, Glu and α-COOH	His	Cys and α- NH_2	Tyr	Lys	Arg	Ser and Thr
N_k	28	2	2	4	15	3	15
pK_a	4	6	8.5	10.4	10.95	12.52	13.22
charge	-1	+1	-1	-1	+1	+1	-1

The net charge of the protein is the summation of negative charges and positive charges from all of the side groups:

$$[protein\ net\ charge] = c_{pt} \sum N_{k,i} z_i \frac{10^{z_i(pK_{ai}-pH)}}{10^{z_i(pK_{ai}-pH)}+1} \qquad (2.6.45)$$

with z_i the charge of different protein side group +1 or -1.

The concentration of undissociated hydrogen in β-lactoglobulin protein is the summation of unprotonated sites calculated by equation (2.6.44):

$$[\text{protein bound } H] = c_{pt} \sum N_{ki} \frac{10^{(pK_{ai}-pH)}}{10^{(pK_{ai}-pH)}+1} \qquad (2.6.46)$$

Figure 2.19 shows the concentration of *H* bounded by protein as a function of pH.

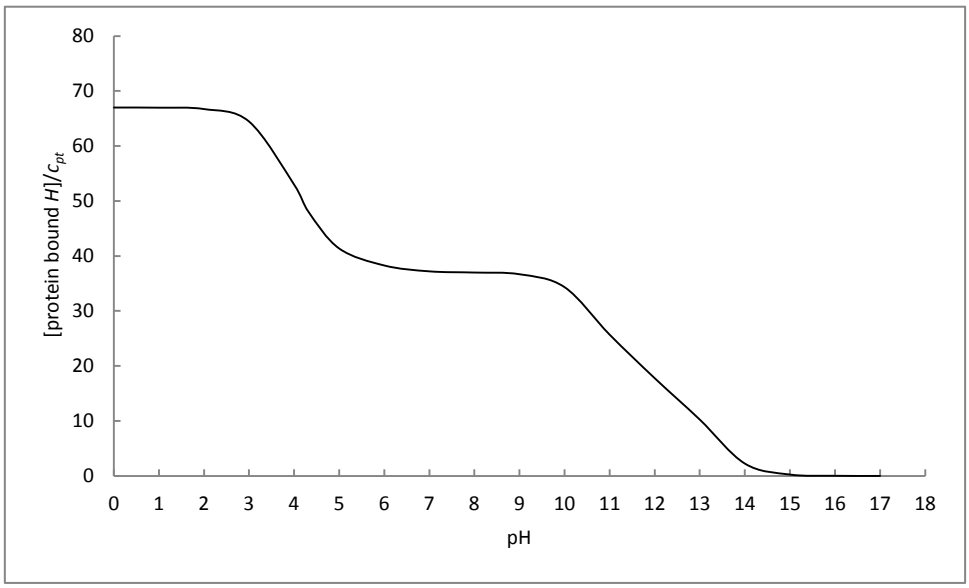

Figure 2.19 Protein bound H in β-lactoglobulin protein as a function of pH calculated by equation (2.6.46)

The total charge in protein is shown in Figure 2.20. It can be seen that at low pH (<4.3 approximately), the protein gives a overall positive charge influence and that means it can be treated as $–NH_3^+$ (proton donor), as the pH increases to about 4.4, often called pI, it has no charge behaving like a zwitterion, and as the pH continuously increases, the protein has a negative charge like $–COO^-$ (proton acceptor).

The approach outlined here assumes that there are no interactions between different side groups or with other components in solution. A more complex calculation procedure is outlined by Bas et al. (2008).

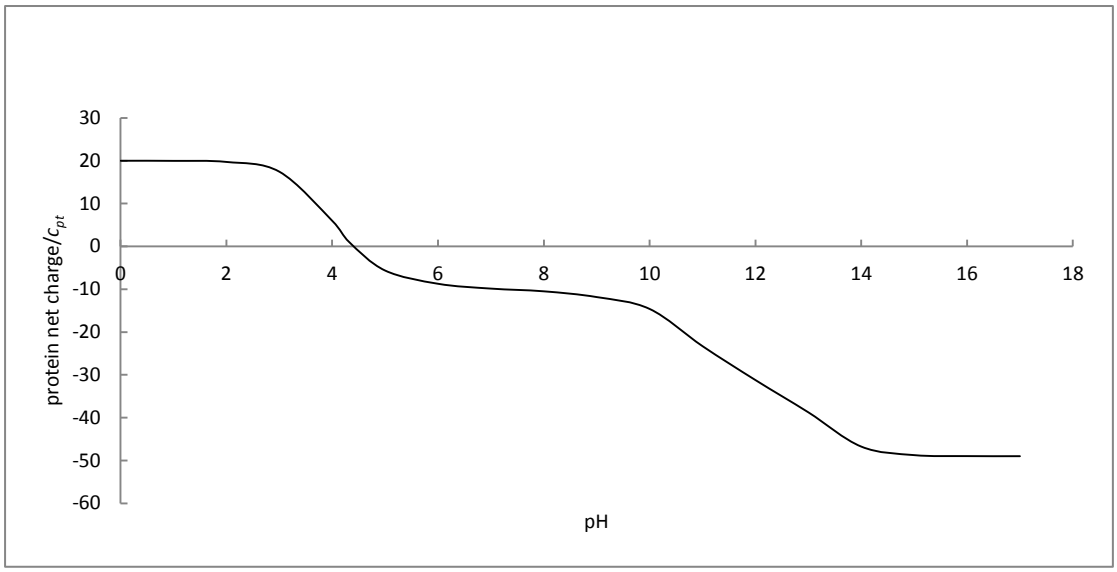

Figure 2.20 The protein net charge

2.7 Material balance

Balance equations for material (on a mole or mass basis) provide the foundation for much of the physical-based modelling in transport phenomena. For example, in the protein gel swelling system, ions transport into the gel region and may react with ions dissociated from the protein, and thus water may be produced. Species transportation can be determined by using the generalised Maxwell-Stefan equations. However, they are spatially dependent and for a time-dependent problem, it is necessary to describe the change in concentration as a function of time. This must be achieved by using the material balances.

Generally speaking the material balance equations are often applied to a fixed control volume. For this system, the gel matrix will swell and thus the control volume is changing with time. Thus it is necessary to examine the fundamental mechanism responsible for material balance in order to validate that the general material balance equations are also applicable to a dynamic problem with a changing control volume.

The following discussion is mainly based on White (1998) and Higgins (2004). To begin with it is helpful to introduce two coordinate systems in fluid dynamics:

Eulerian and Lagrangian coordinate systems.

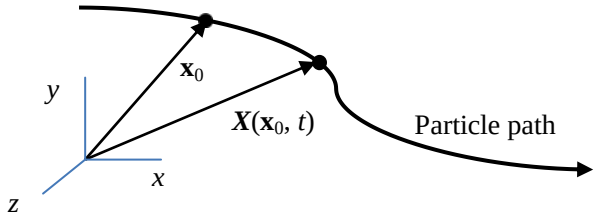

Figure 2.21 Motion of a particle described in Eulerian and Lagrangian coordinates

Figure 2.21 shows the motion of a fluid particle described by Eulerian and Lagrangian. Eulerian coordinates measure position in a fixed frame of reference. The symbols used are the position vectors **x**, and the Cartesian coordinates *x*, *y* and *z*. Although the position of a fluid particle is a function of time the coordinate axes are fixed. This can be visualised as sitting on a river bank and watching the water pass the fixed location. On the other hand from a Lagrangian perspective the position of a particle that was at $\mathbf{x}_0$ at time t_0 has coordinates ***X***, ***Y*** and ***Z***. Because the particle moves, ***X***, ***Y*** and ***Z*** are functions of time. This can be visualised as sitting in a boat and drifting down a river.

In the same manner, there are several possibilities for defining a control volume, based on the kinetics of the surface enveloping the control volume. If we select a control volume *V(t)* with a surface of *S(t)* defined by its outward directed unit normal **n**, and the surface velocity of the control volume moving through the fluid is ***u***, then there are three possibilities of defining a control volume:

1. Material control volume

In this case, the local mass average velocity of the fluid is equal to the surface of the control volume velocity. Since the surface of the control volume moves the same as the velocity of the fluid, there is no mass flux of fluid in or out the surface and thus the control volume retains the material originally present within its control surface. This kind is called material control volume denoted by $V_m(t)$ and its control surface by

$S_m(t)$. Material control volumes are also called Lagrangian control volumes. They are seldom used in the analysis of problems since they move through space, change shape and deform and it is impossible to define boundaries. However, they are often used in the derivation of balance equations.

2. Fixed control volumes

In this case, the surface velocity of the control volume is zero. The control volume is therefore fixed in physical space and thus mass flux can pass through the control surface that defines inflow and outflow boundaries. Fixed control volumes define open systems when mass fluxes can enter or leave through control surfaces.

3. Moving control volumes

In this case, the surface velocity of the control volume is not zero and is not equal to the mass average velocity either. Thus moving control volume will normally have mass flux passing through the control surface that defines inflow and outflow boundaries. The moving control volume is denoted by $V(t)$ and its control surface by $S(t)$.

Having understood the definition of different control volumes, we need to know the Reynolds transport theorems. The Reynolds transport theorem allows one to determine how a given quantity defined within a control volume changes with time as the control volume deforms. In the following discussion it will be shown that the choice of a control volume does not affect the point material balance equation.

Consider a scalar quantity $\psi(\mathbf{x},t)$ defined per unit volume. The total amount of $\psi(\mathbf{x},t)$ in a material control volume $V_m(t)$ is:

$$\int_{V_m(t)} \psi\,(\mathbf{x},t)\,dV \tag{2.7.1}$$

The time rate of change is:

$$\frac{d}{dt}\int_{V_m(t)} \psi(\mathbf{x},t)\,dV \tag{2.7.2}$$

Since the size and shape of $V_m(t)$ are functions of time, the time derivative inside the integral cannot be taken directly. The Reynolds transport theorem allows one to move the time derivative inside the integral and for material control volumes it can be written as:

$$\frac{d}{dt}\int_{V_m(t)} \psi(\mathbf{x},t)\,dV = \int_{V_m(t)} \left(\frac{\partial \psi}{\partial t} + \nabla\cdot(\psi \boldsymbol{v})\right) dV \tag{2.7.3}$$

Here $\boldsymbol{v}$ is the mass average velocity of the fluid.

The divergence theorem (Versteeg and Malalasekera, 2007) relates volume integrals to surface integrals of vector fields. For the vector $\boldsymbol{v}$, it writes:

$$\int_V (\nabla\cdot\boldsymbol{v})\,dV = \int_S (\boldsymbol{v}\cdot\mathbf{n})\,dS \tag{2.7.4}$$

By applying the divergence theorem (2.7.4), the above equation can be written as:

$$\frac{d}{dt}\int_{V_m(t)} \psi(\mathbf{x},t)\,dV = \int_{V_m(t)} \frac{\partial \psi}{\partial t}\,dV + \int_{S_m(t)} \psi\boldsymbol{v}\cdot\mathbf{n}\,dS \tag{2.7.5}$$

If instead the control volume is moving control volume *V(t)* with surface *S(t)*, such that the surface moves with velocity $\boldsymbol{u}$, then the time rate of change of the total amount of ψ in the control volume is:

$$\frac{d}{dt}\int_{V(t)} \psi(\mathbf{x},t)\,dV = \int_{V(t)} \left(\frac{\partial \psi}{\partial t} + \nabla\cdot(\psi\boldsymbol{u})\right) dV \tag{2.7.6}$$

This is called the generalised Reynolds transport theorem. It also applies to vectors and tensors. For example to determine how a vector **G**(**x**,t) changes with time, the direct application of the generalised Reynolds transport theorem gives:

$$\frac{d}{dt}\int_{V(t)} \mathbf{G}(\mathbf{x},t)\,dV = \int_{V(t)} \left(\frac{\partial \mathbf{G}}{\partial t} + \nabla\cdot(\mathbf{G}\boldsymbol{u})\right) dV \tag{2.7.7}$$

Next we are going to derive the general form for a balance quantity. As before let **n** be the outward directed unit normal to a material control volume $V_m(t)$ with a surface

$S_m(t)$. Because a material control volume is considered, the surface velocity of $V_m(t)$ is equal to the mass average velocity of the fluid $\boldsymbol{v}$ evaluated at surface $S_m(t)$. The general form for a balance principle in a material control volume is:

$$\frac{d}{dt}\int_{V_m(t)} \rho\psi \, dV = \int_{V_m(t)} \rho s dV + \int_{S_m(t)} -\mathbf{j}\cdot\mathbf{n} dS = 0 \tag{2.7.8}$$

in which ψ is a physical quantity defined per unit mass, ρ is the density, s is the rate of supply of ψ per unit mass per unit time, and $-\mathbf{j}\cdot\mathbf{n}$ is the influx of ψ per unit area per unit time.

The above equation is an integral statement and it can be formulated as a point equation by applying the Reynolds theorem along with the divergence theorem. The left hand side of the above equation is:

$$\frac{d}{dt}\int_{V_m(t)} \rho\psi \, dV = \int_{V_m(t)} \left(\frac{\partial(\rho\psi)}{\partial t} + \nabla\cdot(\rho\psi\boldsymbol{v})\right) dV \tag{2.7.9}$$

Applying the divergence theorem to the surface integral in the balance principle gives:

$$\int_{S_m(t)} -\mathbf{j}\cdot\mathbf{n} dS = -\int_{V_m(t)} (\nabla\cdot\mathbf{j}) \, dV \tag{2.7.10}$$

Then:

$$\int_{V_m(t)} \left(\frac{\partial(\rho\psi)}{\partial t} + \nabla\cdot(\rho\psi\boldsymbol{v}) - \rho s + \nabla\cdot\mathbf{j}\right) dV = 0 \tag{2.7.11}$$

Since the control volume is arbitrary, it then follows that the integrand must be zero everywhere, which means:

$$\frac{\partial(\rho\psi)}{\partial t} + \nabla\cdot(\rho\psi\boldsymbol{v}) - \rho s + \nabla\cdot\mathbf{j} = \mathbf{0} \tag{2.7.12}$$

This is the point equation for a conserved quantity.

If $\rho(\mathbf{x},t)$ is the local density of the fluid then the total mass in an arbitrary material control volume is given by:

$$M(t) = \int_{V_m(t)} \rho\,(\mathbf{x},t) dV \tag{2.7.13}$$

For the material control volume, the time rate of change of the total mass is zero. Hence

$$\frac{dM}{dt} = \frac{d}{dt}\int_{V_m(t)} \rho\,(\mathbf{x},t)dV = 0 \tag{2.7.14}$$

If we apply the Reynolds transport theorem, we have

$$\frac{d}{dt}\int_{V_m(t)} \rho\,(\mathbf{x},t)dV = \int_{V_m(t)} \left(\frac{\partial \rho}{\partial t} + \nabla\cdot(\rho \boldsymbol{v})\right) dV \tag{2.7.15}$$

The point equation of conservation of mass is then:

$$\frac{\partial \rho}{\partial t} + \nabla\cdot(\rho \boldsymbol{v}) = 0 \tag{2.7.16}$$

For an arbitrary moving control volume the mass balance in the control volume $V(t)$ is:

$$\left\{\begin{matrix}\text{Time rate of change} \\ \text{of mass in } V(t)\end{matrix}\right\} = \left\{\begin{matrix}\text{Net influx of mass} \\ \text{through } S(t)\end{matrix}\right\}$$

In mathematical terms:

$$\frac{d}{dt}\int_{V(t)} \rho\, dV = -\int_{S(t)} \mathbf{j}\cdot\mathbf{n}dS \tag{2.7.17}$$

where **j** is the mass flux vector relative to the surface. At the surface a mass flux $\boldsymbol{n}(\mathbf{x},t)$ can be defined in terms of the mass average velocity of the fluid and the local density:

$$\boldsymbol{n}(\mathbf{x},t) = \rho(\mathbf{x},t)\boldsymbol{v}(\mathbf{x},t) \tag{2.7.18}$$

In the control volume $V(t)$ the surface $S(t)$ is not fixed but moves with velocity $\mathbf{u}(\mathbf{x},t)$ relative to a given reference frame. Thus the mass flux across that surface must also be relative:

$$\boldsymbol{n}_{relative} = \mathbf{j} = \rho \boldsymbol{v}_{relative} \tag{2.7.19}$$

The relative velocity is given by:

$$\boldsymbol{v}_{relative} = \boldsymbol{v} - \boldsymbol{u} \tag{2.7.20}$$

Combining the equation (2.7.17) with (2.7.19) and (2.7.20), the mass balance equation gives:

$$\frac{d}{dt}\int_{V(t)} \rho\, dV = -\int_{S(t)} \mathbf{j}\cdot\mathbf{n}dS = -\int_{S(t)} \rho(\boldsymbol{v}-\boldsymbol{u})\cdot\mathbf{n}dS \tag{2.7.21}$$

This is the integral statement of mass balance in a moving control volume. Compare this result with the integral equation of mass balance in a material control volume given by:

$$\frac{d}{dt}\int_{V_m(t)} \rho \, dV = 0 \tag{2.7.22}$$

Rewrite the mass balance equation in a moving control volume by using the generalised Reynolds transport theorem:

$$\frac{d}{dt}\int_{V(t)} \rho\,(\mathbf{x},t)dV = \int_{V(t)} \left(\frac{\partial \rho}{\partial t} + \nabla \cdot (\rho \boldsymbol{u})\right) dV \tag{2.7.23}$$

$$\int_{S(t)} \rho(\boldsymbol{v}-\boldsymbol{u}) \cdot \mathbf{n} dS = \int_{V(t)} \nabla \cdot \rho(\boldsymbol{v}-\boldsymbol{u})\, dV \tag{2.7.24}$$

$$\int_{V(t)} \left(\frac{\partial \rho}{\partial t} + \nabla \cdot (\rho \boldsymbol{u}) + \nabla \cdot \rho(\boldsymbol{v}-\boldsymbol{u})\right) dV = 0 \tag{2.7.25}$$

$$\int_{V(t)} \left(\frac{\partial \rho}{\partial t} + \nabla \cdot (\rho \boldsymbol{v})\right) dV = 0 \tag{2.7.26}$$

It can be seen that the surface velocity of the moving volume $\boldsymbol{u}$ is cancelled out.

Since $V(t)$ is arbitrary, it should be:

$$\frac{\partial \rho}{\partial t} + \nabla \cdot (\rho \boldsymbol{v}) = 0 \tag{2.7.27}$$

It shows that the point equation describing the mass balance is independent of the choice of a control volume. The same result (equation (2.7.16) and (2.7.27)) is obtained whether a moving control volume or a material control volume is used. Using a material volume one can considerably simplify the deviation of the conservation equations. It is proved that mass balance equations can be used to this dynamic swelling modeling.

At this point it is verified that the general balance principle can be used in any case

whether the system is fixed or moving. Next we consider the point equation of the balance principle using Taylor and Krishna (1993) terminology:

$$\frac{\partial(\rho_t \psi)}{\partial t} + \nabla \cdot (\rho_t \psi \boldsymbol{v}) + \nabla \cdot \boldsymbol{\Phi} = \zeta \tag{2.7.28}$$

where ψ is an arbitrary field quantity per unit mass of mixture, ζ is the rate of production of field per unit volume of bulk phase, $\boldsymbol{\Phi}$ is a diffusion flux of the field quantity through external surface, ρ_t is the mass density of fluid mixture and $\boldsymbol{v}$ is the mass average velocity of fluid mixture. It is the same as equation (2.7.12) with $\boldsymbol{\Phi}$ replaced $\mathbf{j}$ and ζ replaced ρs. We must remember that $\boldsymbol{\Phi}$ is local to the surface for a moving fluid mixture.

For the balance of components in a system with no chemical reactions:

$$\psi = \omega_i \quad \boldsymbol{\Phi} = \boldsymbol{j}_i \quad \zeta = 0 \tag{2.7.29}$$

in which ω_i is the mass fraction of component i and $\boldsymbol{j}_i$ is the mass diffusion flux with respect to a chosen reference velocity.

For the conservation of total mass:

$$\psi = 1 \quad \boldsymbol{\Phi} = 0 \quad \zeta = 0 \tag{2.7.30}$$

Therefore the mass balance equation for continuity of mass of species i in a non-reacting system is:

$$\frac{\partial \rho_i}{\partial t} + \nabla \cdot (\rho_i \boldsymbol{v}) + \nabla \cdot \boldsymbol{j}_i = 0 \tag{2.7.31}$$

with

$$\boldsymbol{j}_i = \rho_i (\boldsymbol{u}_i - \boldsymbol{v}) \tag{2.7.32}$$

The mass balance equation in terms of the velocity of component i, $\boldsymbol{u}_i$, is:

$$\frac{\partial \rho_i}{\partial t} + \nabla \cdot (\rho_i \boldsymbol{u}_i) = 0 \tag{2.7.33}$$

In terms of the component concentration:

$$\frac{\partial c_i}{\partial t} + \nabla \cdot (c_i \boldsymbol{u}_i) = 0 \tag{2.7.34}$$

The molar flux of species i is defined by:

$$\boldsymbol{N}_i = c_i \boldsymbol{u}_i \tag{2.7.35}$$

The mass balance in terms of molar flux:

$$\frac{\partial c_i}{\partial t} + \nabla \cdot \boldsymbol{N}_i = 0 \tag{2.7.36}$$

in which c_i is the concentration of component i and $\boldsymbol{N}_i$ is the molar flux.

The molar diffusion flux can be defined relative to an arbitrary reference velocity $\boldsymbol{u}^a$ by:

$$\boldsymbol{J}_i^a = c_i \boldsymbol{u}_i - c_i \boldsymbol{u}^a \tag{2.7.37}$$

The differential balance equations take the form in terms of the diffusion fluxes with respect to a reference velocity:

$$\frac{\partial c_i}{\partial t} + \nabla \cdot (\boldsymbol{J}_i^a + c_i \boldsymbol{u}^a) = 0 \tag{2.7.38}$$

In a system with chemical reactions, a species is neither lost nor gained. The ζ term is not zero. The mass balance equation for species in a reacting system can be rewritten as:

$$\frac{\partial c_i}{\partial t} + \nabla \cdot (\boldsymbol{J}_i^a + c_i \boldsymbol{u}^a) = \zeta \tag{2.7.39}$$

With ζ defined by:

$$\zeta = \sum_j v^j R^j \tag{2.7.40}$$

where v^j is the stoichiometric coefficient of species i in the jth reaction and R^j is the reaction rate in the jth reaction.

The problem with solving equation (2.7.40) is that the reaction rates for each reaction are sometimes large leading to stiffness of the equations. Stiffness means ordinary differential equations with a wide range of time constants are difficult to solve. The reason for this is that the transport and reaction processes that are included in the model can occur on widely different time scales (Hofmann et al., 2008).

2.7.1 Elimination of reactions in acid-base systems

Di Toro (1976) has given mathematical proof for solving this type of problem by eliminating the reaction terms and solving an alternate set of equations. Later similar approaches can be found in Moe et al. (1995) and Kakhu and Pantelides (2003).

Di Toro (1976) considered carbon dioxide dissolved in water equilibrium:

$$CO_2 + H_2O \overset{K_1}{\Leftrightarrow} H^+ + HCO_3^- \tag{2.7.41}$$

$$HCO_3^- \overset{K_2}{\Leftrightarrow} H^+ + CO_3^{2-} \tag{2.7.42}$$

$$H_2O \overset{K_w}{\Leftrightarrow} H^+ + OH^- \tag{2.7.43}$$

in which K_1, K_2 and K_w are dissociation constants for each corresponding reaction. The major species involved are: CO_2, HCO_3^-, CO_3^{2-}, H^+, H_2O and OH^-. Because the individual species are reactive a total concentration needs to be defined:

$$c_T = [CO_2] + [HCO_3^-] + [CO_3^{2-}] \tag{2.7.44}$$

And the dissociation equilibria for the above reactions are:

$$K_1 = \frac{[H^+][HCO_3^-]}{[CO_2]} \tag{2.7.45}$$

$$K_2 = \frac{[H^+][CO_3^{2-}]}{[HCO_3^-]} \tag{2.7.46}$$

$$K_w = \frac{[H^+][OH^-]}{[HO_2]} \tag{2.7.47}$$

Thus if c_T is known, the concentration of all species involved is easily obtained. It is traditional to write the mass balance equations for each species. However the solution of these differential equations is quite hard to obtain because the large reaction rates cause stiffness of the equations.

Di Toro's method (1976) was to avoid large stiffness by eliminating the reaction terms and solving an alternate set of equations.

Species involved are indentified in a matrix written as:

$$[CO_2 \quad HCO_3^- \quad CO_3^{2-} \quad H^+ \quad H_2O \quad OH^-]^T \tag{2.7.48}$$

Components chosen are:

$$[CO_2 \quad H^+ \quad H_2O]^T \tag{2.7.49}$$

Then vector (2.7.48) can be formulated by matrix multiplication:

$$\begin{aligned}[CO_2 \quad HCO_3^- \quad CO_3^{2-} \quad H^+ \quad H_2O \quad OH^-]^T \\ = \mathbf{F}[CO_2 \quad H^+ \quad H_2O]^T\end{aligned} \tag{2.7.50}$$

F, called the formula matrix, is:

$$\mathbf{F} = \begin{bmatrix} 1 & 0 & 0 \\ 1 & -1 & 1 \\ 1 & -2 & 1 \\ 0 & 1 & 0 \\ 0 & 0 & 1 \\ 0 & -1 & 1 \end{bmatrix} \tag{2.7.51}$$

R, called the reaction matrix, can be written according to species in each reaction:

$$\mathbf{R} = \begin{bmatrix} 1 & -1 & 0 & -1 & 1 & 0 \\ 0 & 1 & -1 & -1 & 0 & 0 \\ 0 & 0 & 0 & -1 & 1 & -1 \end{bmatrix} \tag{2.7.52}$$

Species in each reaction can be obtained by multiplying matrix **R** with species matrix (2.7.48).

Multiplication of reaction matrix **R** with formula matrix **F** results in a zero matrix.

$$\mathbf{RF} = \mathbf{0} \tag{2.7.53}$$

This can be verified:

$$\begin{bmatrix} 1 & -1 & 0 & -1 & 1 & 0 \\ 0 & 1 & -1 & -1 & 0 & 0 \\ 0 & 0 & 0 & -1 & 1 & -1 \end{bmatrix} \begin{bmatrix} 1 & 0 & 0 \\ 1 & -1 & 1 \\ 1 & -2 & 1 \\ 0 & 1 & 0 \\ 0 & 0 & 1 \\ 0 & -1 & 1 \end{bmatrix} = \begin{bmatrix} 0 & 0 & 0 \\ 0 & 0 & 0 \\ 0 & 0 & 0 \end{bmatrix} \tag{2.7.54}$$

The choice of components is arbitrary and has no effect on the formulation. If atoms $[C \quad H \quad O]$ are chosen as components then the formula matrix **F** becomes:

$$\mathbf{F} = \begin{bmatrix} 1 & 0 & 2 \\ 1 & 1 & 3 \\ 1 & 0 & 3 \\ 0 & 1 & 0 \\ 0 & 2 & 1 \\ 0 & 1 & 1 \end{bmatrix} \tag{2.7.55}$$

The reaction matrix is independent of the choice of components such that it is the same as the previous one. Equation (2.7.53) still holds.

$$\begin{bmatrix} 1 & -1 & 0 & -1 & 1 & 0 \\ 0 & 1 & -1 & -1 & 0 & 0 \\ 0 & 0 & 0 & -1 & 1 & -1 \end{bmatrix} \begin{bmatrix} 1 & 0 & 2 \\ 1 & 1 & 3 \\ 1 & 0 & 3 \\ 0 & 1 & 0 \\ 0 & 2 & 1 \\ 0 & 1 & 1 \end{bmatrix} = \begin{bmatrix} 0 & 0 & 0 \\ 0 & 0 & 0 \\ 0 & 0 & 0 \end{bmatrix} \tag{2.7.56}$$

The transformation matrix **TM** is the transpose of the formulation matrix **F**

$$\mathbf{TM} = \mathbf{F}^T \tag{2.7.57}$$

By using the transformation matrix, the mass balance equation for each species can be transformed to each chosen component. Then the reaction term can be eliminated.

In Di Toro's system, there are five species and their concentrations are defined as *c* with different suffixes. The reaction rates are r_1, r_2 and r_3 for the three reactions in sequence. Assuming there is no diffusion, the original differential equations are:

$$\begin{bmatrix} \frac{dc_{CO_2}}{dt} \\ \frac{dc_{HCO_3^-}}{dt} \\ \frac{dc_{CO_3^{2-}}}{dt} \\ \frac{dc_{H^+}}{dt} \\ \frac{dc_{H_2O}}{dt} \\ \frac{dc_{OH^-}}{dt} \end{bmatrix} = \begin{bmatrix} -r_1 \\ r_1 - r_2 \\ r_2 \\ r_1 + r_2 + r_3 \\ -r_1 - r_3 \\ r_3 \end{bmatrix} \tag{2.7.58}$$

When components are chosen as equation (2.7.49) multiplying both sides of equation (2.7.58) with its transformation matrix **TM**:

$$\begin{bmatrix} 1 & 1 & 1 & 0 & 0 & 0 \\ 0 & -1 & -2 & 1 & 0 & -1 \\ 0 & 1 & 1 & 0 & 1 & 1 \end{bmatrix} \begin{bmatrix} \frac{dc_{CO_2}}{dt} \\ \frac{dc_{HCO_3^-}}{dt} \\ \frac{dc_{CO_3^{2-}}}{dt} \\ \frac{dc_{H^+}}{dt} \\ \frac{dc_{H_2O}}{dt} \\ \frac{dc_{OH^-}}{dt} \end{bmatrix} \tag{2.7.59}$$

$$= \begin{bmatrix} 1 & 1 & 1 & 0 & 0 & 0 \\ 0 & -1 & -2 & 1 & 0 & -1 \\ 0 & 1 & 1 & 0 & 1 & 1 \end{bmatrix} \begin{bmatrix} -r_1 \\ r_1 - r_2 \\ r_2 \\ r_1 + r_2 + r_3 \\ -r_1 - r_3 \\ r_3 \end{bmatrix}$$

It is then found that reaction rates are cancelled out in the new equations:

$$\begin{bmatrix} \frac{d\left(c_{CO_2} + c_{HCO_3^-} + c_{CO_3^{2-}}\right)}{dt} \\ \frac{d\left(-c_{HCO_3^-} - 2c_{CO_3^{2-}} + c_{H^+} - c_{OH^-}\right)}{dt} \\ \frac{d\left(c_{HCO_3^-} + c_{CO_3^{2-}} + c_{H_2O} + c_{OH^-}\right)}{dt} \end{bmatrix} = \begin{bmatrix} 0 \\ 0 \\ 0 \end{bmatrix} \tag{2.7.60}$$

When atoms $[C \quad H \quad O]$ are chosen as components then multiplying both sides of equation (2.7.58) with its transformation matrix **TM**:

$$\begin{bmatrix} 1 & 1 & 1 & 0 & 0 & 0 \\ 0 & 1 & 0 & 1 & 2 & 1 \\ 2 & 3 & 3 & 0 & 1 & 1 \end{bmatrix} \begin{bmatrix} \frac{dc_{CO_2}}{dt} \\ \frac{dc_{HCO_3^-}}{dt} \\ \frac{dc_{CO_3^{2-}}}{dt} \\ \frac{dc_{H^+}}{dt} \\ \frac{dc_{H_2O}}{dt} \\ \frac{dc_{OH^-}}{dt} \end{bmatrix} \tag{2.7.61}$$

$$= \begin{bmatrix} 1 & 1 & 1 & 0 & 0 & 0 \\ 0 & 1 & 0 & 1 & 2 & 1 \\ 2 & 3 & 3 & 0 & 1 & 1 \end{bmatrix} \begin{bmatrix} -r_1 \\ r_1 - r_2 \\ r_2 \\ r_1 + r_2 + r_3 \\ -r_1 - r_3 \\ r_3 \end{bmatrix}$$

Then the alternative equations are:

$$\begin{bmatrix} \frac{d\left(c_{CO_2} + c_{HCO_3^-} + c_{CO_3^{2-}}\right)}{dt} \\ \frac{d\left(c_{HCO_3^-} + c_{H^+} + 2c_{H_2O} + c_{OH^-}\right)}{dt} \\ \frac{d\left(2c_{CO_2} + 3c_{HCO_3^-} + 3c_{CO_3^{2-}} + c_{H_2O} + c_{OH^-}\right)}{dt} \end{bmatrix} = \begin{bmatrix} 0 \\ 0 \\ 0 \end{bmatrix} \tag{2.7.62}$$

It is shown that the choice of components is not limited to get the alternative equations with zero reaction rates. Practically atoms are often used as components. In this case three new concentrations can be defined as:

$$c_C = c_{CO_2} + c_{HCO_3^-} + c_{CO_3^{2-}} \tag{2.7.63}$$

$$c_H = c_{HCO_3^-} + c_{H^+} + 2c_{H_2O} + c_{OH^-} \tag{2.7.64}$$

$$c_O = 2c_{CO_2} + 3c_{HCO_3^-} + 3c_{CO_3^{2-}} + c_{H_2O} + c_{OH^-} \tag{2.7.65}$$

At this point all the necessary equations for the polyelectrolyte gel swelling have been obtained from a wide range of literature and their applicability in the modelling has been discussed. The next chapter is about numerical solution.

3 COMSOL Multiphysics

From the literature discussed above, it is clear that the mathematical model of protein gel swelling will include a number of partial differential and algebraic equations. The numerical solution of these equations is not straightforward. In the author's ME thesis, the model equations of a gel swelling were set up and the method of MATLAB ODE15s was used. It was found that the system of equations was stiff. Therefore, in many cases numerical instability, almost certainly caused by the stiffness, led to a failure of the integration. Some of the stiffness arose from the need to make the protein dissociation dynamic and from the range of concentration gradients through the gel. Further, the sudden change in concentration at the gel boundary causes numerical inaccuracy in the solutions. Therefore, there is a need to develop the solution methods for this type of problem.

A numerical software package was going to be used. The alternative of purpose-written software was rejected so that the research could concentrate on modelling and interpretation of numerical simulation results. Current software is based on two principle numerical methods: the finite element method (FEM) and the finite volume method (FVM). Both methods involve subdividing the solution domain into a large number of finite elements (FEM) or control volumes (FVM) and then solving governing equations. The FEM uses simple piecewise functions such as linear or quadratic to describe the local variations of unknown variables. Then the piecewise approximation functions for unknown variables are substituted into the equation and a residual is defined to measure the errors. The residuals are next minimised in some sense by multiplying them by a set of weighting functions and integrating. As a result a set of algebraic equations for the unknown coefficients of the approximation functions is obtained (Burden and Faires, 2005). COMSOL multiphysics uses FEM. COMSOL users are not able to change the numerical methods used. For the FVM, a formal integration of governing equations over all the control volumes of the solution domain is carried out. A variety of finite difference approximation schemes such as

the central differencing and the upwind differencing for the terms in the integrated equation including convection, diffusion and sources are applied. This converts the integral equations into a system of algebraic equations (Versteeg and Malalasekera, 2007). The FVM is used by the computational fluid dynamics (CFD) software such as CFX/ANSYS.

COMSOL Multiphysics version 3.5 was chosen as the numerical solution method in this thesis for two reasons. First of all, the governing equations for the gel swelling are not standard partial differential equations (PDEs). COMSOL Multiphysics has equation based mode which allows one to set up specific PDEs defined for a particular physical problem. Secondly, COMSOL Multiphysics is an integrated environment for solving systems of time dependent, or stationary second order in space, PDEs in one, two and three dimensions. Such equations may be coupled in an almost arbitrary way. This is well suited to this type of gel swelling problem. CFD packages cannot easily solve a user-defined PDE system with algebraic equations.

3.1 Introduction

COMSOL Multiphysics is a powerful interactive environment for solving a variety of problems in science and engineering based on PDEs. A variety of model libraries is supplied, and it is possible to extend conventional models into other domains to solve problems involving coupled phenomena. Although an in-depth knowledge of mathematics and especially PDEs is not a prerequisite for program use, it would certainly help in not only setting up the problems but also in interpreting the results and extending use to the fullest.

By employing built-in modes (for selection and display of relevant parts of the model), it is possible to build more complicated structures and avoid defining each equation. These capabilities may be accessed by the stand-alone product through a graphical user interface (GUI), or by programming through the MATLAB interface. In the

programming environment, MATLAB, C, C++, and FORTRAN programs may be used to define properties, loads, sources and boundary conditions (BC). COMSOL uses the finite element method together with adaptive meshing error control with a variety of numerical solvers while solving the PDEs. The FEM process in COMSOL is presented in Figure 3.1. For linear systems, both direct and iterative solvers (using a range of preconditioners) are available.

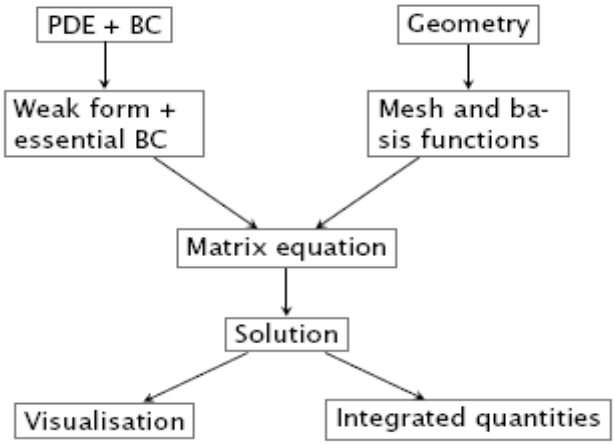

Figure 3.1 The finite element method as implemented in COMSOL

The modelling process in COMSOL Multiphysics includes geometry, physics, mesh, solver and finally post-processing. The first screen appearing when opening COMSOL is called the Model Navigator (Figure 3.2), where the user starts the modeling and controls the program processes. This area allows the selection of the space dimension and application modes for new models, opening of existing models, or entering the model library areas. The program is subtitled multiphysics modeling as this GUI allows one to build and solve models by using predefined 'physics modes,' PDE modes, or a combination of these. The modes are like templates where the user can define properties and boundary conditions and then have the software create the PDEs. This GUI also has a set of computer assisted design (CAD) tools for geometry modeling in 1-D, 2-D, and 3-D. Alternatively, for some complex problems, the geometry can be imported from professional CAD software. Various dialog boxes will display the values of the variables and the equation used (Figure 3.3). There is much detail here and the coefficients for each term in the model can be quickly

displayed. Once the multiphysics mode is entered and the type of problem defined, the initial and boundary conditions may be set, so that the equations can be solved and graphics generated (Figure 3.4).

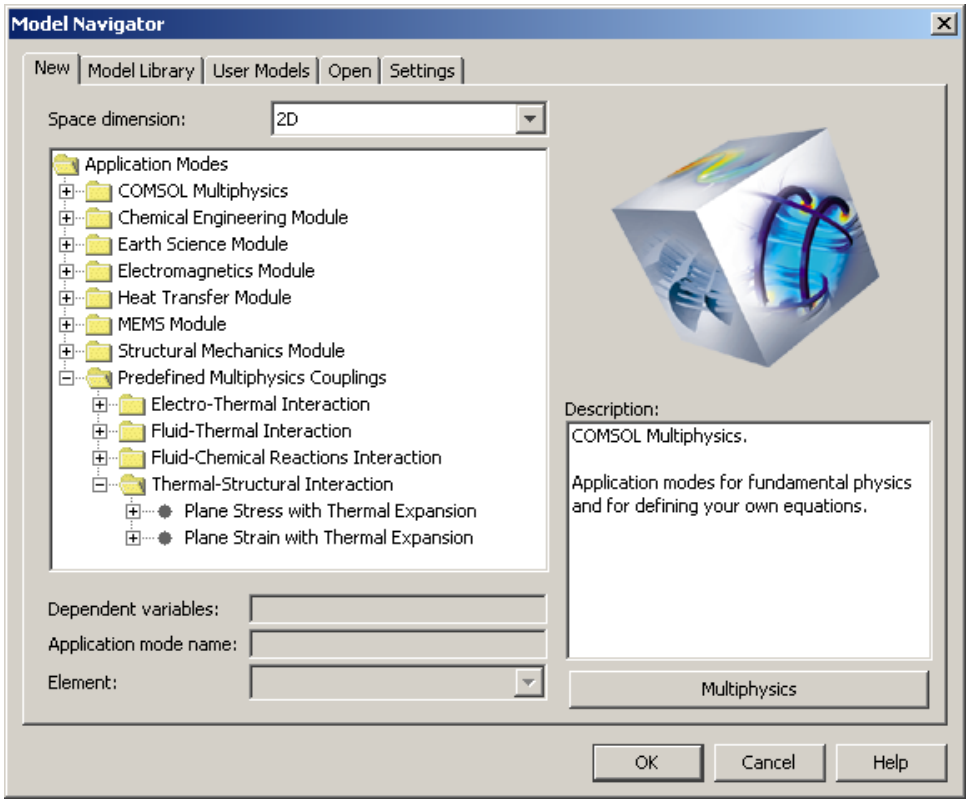

Figure 3.2 Starting a new COMSOL model

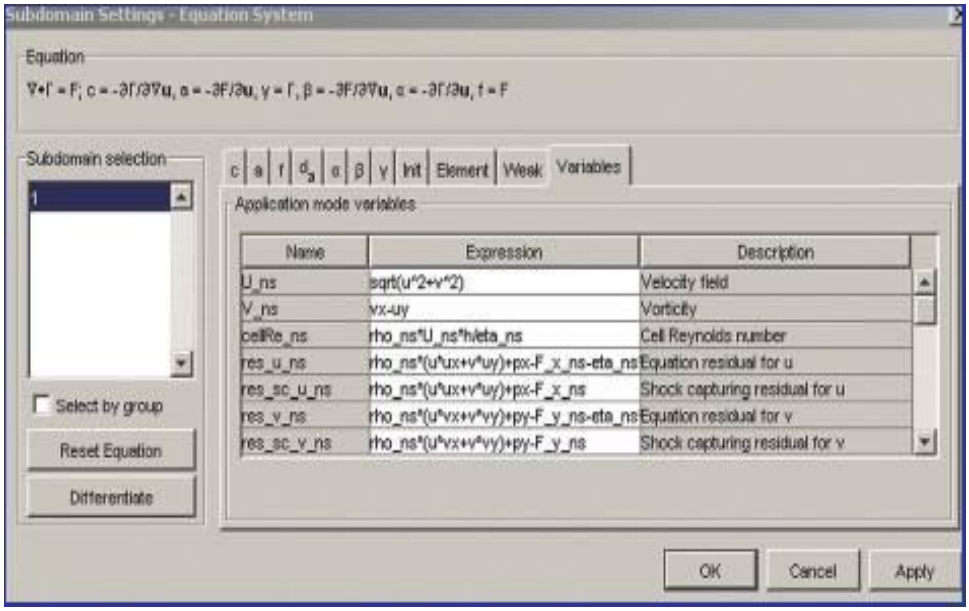

Figure 3.3 Equation systems display in COMSOL

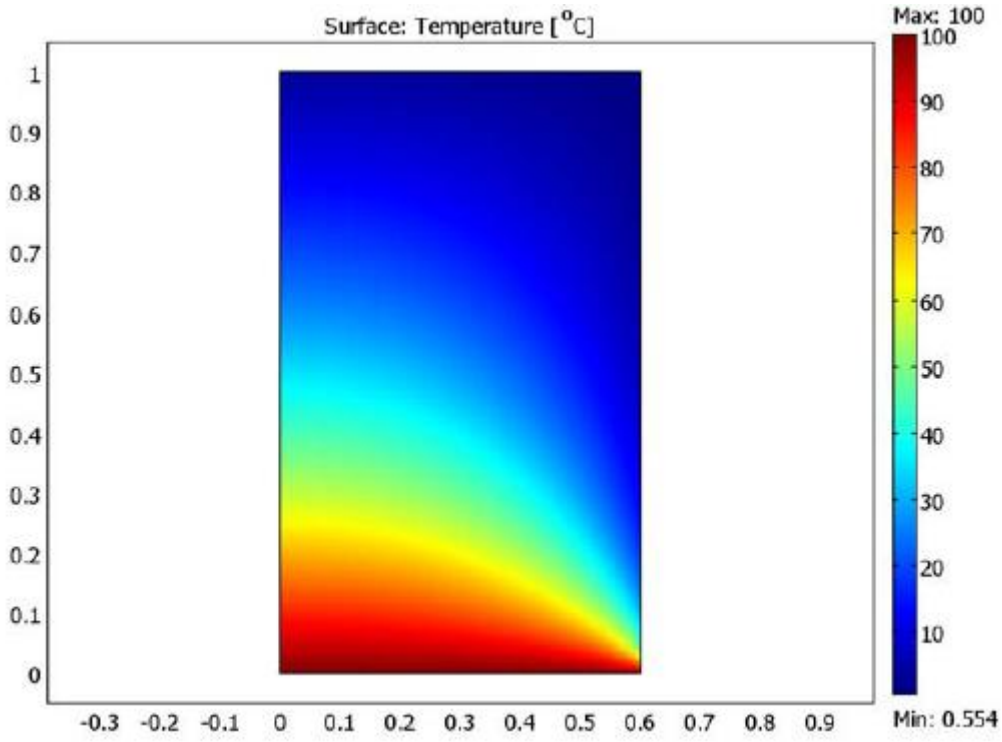

Figure 3.4 2-D surface plot example: temperature distribution in a 2-D plate resulting from external convection heating and internal conduction

3.2 Using the general form of PDE in COMSOL

COMSOL can solve systems of coupled PDEs. The specified PDEs may be non-linear and time dependent and act on a 1D, 2D or 3D geometry. The PDEs and boundary values can be represented by three forms: the coefficient form, the general form and the weak form (COMSOL Multiphysics 3.5, 2008). COMSOL also provides a number of predefined models for many standard problems. These models consist of predefined templates and user interfaces already set up with equations and variables for specific areas of physics in order to hide much of the complex details of modelling by equations. Although predefined models are convenient, equation based modelling was used in this thesis. For one reason, the pre-defined Maxwell-Stefan diffusion model does not cover our coupled system such that diffusion potential and swelling pressure are not included. For another reason, it would certainly help in not only understanding the underlying physics of the problem but also in interpreting the results and extending use to the fullest.

Equation based physical problems can be defined by three forms in COMSOL: coefficient form, general form and weak form. Because the general form will be used, we will only discuss the general form of the PDEs in COMSOL.

The general form reads:

$$\begin{cases} e_a \dfrac{\partial^2 u}{\partial t^2} + d_a \dfrac{\partial u}{\partial t} + \nabla \cdot \Gamma = F \quad \text{in domain} \\ -n \cdot \Gamma = G + \left(\dfrac{\partial R}{\partial u}\right)^T \mu \quad \text{on boundary} \\ 0 = R \quad \text{on boundary} \end{cases} \tag{3.2.1}$$

where u is the unknown solution of any number of variables over time and space, **n** is the outward unit normal vector on boundary and e_a, d_a, Γ, F, G, R and μ are coefficients.

The first equation in equation (3.2.1) is the PDE. The second is a generalised Neumann boundary condition and the third is a Dirichlet boundary condition. Dirichlet conditions often represent constraints.

The coefficients Γ and F can be functions of the space, time, the solution u and its gradient. G and R can be functions of the space, time and the unknown, u. F and G and R are scalar, while Γ represents the flux vector. The variable μ is the Lagrange multiplier.

To solve a problem within COMSOL Multiphysics, we must perform the following steps:

- Define the geometry of interest including discretisation
- Set the equation coefficients
- Specify the boundary conditions
- Set solution parameters and solve the problem
- Perform post processing and analysis of the result

Two cases are presented to illustrate how COMSOL Multiphysics can be used to solve a variety of general problems of interest.

Case 1: Solving linear systems of ODEs

Consider the isomerisation reactions:

$$A \underset{k_2}{\overset{k_1}{\rightleftarrows}} B \underset{k_4}{\overset{k_3}{\rightleftarrows}} C \tag{3.2.2}$$

First order kinetics leads to the following system of ODEs:

$$\begin{aligned} \frac{dc_A}{dt} &= -k_1 c_A + k_2 c_B \\ \frac{dc_B}{dt} &= k_1 c_A - k_2 c_B - k_3 c_B + k_4 c_c \\ \frac{dc_c}{dt} &= k_3 c_B - k_4 c_c \end{aligned} \tag{3.2.3}$$

where c are concentrations for three components A, B and C, and k represent reaction rates with k_1=1, k_2=0, k_3=2 and k_4=3.

In the Model Navigator, a one-dimensional (1D), PDE general form is chosen with dependent variables: c_A, c_B and c_C representing the concentrations of three components. Users can freely choose the variable names according to the problems. For a new model, COMSOL Multiphysics automatically puts users in Draw Mode. Since this is a 1D geometry case and the problem is space independent, a line of any dimension will do and the line of 1 dimension is chosen for its simplicity. Constants of the equation, reaction rates in this case, can be set in Constants. Then, the physics of the problem needs setting. Comparing equation (3.2.3) with the PDE general form equation (3.2.1), Γ is set to zeros for each variable. The setting of F is shown in Figure 3.5. The problem starts with pure c_A=1, thus the initial setting is needed with $c_A(0)$=1. Because the current problem is only time dependent, the boundaries have Neumann boundary conditions (Figure 3.6). Once the geometry, equation coefficients and BCs have been specified, it is now ready to discretise the independent variables, that is, to create a finite element mesh for the geometry of interest. For this 1D problem, this is relatively straightforward. For more complex 2D and 3D geometries, this step may

require more care to get an accurate solution throughout the full system. COMSOL Multiphysics has a number of user options for refining the mesh grid for particularly difficult problems. Many general PDE problems are difficult to solve, but this one is not. This problem is solved with the time dependent solver with a final of 10 seconds. For more difficult problems, the solver parameters and the solver manager need to be modified. After COMSOL has solved the problem of interest, the Postprocessing Mode can be used to visualise and analyse the system. In this case, the concentration of component *A* is plotted (Figure 3.7).

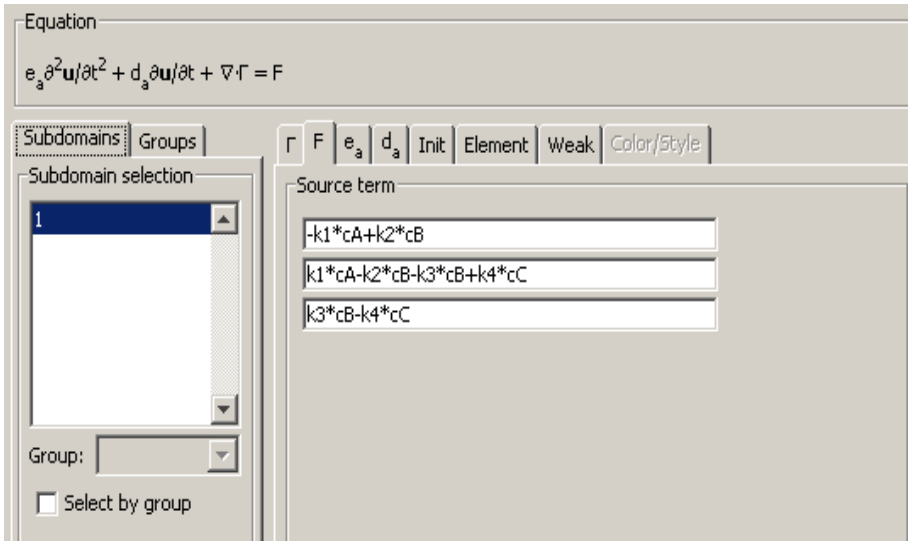

Figure 3.5 Equation setting

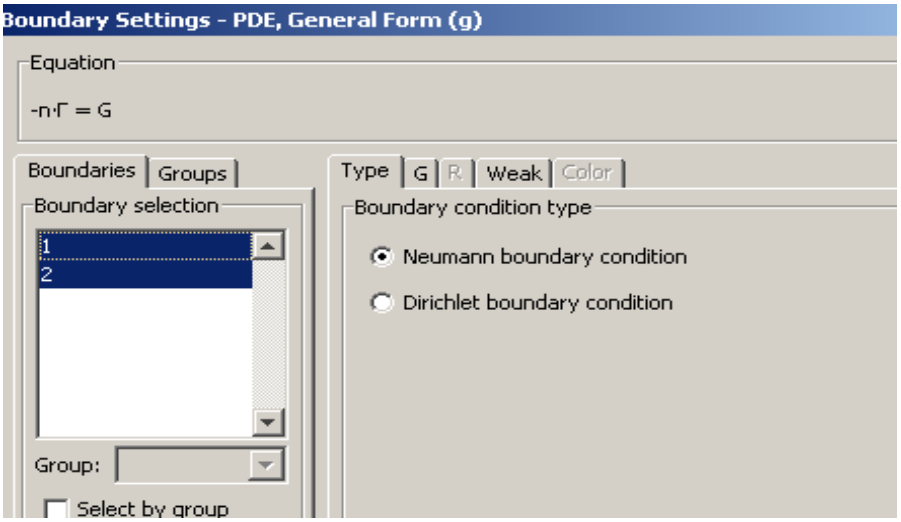

Figure 3.6 Boundary conditions

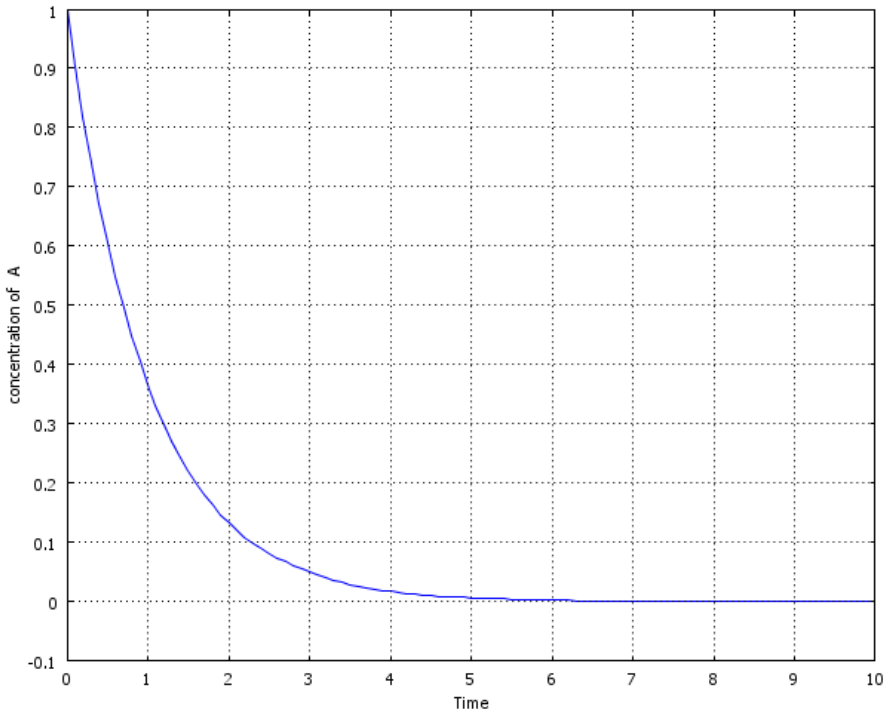

Figure 3.7 The concentration of component *A* plot versus time

Case 2: Diffusion in a Stefan tube

The second example is more complicated than the first one and it was the initial try to solve a Maxwell-Stefan diffusion problem using the COMSOL PDE general form. The detailed description of the problem can be found in Taylor and Krishna (1993, p21-23). The model represents steady state diffusion of acetone and methanol through stagnant air in a Stefan tube. The model description will be presented in Appendix A. The model equations are simply presented as:

$$\begin{gathered} \nabla \cdot N_i = 0 \\ \frac{dx_i}{dz} = \sum_{\substack{j=1 \\ j \neq i}}^{3} \frac{x_i N_j - x_j N_i}{c_t \mathcal{D}_{ij}} \\ N_3 = 0 \end{gathered} \tag{3.2.4}$$

where *N* is the molar diffusion fluxes an *x* is the mole fraction of the components.

We are already familiar with the matrix form:

$$\begin{gathered} \nabla \cdot N_i = 0 \\ -c_t(\nabla x) = [B](N) \end{gathered} \tag{3.2.5}$$

with

$$B_{ii} = \sum_{\substack{k=1 \\ k \neq i}}^{3} \frac{x_k}{\mathcal{D}_{ik}}$$
$$B_{ij} = -\frac{x_i}{\mathcal{D}_{ij}} \qquad (3.2.6)$$

This is a one-dimensional, PDE general form problem with dependent variables x_1, x_2, N_1 and N_2 representing different mole fraction (x) and molar diffusion flux (N) respectively. In the same procedure as in Case 1, the diffusion in a Stefan tube can be solved. The following (Figure 3.8-3.12) presents some of the settings involved in this modelling.

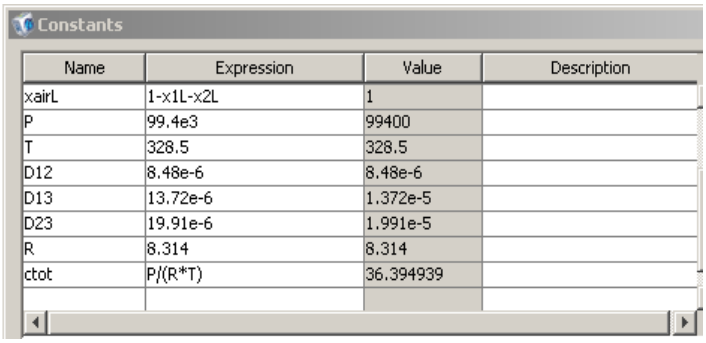

Figure 3.8 Constant setting

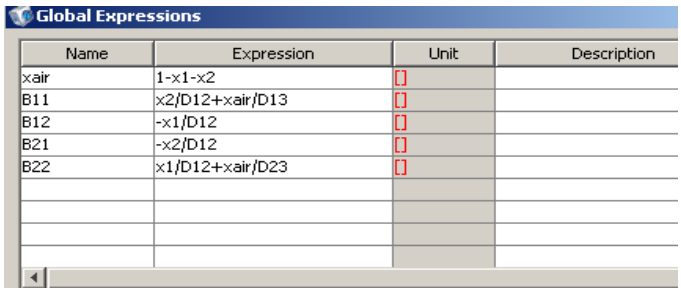

Figure 3.9 Variable setting

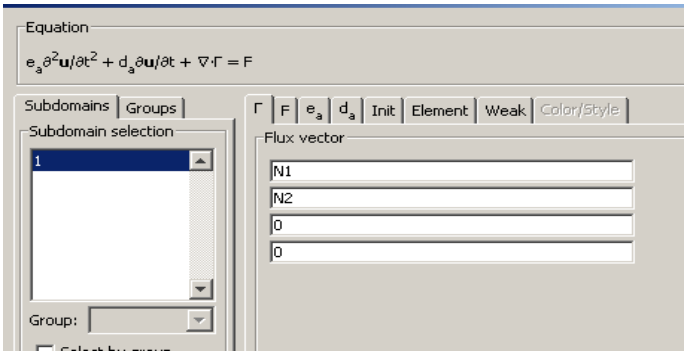

Figure 3.10 Equation setting for Γ

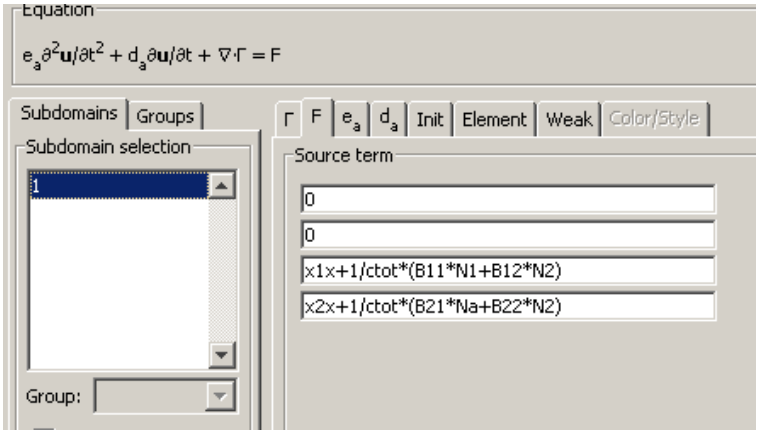

Figure 3.11 Equation setting for *F*

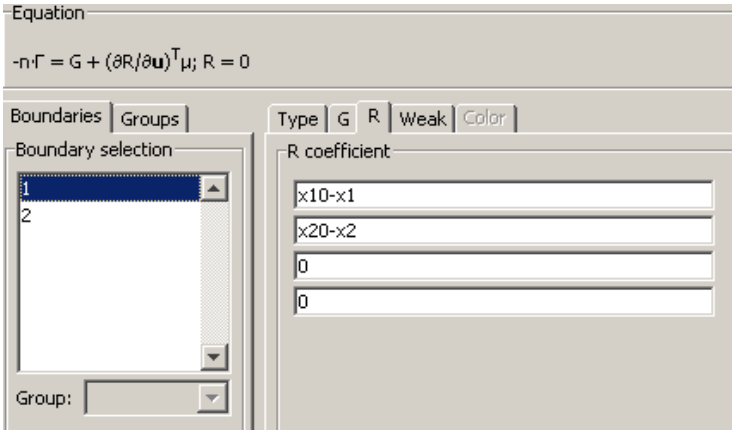

Figure 3.12 Dirichlet boundary setting

The COMSOL numerical results are obtained with 120 meshes and then are compared with analytical results. With 60 meshes the results were clearly different from the exact values. The numerical fluxes are: $N_1 = 1.7831 \times 10^{-3}$ and $N_2 = 3.1282 \times 10^{-3}$ mol/m^{2}s. They are in excellent agreement with the exact values ($N_1 = 1.783 \times 10^{-3}$ and $N_2 = 3.127 \times 10^{-3}$ mol/m^{2}s) given by Taylor and Krishna. The results are plotted in Figure 3.13.

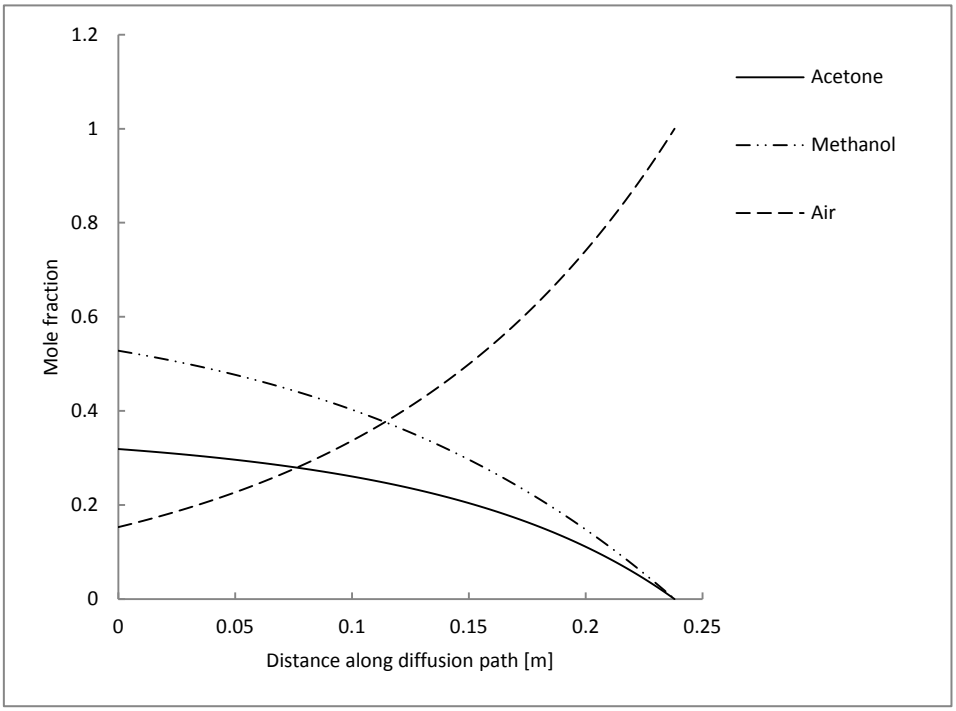

Figure 3.13 Composition profiles in the Stefan diffusion tube

3.3 COMSOL solutions for GMS diffusion in electrolytes

In the author's ME thesis, the model to simulate the diffusion of HCl through a membrane with the length of 0.001 m was set up and solved by MATLAB ODE15s solver. In this example, we want to check the ability of COMSOL Multiphysics to deal with difficult problems and in this case it is the diffusion potential which is not explicitly defined and difficult to solve. HCl is treated as two components: H^+ and Cl^-. Thus, the system is composed of three components: H^+ (1), Cl^- (2) and water (3).

The model equations are:

$$\begin{aligned} \frac{\partial c_i}{\partial t} + \nabla \cdot \boldsymbol{J}_i = 0 \quad i = 1,2 \\ (\boldsymbol{J}) = -c_t[B]^{-1}\left(\nabla x + \frac{x_i z_i}{RT}\Im \nabla \varphi\right) \end{aligned} \tag{3.3.1}$$

Matrix, *B*, is described as:

$$
\begin{gathered}
B_{ii} = \sum_{\substack{j=1 \\ j \neq i}}^{3} \frac{x_j}{\mathcal{D}_{ij}} \quad i = 1,2 \\
B_{ij} = -\frac{x_i}{\mathcal{D}_{ij}} \;\; i,j = 1,2 \\
B_{i3} = c_i z_i \;\; i = 1,2 \\
B_{3j} = z_j \;\; j = 1,2 \\
B_{33} = 0
\end{gathered}
\tag{3.3.2}
$$

x_i is the mole fraction of component i, z_i is the charge number of component i and c_i is the concentration of component i. z_i is the parameter with +1 and -1.

If the matrix B needs to be inverted there is no way to do this in the COMSOL GUI and COMSOL script must be used. Since the matrix inversion will be done externally of the solver this will be a slow process. However we can use an alternative equation:

$$
\left(\nabla x + \frac{\mathrm{x} \cdot \mathrm{z}}{RT} \Im \nabla \varphi\right) = -\frac{1}{c_t}[B](\boldsymbol{J}) \tag{3.3.3}
$$

when i =3, ∇x_3=0 and for convenience $\boldsymbol{J}_3$, which is not a real flux, is introduced:

$$
\boldsymbol{J}_3 = \frac{\Im}{RT} \nabla \varphi \tag{3.3.4}
$$

Here $\Im$ is the Faraday's constant and φ is the diffusion potential.

Because this is an electrolyte system and a diffusion potential is included in the equation, the Maxwell-Stefan diffusion predefined model in COMSOL cannot be used. In order to get a COMSOL solution, the PDE equations in COMSOL are:

$$
\begin{gathered}
\begin{bmatrix} 1 & 0 & 0 & 0 & 0 \\ 0 & 1 & 0 & 0 & 0 \\ 0 & 0 & 0 & 0 & 0 \\ 0 & 0 & 0 & 0 & 0 \\ 0 & 0 & 0 & 0 & 0 \end{bmatrix} \frac{\partial}{\partial t} \begin{bmatrix} c_1 \\ c_2 \\ \boldsymbol{J}_1 \\ \boldsymbol{J}_2 \\ \boldsymbol{J}_3 \end{bmatrix} + \nabla \cdot \begin{bmatrix} \boldsymbol{J}_1 \\ \boldsymbol{J}_2 \\ 0 \\ 0 \\ 0 \end{bmatrix} = \begin{bmatrix} 0 \\ 0 \\ c_t \nabla x_1 + B_{11}\boldsymbol{J}_1 + B_{12}\boldsymbol{J}_2 + B_{13}\boldsymbol{J}_3 \\ c_t \nabla x_2 + B_{21}\boldsymbol{J}_1 + B_{22}\boldsymbol{J}_2 + B_{23}\boldsymbol{J}_3 \\ B_{31}\boldsymbol{J}_1 + B_{32}\boldsymbol{J}_2 + B_{33}\boldsymbol{J}_3 \end{bmatrix} \\
\begin{bmatrix} 0 & 0 \\ 0 & 0 \end{bmatrix} \frac{\partial}{\partial t} \begin{bmatrix} \varphi \\ d\varphi \end{bmatrix} + \nabla \cdot \begin{bmatrix} 0 \\ 0 \end{bmatrix} = \begin{bmatrix} \nabla \varphi - d\varphi \\ \boldsymbol{J}_3 - \frac{\Im}{RT} d\varphi \end{bmatrix}
\end{gathered}
\tag{3.3.5}
$$

For the boundary conditions and initial conditions, readers can refer to the author's ME thesis (Lu, 2007). The COMSOL Multiphysics solution is then compared with MATLAB solution in Figure 3.14:

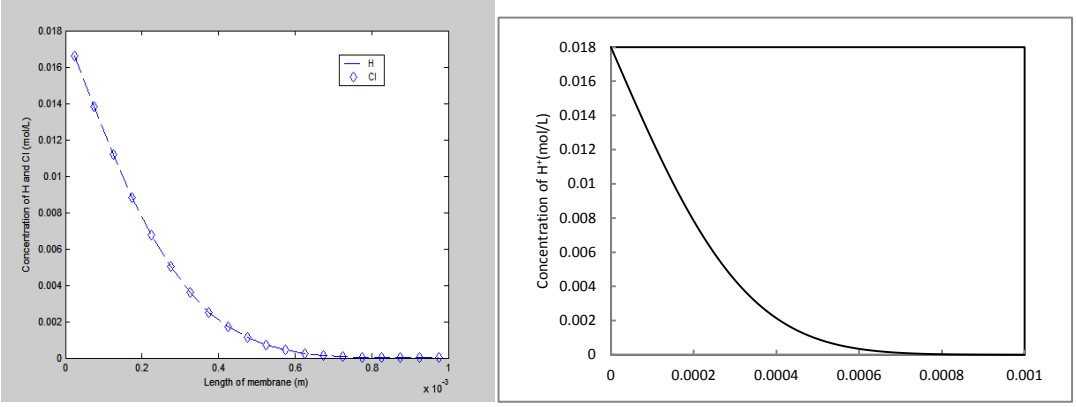

Figure 3.14 The concentration profile of H^+ across the membrane
Left: MATLAB solution (Lu, 2007). Right: COMSOL solution

Then one more component was added and the model was set up to simulate the diffusion of HCl and NaCl through the distance of 0.001m. There are four components in the model: H^+(1), Cl^-(2), Na^+(3) and H_2O(4).

The model equations are:

$$\frac{\partial c_i}{\partial t} + \nabla \cdot \boldsymbol{J}_i = 0 \quad i = 1,2,3$$
$$(\boldsymbol{J}) = -c_t[B]^{-1}\left(\nabla x + \frac{x_i z_i}{RT}\Im \nabla\varphi\right) \tag{3.3.6}$$

in which

$$B_{ii} = \sum_{\substack{j=1 \\ j\neq i}}^{4} \frac{x_j}{\mathcal{D}_{ij}} \quad i = 1,2,3$$
$$B_{ij} = -\frac{x_i}{\mathcal{D}_{ij}} \quad i,j = 1,2,3 \tag{3.3.7}$$
$$B_{i4} = c_i z_i \quad i = 1,2,3$$
$$B_{4j} = z_j \quad j = 1,2,3$$
$$B_{44} = 0$$

$\boldsymbol{J}_4$ is also not a real flux, $J_4 = \frac{\Im}{RT}\nabla\varphi$, and there are 7 variables: x_i (there are 3), $\boldsymbol{J}_i$ (there are 3) and $\nabla\varphi$ with 7 equations. In COMSOL an additional equation is required to obtain φ as seen in equations (3.3.8).

In COMSOL the PDE setting is:

$$\begin{bmatrix} 1 & 0 & \dots & \dots & \dots & \dots & \dots & \dots & 0 \\ 0 & 1 & 0 & & & & & & \vdots \\ \vdots & & 1 & & & & & & \vdots \\ \vdots & & & 0 & & & & & \vdots \\ \vdots & & & & 0 & & & & \vdots \\ \vdots & & & & & 0 & & & \vdots \\ \vdots & & & & & & 0 & & \vdots \\ \vdots & & & & & & & 0 & \vdots \\ 0 & \dots & \dots & \dots & \dots & \dots & \dots & \dots & 0 \end{bmatrix} \frac{\partial}{\partial t} \begin{bmatrix} c_1 \\ c_2 \\ c_3 \\ \boldsymbol{J}_1 \\ \boldsymbol{J}_2 \\ \boldsymbol{J}_3 \\ \boldsymbol{J}_4 \\ \varphi \\ d\varphi \end{bmatrix} + \nabla \cdot \begin{bmatrix} \boldsymbol{J}_1 \\ \boldsymbol{J}_2 \\ \boldsymbol{J}_3 \\ 0 \\ 0 \\ 0 \\ 0 \\ 0 \\ 0 \end{bmatrix}$$

$$= \begin{bmatrix} 0 \\ 0 \\ 0 \\ c_t \nabla x_1 + B_{11}\boldsymbol{J}_1 + B_{12}\boldsymbol{J}_2 + B_{13}\boldsymbol{J}_3 + B_{14}\boldsymbol{J}_4 \\ c_t \nabla x_2 + B_{21}\boldsymbol{J}_1 + B_{22}\boldsymbol{J}_2 + B_{23}\boldsymbol{J}_3 + B_{24}\boldsymbol{J}_4 \\ c_t \nabla x_3 + B_{31}\boldsymbol{J}_1 + B_{32}\boldsymbol{J}_2 + B_{33}\boldsymbol{J}_3 + B_{34}\boldsymbol{J}_4 \\ B_{41}\boldsymbol{J}_1 + B_{42}\boldsymbol{J}_2 + B_{43}\boldsymbol{J}_3 + B_{44}\boldsymbol{J}_4 \\ \nabla\varphi - d\varphi \\ \boldsymbol{J}_4 - \frac{\mathfrak{F}}{RT} d\varphi \end{bmatrix} \tag{3.3.8}$$

The details of this simulation can be found in Appendix C. Figures 3.15 and 3.16 show the concentration profiles of three ions in the centre segment of the membrane over 800 seconds. The comparison between the COMSOL Multiphysics and MATLAB solution shows almost identical concentration results.

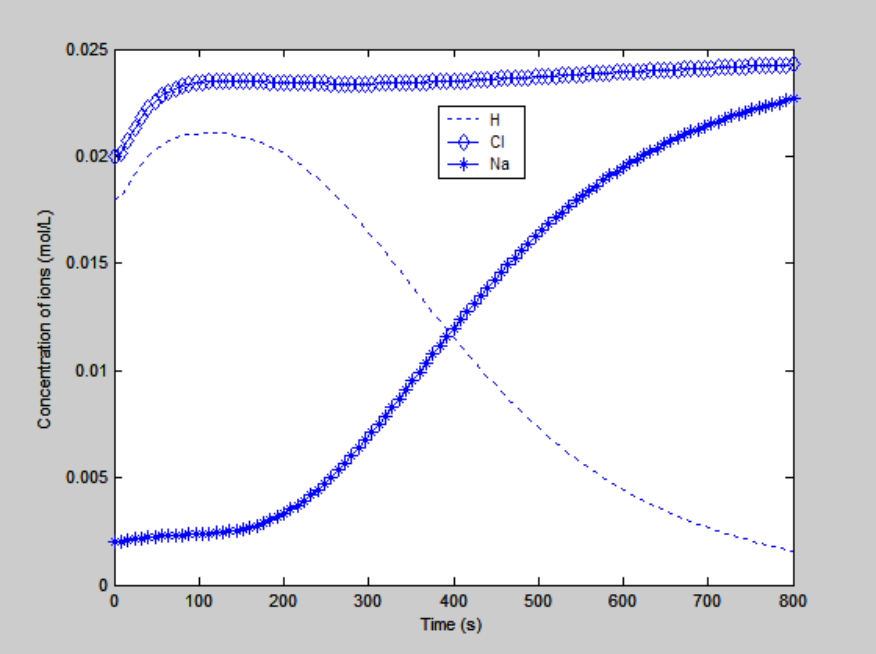

Figure 3.15 MATLAB solutions of concentrations in the centre segment of the membrane over 800 seconds

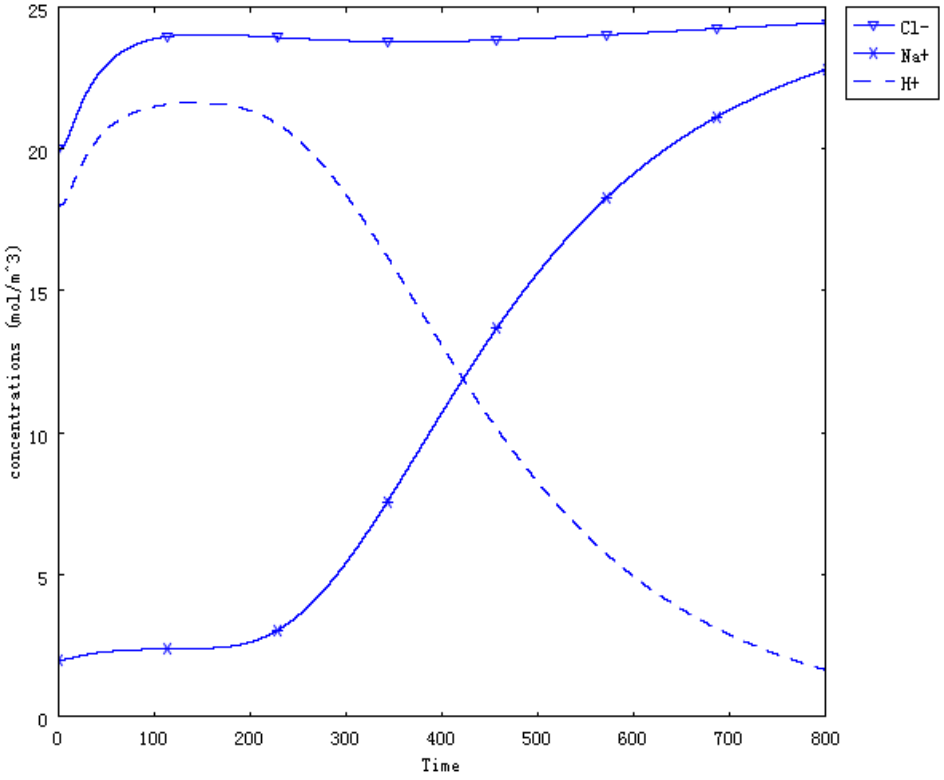

Figure 3.16 COMSOL solution for the same problem of Figure 3.15

In the Sections 2.2.2 and 2.2.3, two diffusion theories were presented. The MS diffusion theory was chosen over the Fick's diffusion theory because the latter does not include other driving forces such as diffusion potential. To show the inadequacy of the Fick's diffusion theory, we will simulate the above same problem by using Fick's theory with no ion-ion interactions and then compare the results with those obtained by Maxwell-Stefan diffusion theory.

The model equations by Fick's diffusion write:

$$\frac{\partial c_i}{\partial t} + \nabla \cdot \boldsymbol{J}_i = 0 \quad i = 1,2,3$$
$$(\boldsymbol{J}) = -c_t[D]\nabla(x) \tag{3.3.9}$$

For the comparison, the initial conditions are:

$$c_{H^+0} = 18 \quad c_{Cl^-0} = 20 \quad c_{Na^+0} = 2 \ \text{mol/m}^3 \tag{3.3.10}$$

The left boundary is set to insulation symmetry. The right boundary has the concentration:

$$c_{H^+} = 18 \quad c_{Cl^-0} = 48 \quad c_{Na^+0} = 30 \ \text{mol/m}^3 \tag{3.3.11}$$

Figures 3.17, 3.18 and 3.19 show the comparison of concentrations in the centre between the Maxwell-Stefan diffusion and Fickian diffusion models.

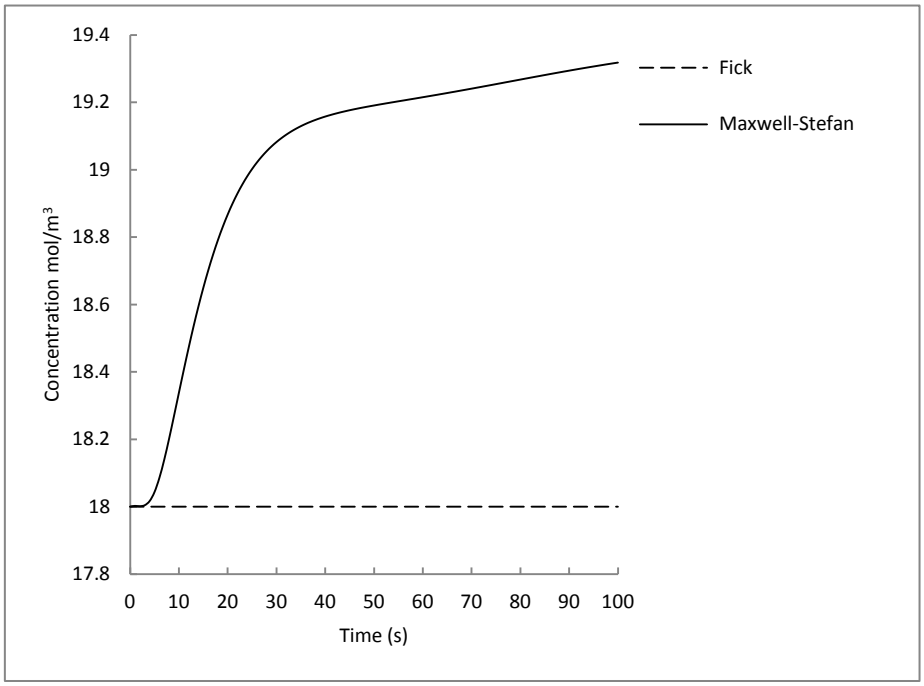

Figure 3.17 Concentration comparison of H^+

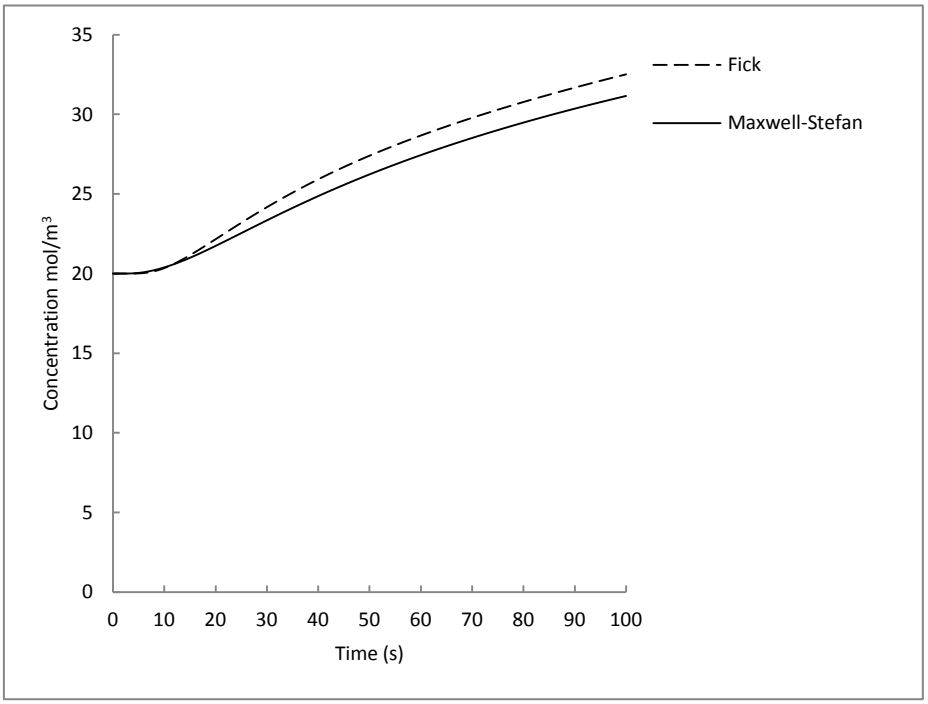

Figure 3.18 Concentration comparison of Cl^-

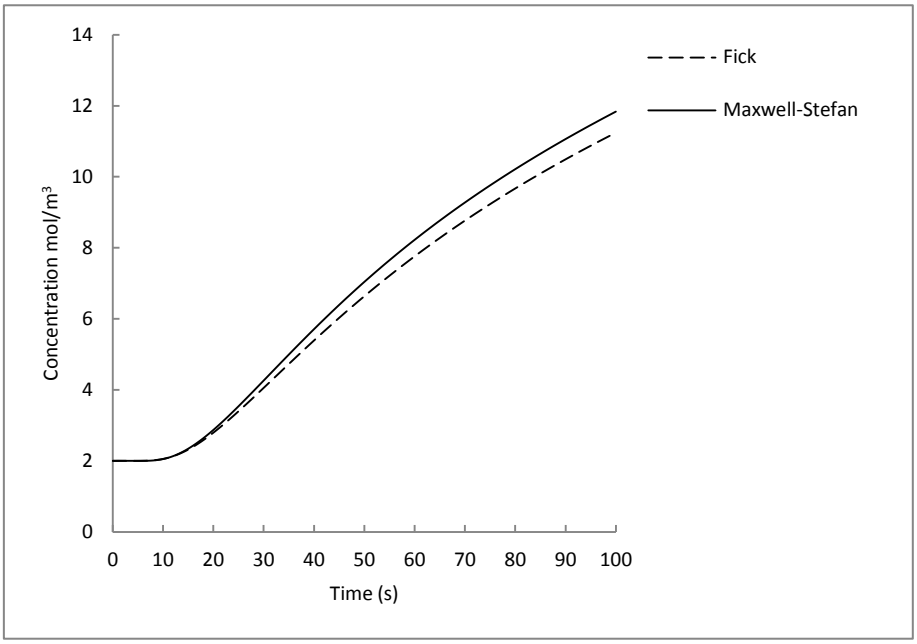

Figure 3.19 Concentration comparison of Na^+

The behaviours of Cl^- and Na^+ obtained by Fick and Maxwell-Stefan computations are very similar, as one can see on Figure 3.18 and 3.19. Nevertheless, there are some significant variations on the values of H^+ shown by Figure 3.17. These variations can be explained by the diffusion potential. The high concentration gradients of Cl^- and Na^+ generate strong fluxes. If the diffusion of Cl^- is a little faster than that of Na^+, the electroneutrality condition of the region is not satisfied any more. An electrical potential across the region is then set up due to the excess of Cl^- over Na^+ and this electrostatic force will drag H^+ moving with Na^+ to recover the electroneutrality condition. This cannot be explained by Fick's diffusion theory. By Fick's diffusion theory H^+ will not move because there is no concentration gradient for H^+ across the region. Wesselingh and Krishna (2000) have also observed that in a solution of sodium chloride and hydrogen chloride, sodium will diffuse against its gradient, in the direction opposite to what we expect from Fick's law.

In summary COMSOL Multiphysics has some advantages in solving PDEs over other softwares. Firstly, COMSOL Multiphysics is flexible. Users can freely define their own equations in its general form. The above examples were all solved by using COMSOL Multiphysics general form. Secondly COMSOL Multiphysics can solve a

wide range of problems. It can solve linear systems of ODEs. This is illustrated by the isomerisation reactions in Section 3.2. Most importantly, COMSOL Multiphysics has the ability to solve multicomponent diffusion problems based on the GMS equations. It can solve the diffusion of three gases in a Stefan tube as shown in Section 3.2. It can also solve a multicomponent diffusion problem in electrolytes with an implicitly defined diffusion potential shown by the diffusion of HCl and NaCl. Because the GMS equations in electrolytes are the basic equations in the protein gel modelling, COMSOL Multiphysics version 3.5 was chosen as the numerical tool for the remainder of this project.

4 The mathematical model of protein gel swelling

In this chapter, the mathematical model of protein gel swelling will be set up. From the discussion in Chapter 2, it can be seen that the model will include molar diffusion, chemical reaction and mechanical structures. This multiphysical process needs a suitable mathematical model that can reflect the inside physics and at the same time avoid unnecessarily over-complicating the problem. Therefore, the protein gel under study has a simple geometry and a 2-dimensional rectangular gel is considered. The system considered is a two phase system: a protein matrix immersed in a solution of NaOH and NaCl (or HCl and NaCl). The schematic picture is shown in Figure 4.1.

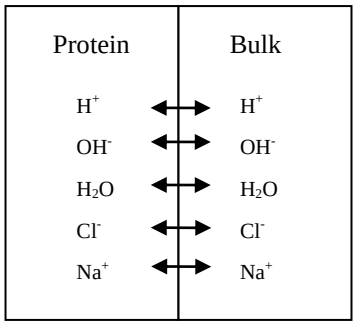

Figure 4.1 Schematic of protein gel immersed in a solution

The whole physical and chemical process involved can be described as follows. The solution components, H_2O, OH^-, H^+, Na^+ and Cl^-, diffuse into the protein gel. The protein in the gel dissociates losing or gaining hydrogen ions (H^+) depending on the pH of the solution. Hydrogen ions react with hydroxide ions (OH^-) and then extra water is produced. This extra water, in association with water diffusing into the gel, will cause the gel network structure to swell. This is a multicomponent system with 7 species in the system: H^+, OH^-, H_2O, Cl^-, Na^+, total protein and undissociated hydrogen ion in the protein (HProtein).

Although we want as few assumptions as possible in the model, there are still some assumptions. The frictional forces experienced by the gel are negligible because the

solution surrounding the gel acts as a lubricant. The system is at the constant temperature and external pressure.

As ions move into a charged gel network, they may react with the fixed charged side groups as shown in Figure 4.2. That is, diffusing H^+ or OH^- in solvent can react with corresponding basic or acidic structures on the network, and such diffusion-reaction can significantly slow down the overall ion transport process (Lee, 1996).

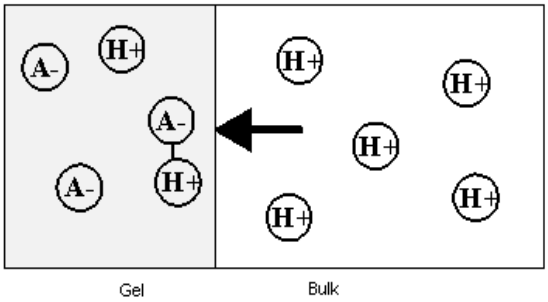

Figure 4.2 Reaction of H^+ with basic structure of gel network (A- represents charged protein)

The protein dissociation reaction can be written as:

$$\text{Protein with H} \leftrightarrow \text{Protein}^- + H^+ \quad r_1$$

and

$$H^+ + OH^- \leftrightarrow H_2O \quad r_2$$

in which the rates, *r*, are the reaction rates to the right.

The dissociation equilibria for the two reactions are:

$$K_a = \frac{[H^+][Protein^-]}{[HProtein]} \qquad (4.1)$$
$$K_w = [H^+][OH^-]$$

There are 7 species in the system: H^+, OH^-, H_2O, Cl^-, Na^+, total protein and HProtein. Their concentrations are denoted by c_1, c_2, c_3, c_4, c_5, c_6 and c_7 respectively. Their diffusion fluxes relative to the protein matrix are $\boldsymbol{J}_1$, $\boldsymbol{J}_2$, $\boldsymbol{J}_3$, $\boldsymbol{J}_4$, $\boldsymbol{J}_5$, $\boldsymbol{J}_6$ and $\boldsymbol{J}_7$. Since no protein molecule diffuses relative to itself, $\boldsymbol{J}_6$ and $\boldsymbol{J}_7$ are equal to zero. For

convenience, some important variables and parameters are tabulated in Table 4.1.

Table 4.1 Modelling variables and parameters

species	H^+	OH^-	H_2O	Cl^-	Na^+	Total Protein	HProtein
concentration	c_1	c_2	c_3	c_4,	c_5	c_6	c_7
reaction rate	r_1-r_2	-r_2	r_2	0	0	0	-r_1
diffusion flux	$\boldsymbol{J}_1$	$\boldsymbol{J}_2$	$\boldsymbol{J}_3$	$\boldsymbol{J}_4$	$\boldsymbol{J}_5$	$\boldsymbol{J}_6$=0	$\boldsymbol{J}_7$=0
charges	+1	-1	0	-1	+1	z_p	0

In the following parts, a detailed mathematical model consisting of diffusion, mass balance, and mechanical swelling will be presented. Figure 4.3 shows the model components.

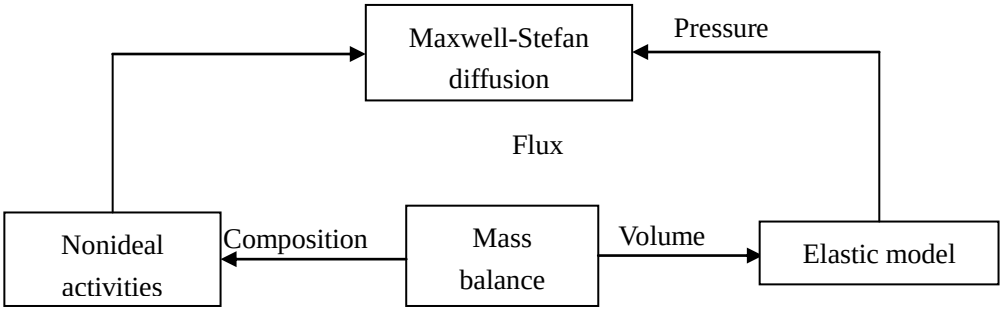

Figure 4.3 Model components

4.1 Diffusion model

As discussed in Chapter 2, the generalised Maxwell-Stefan equation will be used to describe the diffusion process. Although many studies have been based on Fickian diffusion, a proof of the inadequacy of Fick's diffusion theory has been given in Chapter 3. From equation (2.3.10) in Chapter 2, the generalised Maxwell-Stefan equation for electrolytes can be written for each of the *n* components as:

$$-\frac{x_i}{RT}\nabla_{T,P}\mu_i+\frac{(\omega_i-c_i\bar{V}_i)}{c_tRT}\nabla P-\frac{x_iz_i}{RT}\Im\nabla\varphi=\sum_{\substack{j=1\\ j\neq i}}^{n}\frac{x_j\boldsymbol{J}_i^n-x_i\boldsymbol{J}_j^n}{c_t\text{Đ}_{ij}}\quad i \tag{4.1.1}$$

$$=1,2,\dots,n$$

where x_i - mole fraction of component *i*

ω_i - mass fraction of component *i*

μ_i - chemical potential,

R - idea gas constant, 8.31414 [J/mol K]

T - temperature [K]

P - system pressure, [Pa]

$\bar{V}_i$ - partial molar volume of component *i* [m^3/mol]

z_i - charge number of component *i*

$\Im$ - Faraday's constant, 9.65×10^4 [C/mol]

ϕ - electrical potential [V]

c_t - total molar concentration [mol/m^3]

$\boldsymbol{J}_i^n$- molar flux of component *i* relative to component *n* [mol/m^2 s]

Đ_{ij}- Maxwell-Stefan diffusivity between species *i* and *j* [m^2/s]

Looking at equation (4.1.1), one can see that the generalised Maxwell-Stefan (GMS) equation is very flexible. It does yield Fick's equation as a limiting case for some simple problems, such as dilute and thermodynamically ideal solutions. It can also take into account effects such as viscous flow, electrostatic potential, pressure, and thermodynamic activity.

Therefore, the diffusion flux of component *i*, $\boldsymbol{J}_i^n$, is governed by the Generalised Maxwell-Stefan equations (4.1.1). This can be expressed in matrix form:

$$\Gamma\nabla\mathrm{x}+\frac{(\mathrm{c}\cdot\overline{\mathrm{V}}-\omega)}{c_tRT}\nabla P+\frac{\mathrm{x}\cdot\mathrm{z}}{\mathrm{RT}}\Im\nabla\varphi=-\frac{1}{c_t}\mathrm{B}\mathbf{J}^n \tag{4.1.2}$$

where Γ is a *n*-1 square matrix.

$$\Gamma_{ij} = \delta_{ij} + x_i \left.\frac{\partial \ln \gamma_i}{\partial x_j}\right|_{T,P,\Sigma} \tag{4.1.3}$$

Here γ_i is the activity coefficient and δ_{ij} equals one only when $i=j$. In the case of an ideal solution, the activity coefficients are unity and thus Γ is an identity matrix.

B is an n-1 square matrix with elements:

$$\begin{aligned} B_{ii} &= \sum_{j \neq i} \frac{x_j}{\mathcal{D}_{ij}} \quad i = 1, \ldots, n-1 \\ B_{ij} &= -\frac{x_i}{\mathcal{D}_{ij}} \quad i \neq j \end{aligned} \tag{4.1.4}$$

It can be assumed that initially a system is electrically neutral everywhere:

$$\sum_i z_i x_i(t_0) = 0 \tag{4.1.5}$$

and to retain neutrality there must be no net current:

$$\sum_i z_i \boldsymbol{J}_i^n = 0 \tag{4.1.6}$$

Krishna (1987) combined equations (4.1.2) and (4.1.6) to give an augmented matrix from which $\boldsymbol{J}_i$ and $\nabla\phi$ could be determined.

$$\begin{bmatrix} -c_t \left(\Gamma \nabla \mathrm{x} + \dfrac{(\mathrm{c} \cdot \bar{\mathrm{V}} - \omega)}{c_t RT} \nabla P \right) \\ \cdots\cdots\cdots\cdots\cdots\cdots\cdots\cdots\cdots\cdots\cdots\cdots \\ 0 \end{bmatrix} = \begin{bmatrix} [\mathrm{B}] & \vdots & [\mathrm{c} \cdot \mathrm{z}] \\ \cdots\cdots\cdots & \vdots & \cdots\cdots\cdots \\ [\mathrm{z}] & \vdots & 0 \end{bmatrix} \begin{bmatrix} [\mathbf{J}^n] \\ \cdots\cdots \\ \dfrac{\Im}{RT} \nabla\varphi \end{bmatrix} \tag{4.1.7}$$

In the system concerned, diffusion only happens when electrolytes such as NaOH and NaCl diffuse into and out the system. The protein matrix is considered as a reference structure and no protein molecule diffuses into the solution from the matrix. Therefore, equation (4.1.7) does not apply to protein.

One advantage of the Maxwell-Stefan equation is its ability to deal with thermodynamic non-idealities with the matrix Γ. If the solution is non-ideal, activity coefficients are required to calculate Γ by equation (4.1.3). Many researchers have shown that ideal solution modelling can get diffusion behaviours in good agreement with experiments and thus in most models found in literature, an ideal solution is assumed. However in this research this assumption was not made as doing so would

defeat the purpose of using the Maxwell-Stefan equations. A thorough explanation of how to obtain the thermodynamic matrix can be found in the appendix of Taylor and Krishna (1993) and some binary and multicomponent models are also given. The procedure of obtaining the matrix Γ is reproduced in the following section.

4.2 Thermodynamic matrix Γ

In GMS diffusion, the elements of the thermodynamic matrix are defined by equation (4.1.3):

$$\Gamma_{ij} = \delta_{ij} + x_i \left.\frac{\partial \ln \gamma_i}{\partial x_j}\right|_{T,P,\sum} \tag{4.2.1}$$

The symbol $\sum$ is used to indicate that the differentiation of $\ln\gamma_i$ with respect to mole fraction x_j is to be carried out while keeping the mole fractions of all other components constants except the nth. The mole fraction of species n must be eliminated using the fact that the summation of x_i is unity.

Let Q be the dimensionless excess Gibbs energy:

$$Q = \frac{G^{EX}}{RT} = \sum_{i=1}^{n} x_i \ln \gamma_i \tag{4.2.2}$$

γ_i is defined by:

$$\ln \gamma_i = \left.\frac{\partial (n_t Q)}{\partial n_i}\right|_{T,P,n_k,k\neq i=1,\ldots n} \tag{4.2.3}$$

where n_i is the number of moles of species i in solution and n_t is the total number of moles in the mixture.

$$n_t = \sum_{i=1}^{n} n_i \tag{4.2.4}$$

The partial derivative in equation (4.2.3) may be expanded to give:

$$\ln \gamma_i = Q + n_t \left.\frac{\partial Q}{\partial n_i}\right|_{T,P,n_k,k\neq i=1,\ldots n} \tag{4.2.5}$$

It is useful to replace the partial derivative of Q with respect to the number of moles

with the partial derivatives of Q with respect to the mole fractions x_i defined by:

$$x_i = \frac{n_i}{n_t} \tag{4.2.6}$$

A change in the number of moles of species *i* changes the mole fractions of all species, not just the mole fraction of species *i*. Thus we may express the partial derivatives in equation (4.2.5) as:

$$\frac{\partial Q}{\partial n_i} = \sum_{j=1}^{n} Q_j \left.\frac{\partial x_j}{\partial n_i}\right|_{n_k} \tag{4.2.7}$$

where

$$Q_j = \left.\frac{\partial Q}{\partial x_j}\right|_{\bar{\Sigma}} \tag{4.2.8}$$

The symbol $\bar{\Sigma}$ is to emphasise that the mole fractions of all species except the *j*th are kept constant while performing the differentiation. The requirement that the mole fractions sum to unity is not used to eliminate any mole fraction before the differentiation has been carried out.

The mole fraction derivatives may be obtained by differentiating equation (4.2.6):

$$\left.\frac{\partial x_j}{\partial n_i}\right|_{n_k} = \frac{\delta_{ij} - x_j}{n_t} \tag{4.2.9}$$

with δ_{ij} is the Kronecker delta.

By combining equation (4.2.5) with equations (4.2.7) and (4.2.9) the expression for the activity coefficients γ_i can be obtained:

$$\ln \gamma_i = Q + Q_i - \sum_{k=1}^{n} x_k Q_k \tag{4.2.10}$$

The derivatives of $\ln\gamma_i$ with respect to mole fraction x_j are obtained on differentiation of the above equation as:

$$\left.\frac{\partial \ln \gamma_i}{\partial x_j}\right|_{\bar{\Sigma}} = Q_{ij} - \sum_{k=1}^{n} x_k Q_{kj} \tag{4.2.11}$$

in which

$$Q_{ij} = \left.\frac{\partial Q_i}{\partial x_j}\right|_{\Sigma} \tag{4.2.12}$$

They are the partial derivatives of Q_i with respect to mole fraction x_j. The Q_{ij} are symmetric:

$$Q_{ij} = Q_{ji} \tag{4.2.13}$$

Equation (4.2.11) provides the unconstrained mole fraction derivatives of $\ln\gamma_i$, and the differentiation of Q_i must be done with the fact that mole fractions sum to unity in order to simplify the expression for Q_i. The constrained mole fraction derivatives needed in the thermodynamic matrix Γ_{ij} are given in terms of the unconstrained derivatives by:

$$\left.\frac{\partial \ln\gamma_i}{\partial x_j}\right|_{\Sigma} = \left.\frac{\partial \ln\gamma_i}{\partial x_j}\right|_{\Sigma} - \left.\frac{\partial \ln\gamma_i}{\partial x_n}\right|_{\Sigma} = Q_{ij} - Q_{in} - \sum_{k=1}^{n} x_k\left(Q_{kj} - Q_{kn}\right) \tag{4.2.14}$$

Finally, the elements of the thermodynamic matrix are given by:

$$\Gamma_{ij} = \delta_{ij} + x_i\left\{Q_{ij} - Q_{in} - \sum_{k=1}^{n} x_k\left(Q_{kj} - Q_{kn}\right)\right\} \tag{4.2.15}$$

The Pitzer's model discussed in Chapter 2 is based on molalities. However, in order to obtain thermodynamic matrix in Maxwell-Stefan diffusion it is necessary to develop an equation based on a mole fraction rather than on a molality. That means a mole-fraction-based excess Gibbs free energy is needed. Such mole-fraction-based model has been developed by Pitzer and his co-workers. The excess Gibbs energy of the mixed solution is assumed to consist of two parts: short-range force terms accounted for by a Margules expansion and a long range force by Pitzer-Debye-Hückel term. A general Margules expansion is based on three suffixes:

$$\begin{aligned} Q = \frac{G^S}{RT} = &\sum_{n'}\sum_{n} x_{n'}x_n W_{n',n} + \sum_{n}\sum_{c}\sum_{a} x_n x_I F_c F_a W_{n,ca} \\ &+ \frac{x_I^2}{2}\left[\sum_{c'}\sum_{c}\sum_{a} F_{c'}F_c F_a W_{c'a,ca}\right. \\ &\left. + \sum_{a'}\sum_{a}\sum_{c} F_{a'}F_a F_c W_{ca',ca}\right] \end{aligned} \tag{4.2.16}$$

x_n and $x_{n'}$ represent the mole fractions of neutral species, and x_I is the total mole

fraction of ions. For the ions the cation fractions are F_c, $F_{c'}$, the anion fractions are F_a, $F_{a'}$, and W's are binary and ternary parameters. Technically all of the binary parameters can be determined from two component systems. Presumably all ternary parameters could be determined from three-component systems. However, practically most of these parameters are not available.

In this study, moderate concentrations are involved and to avoid many unknown parameters it is reasonable to only consider the long range Gibbs excess energy. If the excess Gibbs energy is described by Pitzer-Debye-Hückel:

$$Q = \frac{G^{DH}}{RT} = -\frac{4A_x I_x}{b_x} ln\left[\frac{1 + b_x I_x^{1/2}}{1 + b_x (I_x^0)^{1/2}}\right] + \sum_c \sum_a x_c x_a B_{ca} \mathrm{g}\left(\alpha I_x^{1/2}\right) \quad (4.2.17)$$

A_x is the Debye-Hückel parameter on a mole fraction basis (2.917 for water at 298.15K). The term I_x^0 is the ionic strength corresponding to the reference state upon which the activity coefficients of the ions are based. For the pure fused salt reference state, it is $z_j^2/2$ for a symmetrical electrolyte. For a reference state of infinite dilution, it is zero. This study belongs to the latter.

The parameter b_x is the closest approach parameter. It can be calculated (Pitzer and Simonson, 1986). However, in practice b_x is treated empirically. In multicomponent systems it complicates the equations greatly to make b_x dependent on the composition of ionic components. It has been found satisfactory to set b_x constant and equal to 14.9 for all electrolytes as suggested by Pitzer et al (Pitzer, 1991; Pitzer and Simonson, 1986).

The parameter α can be written as α_x to avoid ambiguity with that in molal basis equations. Its magnitude is expected to be larger than the α in the molality equations by the factor of 7.45. Therefore values in the range 10 to 15 are expected. The B_{ca} term is related to $\beta^{(1)}$ term in the molality based equations and it is specific to each electrolyte.

The function g(x) is the same as that described in the molality system:

$$\mathrm{g}(x) = \frac{2[1-(1+x)\exp(-x)]}{x^2} \tag{4.2.18}$$

Ionic strength on a mole fraction basis is defined as:

$$I_x = \frac{1}{2}\sum_i x_i z_i^2 \tag{4.2.19}$$

The activity coefficients of the solvent and ions are derived as:

$$ln\gamma_w = \frac{2A_x I_x^{3/2}}{1+b_x I_x^{1/2}} + \sum_c \sum_a x_c x_a B_{ca} \exp\left(-\alpha_x I_x^{1/2}\right) \tag{4.2.20}$$

and

$$\begin{aligned} ln\gamma_M = -z_M^2 A_x \left[\frac{2}{b_x} ln\left(1+b_x I_x^{1/2}\right) + \frac{I_x^{1/2}\left(1-2\frac{I_x}{z_M^2}\right)}{1+b_x I_x^{1/2}}\right] \\ + \sum_a x_a B_{Ma} \mathrm{g}\left(\alpha_x I_x^{1/2}\right) \\ - \sum_c \sum_a x_c x_a B_{ca} \left[\frac{z_M^2 \mathrm{g}\left(\alpha_x I_x^{1/2}\right)}{2I_x} \right. \\ \left. + \left(1-\frac{z_M^2}{2I_x}\right)\exp(-\alpha_x I_x)\right] \end{aligned} \tag{4.2.21}$$

For an anion *X*, one changes *M* to *X*, *c* to *a*, and *a* to *c* in the above equation.

Figure 4.4 shows the activity coefficient of Na^+ in NaCl and NaOH solution calculated by Pitzer's method and Pitzer-Debye-Hückel respectively. The two methods produce very close results when the concentration of Na^+ is less than 0.2 M. When the concentration of Na^+ is between 0.2 and 0.6 M, the activity of Na^+ by Pitzer-Debye-Hückel is slightly lower than that by Pitzer's method. This is simply because the former method ignored the short range interaction between ions. The long range Pitzer-Debye-Hückel equation can be used to describe thermodynamics because the range of Na^+ concentration in this research is under 0.2 M.

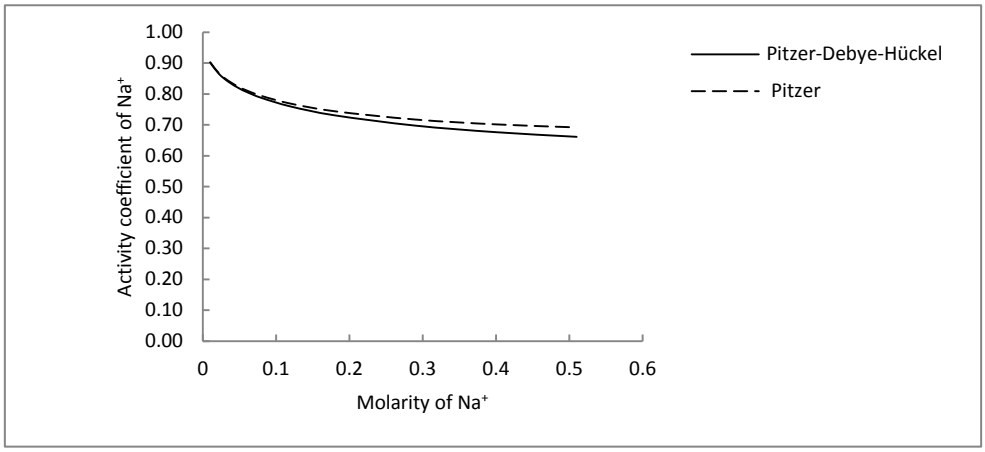

Figure 4.4 Activity coefficient of Na^+ in NaCl and NaOH solution by two methods

The presence of a polyelectrolyte is likely to lower the activity of the surrounding ions and it is possible that counter-ion condensation will occur (Manning, 1969a; 1969b). As has been discussed in Section 2.4.3, the influence of protein charged number on activity coefficients can be solved by Manning's condensation theory. Using equations (2.4.60) and (2.4.61) presented in Section 2.4.3 one can easily calculated activity coefficients of ions in polyelectrolyte solutions.

In summary the calculation of thermodynamics of ions in a polyelectrolyte gel is divided into two parts. Pitzer's method is used to get activity coefficients of ions in electrolytes and equations (2.4.38) to (2.4.47) are presented in Section 2.4.2. Manning condensation theory (equations (2.4.60) and (2.4.61)) is needed to have activity coefficients of ions with protein gel influence. Then the overall activity coefficients can be obtained by equation (2.4.68). For water activity coefficients, the similar procedure is carried out. The osmotic coefficient in electrolytes can be obtained by equation (2.4.40). The osmotic coefficient with the influence of a protein gel is obtained by equation (2.4.62). The overall osmotic coefficient is obtained by equation (2.4.69). Water activity coefficient in the protein gel is then calculated by equation (2.4.48). Finally equation (4.2.1) is used to calculate the thermodynamic factor in the GMS equations.

An alternative way is to use equation (4.2.15) to obtain the thermodynamic matrix Γ.

Equation (4.2.15) does not required the activity coefficients but the derivatives of the excess Gibbs energy. However, the excess Gibbs energy cannot be found from Manning's condensation theory. Therefore, this method cannot be applied in this thesis. However, for the GMS equations in pure electrolyte systems it is easy to use because the complicated calculation of activity coefficients of ions is avoided.

In this thesis, the overall activity coefficients were obtained first and then equation (4.2.1) was used to obtain the thermodynamic matrix. In COMSOL numerical derivatives can be obtained for equation (4.2.1) using the built-in function "diff".

4.3 Diffusivities

In order to solve the Maxwell-Stefan equations, the values for the Maxwell-Stefan diffusivities between component pairs, namely anion, cation, water and gel, are needed. The first major problem here is simply that there is no tabulated data available for the diffusivities between polymer and either ions or water. Additionally, there is no data for the diffusivities between likely charged ions. Fortunately, Wesselingh et al. (1995) provides sufficient information to make it possible to estimate the order of magnitude of these values.

For a gel free solution, the diffusion coefficients of plus/plus and minus/minus ion pair are negative, with the order of magnitude between 10^{-10} and 10^{-13} m^2s^{-1}. For a solution containing a negatively charged gel, if the gel is considered as a solid matrix, the diffusion coefficients of water/gel, cation/water, anion/water and anion/gel are the values in free solution with a tortuosity correction, between 10^{-9} and 10^{-10} m^2s^{-1}. The diffusivity of cations/gel depends on several things, such as swelling, polymer morphology, ion size, etc. For ions with a single charge, the diffusivity is about 10^{-12} m^2s^{-1}. For ions with a double and triple charge, it is somewhere between 10^{-13} and 10^{-14} m^2s^{-1}. The diffusion coefficients are obtained from Wesselingh and co-workers and they are shown in Table 4.2. In some cases typical values are selected from

graphs.

When only one electrolyte is involved in diffusion, the diffusion coefficient of ion-ion can be calculated by the equation (4.3.1) (Wesselingh and Krishna, 2000):

$$\mathbb{D}_{+,-} = 2\left(\frac{1}{\mathbb{D}_{+,w}} + \frac{1}{\mathbb{D}_{-,w}}\right)^{-1} \tag{4.3.1}$$

where $\mathbb{D}_{+,w}$ and $\mathbb{D}_{-,w}$ represent the diffusion coefficients of cation/water and anion/water respectively.

Table 4.2 Diffusion coefficients used

Coefficient	Value	Ref
$Đ_{H+,water}$	$9.3\text{x}10^{-9}$	Wesselingh and Krishna (2000)
$Đ_{Na+,water}$	$1.3\text{x}10^{-9}$	Wesselingh and Krishna (2000)
$Đ_{Na+,protein}$	$5\text{x}10^{-11}$	Wesselingh et al. (1995)
$Đ_{OH-,water}$	$5.3\text{x}10^{-9}$	Wesselingh and Krishna (2000)
$Đ_{OH-,protein}$	$5.3\text{x}10^{-10}$	Kraaijeveld et al. (1995)
$Đ_{Cl-,water}$	$2\text{x}10^{-9}$	Wesselingh and Krishna (2000)
$Đ_{Cl-,protein}$	$2\text{x}10^{-10}$	Kraaijeveld et al. (1995)
$Đ_{water,protein}$	$1.8\text{x}10^{-9}$	Wesselingh et al. (1995)

When there is more than one electrolyte, Wesselingh and Krishna (2000) also presented an empirical equation for ion-ion diffusion coefficients relating them to ion-water diffusion coefficients:

$$\mathbb{D}_{+,-} = \frac{\mathbb{D}_{+,w} + \mathbb{D}_{-,w}}{2} \frac{i^{0.55}}{|z_+ z_-|^{2.3}} \tag{4.3.2}$$

where

$$i = 0.5 \sum_i z_i^2 x_i \tag{4.3.3}$$

The same equation applied for $\mathbb{D}_{-,-}$, but with a negative sign.

Generally, the accuracy of the model will be limited by the accuracy of these values due to such estimation.

4.4 Mass balance

It was found that there were two obstacles for setting up mass balance equations in this thesis. Firstly the general material balance equations in literature are mostly applied for fixed geometries. It is necessary to verify that those equations are also applicable for moving geometries. Secondly the reaction rates in equations can cause stiffness and hence numerical instability in the simulation. Therefore an alternate set of equations is required not only to avoid the numerical instability but also to keep the physics unchanged. These two obstacles were overcome in Section 2.7.

In Section 2.7, it was shown that the point equation describing the mass balance is independent of a control volume. In a system with chemical reactions, the mass balance equation for species can be rewritten as:

$$\frac{\partial c_i}{\partial t} + \nabla \cdot (\boldsymbol{J}_i^a + c_i \boldsymbol{u}^a) = \boldsymbol{\zeta} \tag{4.4.1}$$

with $\boldsymbol{\zeta}$ defined by:

$$\boldsymbol{\zeta} = \sum_j v^j R^j \tag{4.4.2}$$

where v^j is the stoichiometric coefficient of species i in the jth reaction and R^j is the reaction rate in the jth reaction. Here the arbitrary reference velocity, $\boldsymbol{u}^a$, is the velocity of the protein structure swelling and will be denoted by $\boldsymbol{u}_p$ later.

The reaction rates can cause stiffness so an alternate set of equations are to be solved instead of equation (4.4.1) by using Di Toro's (1976) transformation method. Details of the mathematical proof of Di Toro method can be found in Section 2.7.1.

Reactions involved in the system under study have already been presented in the beginning of this chapter as:

$$\begin{aligned} Protein\ with\ H &\leftrightarrow Protein\ dissociated + H^+ \quad r_1 \\ H^+ + OH^- &\leftrightarrow H_2O \quad r_2 \end{aligned} \tag{4.4.3}$$

in which r represents the reaction rate. Concentration variables can be found in Table 4.1 and the mass balance equation for each component can be written as:

$$\begin{aligned} \frac{\partial c_1}{\partial t} &= -\nabla \cdot \boldsymbol{N}_1 + r_1 - r_2 \\ \frac{\partial c_2}{\partial t} &= -\nabla \cdot \boldsymbol{N}_2 - r_2 \\ \frac{\partial c_3}{\partial t} &= -\nabla \cdot \boldsymbol{N}_3 + r_2 \\ \frac{\partial c_4}{\partial t} &= -\nabla \cdot \boldsymbol{N}_4 \\ \frac{\partial c_5}{\partial t} &= -\nabla \cdot \boldsymbol{N}_5 \\ \frac{\partial c_6}{\partial t} &= -\nabla \cdot \boldsymbol{N}_6 + r_1 \\ \frac{\partial c_7}{\partial t} &= -\nabla \cdot \boldsymbol{N}_7 - r_1 \end{aligned} \tag{4.4.4}$$

As has been discussed in Section 2.7.1, in a system with chemical reactions, mass balance equations can be solved without the presence of reaction terms if the reactions are significantly faster than other processes. To eliminate the reaction terms and obtain alternative equations two new variables, c_H and c_O, representing the concentrations of atomic hydrogen and oxygen, need to be introduced:

$$\begin{aligned} c_H &= c_1 + c_2 + 2c_3 + c_7 \\ c_O &= c_2 + c_3 \end{aligned} \tag{4.4.5}$$

A new set of partial differential equations can be obtained by using c_H and c_O:

$$\begin{aligned} \frac{\partial c_H}{\partial t} + \nabla \cdot \boldsymbol{N}_H &= 0 \\ \frac{\partial c_O}{\partial t} + \nabla \cdot \boldsymbol{N}_O &= 0 \end{aligned} \tag{4.4.6}$$

with $\boldsymbol{N}_H$ and $\boldsymbol{N}_O$ defined by:

$$\begin{aligned} \boldsymbol{N}_H &= \boldsymbol{N}_1 + \boldsymbol{N}_2 + 2\boldsymbol{N}_3 + \boldsymbol{N}_7 \\ \boldsymbol{N}_O &= \boldsymbol{N}_2 + \boldsymbol{N}_3 \end{aligned} \tag{4.4.7}$$

The mass balance equations for Cl^- and Na^+ remain unchanged:

$$\begin{aligned} \frac{\partial c_4}{\partial t} + \nabla \cdot \boldsymbol{N}_4 &= 0 \\ \frac{\partial c_5}{\partial t} + \nabla \cdot \boldsymbol{N}_5 &= 0 \end{aligned} \tag{4.4.8}$$

Electrical neutrality is everywhere:

$$c_1 - c_2 - c_4 + c_5 + z_p c_6 = 0 \tag{4.4.9}$$

z_p is the protein charge which is defined below.

Applying water dissociation equilibrium in equation (4.1):

$$c_1 c_2 = K_w \tag{4.4.10}$$

Applying the concentration of undissociated hydrogen in β-Lactoglobulin equation in Section 2.6, c_7 is then calculated:

$$c_7 = c_6 \sum_{j=amino\ acids} N_{k,j} \frac{1}{10^{(pH-pK_{aj})} + 1} \tag{4.4.11}$$

with

$$pH = -\log_{10} c_1 \tag{4.4.12}$$

The total protein concentration c_6 is independently determined by the protein gel swelling:

$$c_6 \bar{V}_p + c_3 \bar{V}_3 = 1 \tag{4.4.13}$$

in which $\bar{V}_3$ is the molar volume of water and $\bar{V}_p$ is the molar volume of protein in [m^3/mol]. Note here the assumption that ions occupy negligible volume.

Protein charge z_p can be obtained by equation (2.6.45) in Section 2.6:

$$z_p = \sum_{j=amino\ acids} N_{k,j} z_j \frac{10^{z_j(pK_{aj}-pH)}}{10^{z_j(pK_{aj}-pH)} + 1} \tag{4.4.14}$$

After carefully checking variables and equations, there are 11 equations with 10 variables namely c_H, c_O, c_1, c_2, c_3, c_4, c_5, c_6, c_7 and protein charge z_p. It is found that concentrations of salts (c_4 and c_5) are tied together by electrical neutrality equation (4.4.9). Therefore only one mass balance equation for salts, either for Na^+ or for Cl^-, is independent.

The molar fluxes $\boldsymbol{N}$ in equations are not counted as variables since they are related to the relative diffusion flux, $\boldsymbol{J}^n$, in the GMS diffusion equation (4.1.7). In many systems, the solvent is stationary and thus it is convenient to work in terms of diffusion flux

with respect to the solvent:

$$\boldsymbol{J}_i^n = \boldsymbol{N}_i - x_i \boldsymbol{N}_n \tag{4.4.15}$$

There is no external potential applied to the system and thus there is no flow of current, *i.e.*

$$\sum_{i=1}^{n-1} z_i \boldsymbol{N}_i = \sum_{i=1}^{n-1} z_i \boldsymbol{J}_i^n = 0 \tag{4.4.16}$$

In a system containing a charged protein gel which is considered as an additional component to the electrolyte system, there are some different features. Firstly, the polymer is now moving and not stationary. The protein matrix velocity, $\boldsymbol{u}_p$, arises from the change in volume (density) of the gel. If the protein matrix is chosen as the reference frame the molar diffusion flux of species *i* can be written by equation (2.2.11):

$$\boldsymbol{N}_i = \boldsymbol{J}_i^n + c_i \boldsymbol{u}_p \tag{4.4.17}$$

Secondly the protein gel is charged so the net current flux should include component *n* which is the protein matrix:

$$\sum_{i=1}^{n} z_i \boldsymbol{N}_i = \sum_{i=1}^{n} z_i \boldsymbol{J}_i^n + \boldsymbol{u}_p \sum_{i=1}^{n} z_i c_i \tag{4.4.18}$$

By electroneutrality the second term of the right hand side equation (4.4.18) is zero, so:

$$\sum_{i=1}^{n} z_i \boldsymbol{N}_i = \sum_{i=1}^{n} z_i \boldsymbol{J}_i^n = 0 \tag{4.4.19}$$

which is the same as equation (4.4.16). The no net current flux condition still holds for the charged protein gel as the *n* component.

To obtain the molar flux $\boldsymbol{N}$ in the mass balance equations from the relative diffusion flux $\boldsymbol{J}^n$ we need to define the velocity of protein matrix. Equation (4.4.1) is considered when there is no reaction. Each side of equation (4.4.1) is multiplied by the corresponding molar volume:

$$\bar{V}_i \frac{\partial c_i}{\partial t} = -\bar{V}_i \nabla \cdot \boldsymbol{N}_i \,, \quad i = 1,2,\ldots,6 \tag{4.4.20}$$

where $\boldsymbol{N}_i$ is the molar flux of component *i* in mol/m^{2}s and $\bar{V}_i$ is the molar volume of component *i* in m^3/mol.

Summing for all components:

$$\frac{\partial\left(\sum_{i=1,n} \bar{V}_i \, c_i\right)}{\partial t} = -\nabla \cdot \sum_{i=1}^{\mathrm{n}} \boldsymbol{N}_i \bar{V}_i \tag{4.4.21}$$

The left hand side of equation (4.4.21) represents the rate of change in volume so equals zero.

Further:

$$\boldsymbol{N}_6 = c_6 \boldsymbol{u}_p \tag{4.4.22}$$

By combining equation (4.4.17), (4.4.21) and (4.4.22), $\boldsymbol{u}_p$ can be determined:

$$0 = \nabla \cdot \left(\sum_{i=1,5} \left(\boldsymbol{J}_i^n + c_i \boldsymbol{u}_p \right) \bar{V}_i + c_6 \boldsymbol{u}_p \bar{V}_p \right) \tag{4.4.23}$$

It is assumed molar volumes of ions are neglected and therefore the above equation can be simplified.

$$0 = \nabla \cdot \left(\left(\boldsymbol{J}_3^n + c_3 \boldsymbol{u}_p \right) \bar{V}_3 + c_6 \boldsymbol{u}_p \bar{V}_p \right) \tag{4.4.24}$$

It is further simplified so that $\boldsymbol{u}_p$ is defined together with the boundary condition of velocity at a fixed boundary or on a symmetry plane:

$$0 = \nabla \cdot \left(\boldsymbol{J}_3^n \bar{V}_3 + \boldsymbol{u}_p \right) \tag{4.4.25}$$

The flux $\boldsymbol{N}_7$ can be calculated the same way as $\boldsymbol{N}_6$:

$$\boldsymbol{N}_7 = c_7 \boldsymbol{u}_p \tag{4.4.26}$$

4.5 Swelling pressure

The Maxwell-Stefan diffusion description has the ability to include all the factors in diffusion process. Krishna (1987) said “in many cases of practical interest the pressure gradients are negligibly small and this term may therefore be neglected”. This is true when a system is only composed of electrolytes because the molar volume

of ions is very small. However for a system involved a macromolecular structure like protein, water diffusing into the structure is taken into account and this causes the gel to swell. The swelling pressure is directly related to the elasticity of the network.

In Section 2.5 two approaches to describe the swelling mechanics were discussed. The mechanic structure approach states that a deformed material body (the strain) is linearly related to the force causing the deformation (the stress) by the Hooke's law. The moduli are material independent and keep constant during swelling. The rubber elasticity theory uses deformation free energy to describe a swelling structure. The modulus of a rubber is material dependent shown by equation (2.5.47). Equation (2.5.71) suggests that the modulus of a swollen rubber decreases as the rubber swelling ratio increases.

Protein gels are rubber-like materials. Therefore in this study rubber elasticity theory is used to describe the gel deformation. Like a rubber, a gel is composed of a polymer network with the important difference that a gel also contains a considerable fraction of liquid. Swelling pressure is to be calculated from an expression for the Helmholtz elastic energy of a network similar to Maurer and Prausnitz's method (Maurer and Prausnitz, 1996; Sassi et al., 1996). The Helmholtz energy of the elastic network depends on the deformation of the network from its initial state, which is the state where it is produced. That deformation is expressed by the ratio of the volume of the gel, V, to the volume of the gel in the initial state, V_0:

$$A = \frac{3}{2} NkT \left[\left(\frac{V}{V_0} \right)^{\frac{2}{3}} - 1 \right] + f\left(\frac{V}{V_0} \right) \tag{4.5.1}$$

where N is the number of crosslinked chains in the protein network structure, k is the Boltzmann's constant and $f(V/V_0)$ stands for the different methods (Flory, Kuhn-Wall-Flory and Treloar etc).

For Flory:

$$A = \frac{1}{2}NkT\left[3\left(\frac{V}{V_0}\right)^{\frac{2}{3}} - 3 - \ln\frac{V}{V_0}\right] \tag{4.5.2}$$

For Kuhn-Wall-Flory:

$$A = \frac{NkT}{2}\left[3\left(\frac{V}{V_0}\right)^{\frac{2}{3}} - 3 - 2\ln\frac{V}{V_0}\right] \tag{4.5.3}$$

For Treloar:

$$A = \frac{3}{2}NkT\left[\left(\frac{V}{V_0}\right)^{\frac{2}{3}} - 1\right] \tag{4.5.4}$$

Combining with Maurer and Prausnitz's (1996) concept: the pressure difference between the gel and its surroundings is caused by the elastic properties of the network. This can be written as:

$$P - P_0 = \left(\frac{\partial A}{\partial V}\right)\Big|_T \tag{4.5.5}$$

in which P_0 is the surrounding pressure.

Therefore the elastic contribution to the driving force for the swelling process is obtained by equation (4.5.5).

For the Flory free energy:

$$\Delta P = P - P_0 = \frac{NkT}{2V}\left[2\left(\frac{V}{V_0}\right)^{\frac{2}{3}} - 1\right] \tag{4.5.6}$$

Maurer and Prausnitz (1996) used equation (4.5.6) to describe the swelling pressure. However this was proved to be wrong in Section 2.5.1 because the free energy did not obey Edwards' principle.

Different pressure models were presented in Section 2.5.1. The following equations are the representation of the equations (2.5.48) to (2.5.51) in Section 2.5.1.

For the Kuhn-Wall-Flory free energy:

$$\Delta P = P - P_0 = \frac{NkT}{V}\left[\left(\frac{V}{V_0}\right)^{\frac{2}{3}} - 1\right] \tag{4.5.7}$$

Or for the Treloar free energy:

$$\Delta P = P - P_0 = \frac{NkT}{V_0}\left(\frac{V}{V_0}\right)^{-\frac{1}{3}} \tag{4.5.8}$$

Or Ogden:

$$\Delta P = P - P_0 = G_{elr}\left[\nu_2^{-\frac{1}{3}(\alpha_r - 3)} - \nu_2^{\frac{1}{3}(2\alpha_r + 3)}\right] \tag{4.5.9}$$

and Mooney:

$$\Delta P = P - P_0 = C_1\left(\nu_2^{1/3} - \nu_2^{7/3}\right)\left(1 + \frac{C_2}{C_1}\nu_2^{-2/3}\right) \tag{4.5.10}$$

It is shown by James and Guth (Treloar, 2005) that the initial shear modulus G is equivalent to:

$$G = NkT \tag{4.5.11}$$

Protein cannot diffuse out into the bulk and thus the number of moles of protein is a constant:

$$c_{60}V_0 = c_6V \tag{4.5.12}$$

where c_{60} represents the initial concentration of total protein.

Therefore the ratio,V/V_0, is written by:

$$\frac{V}{V_0} = \frac{c_{60}}{c_6} \tag{4.5.13}$$

Figure 4.5 shows the pressure against the ratio of the volume of the gel, V, to the volume of the gel in the initial state, V_0. The parameters used are the same as those in Section 2.5.1.

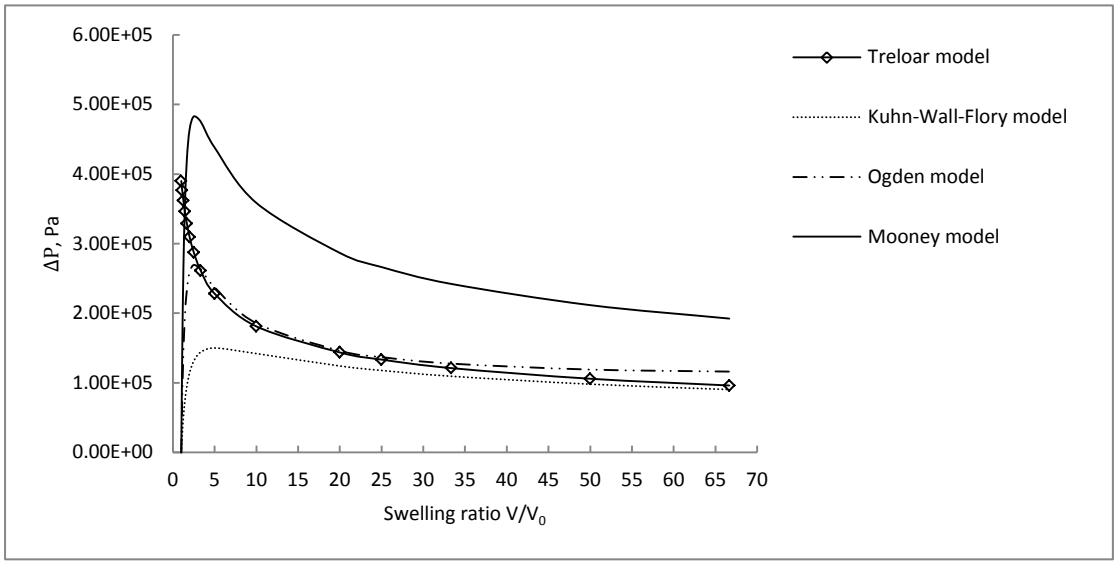

Figure 4.5 Different pressure models

In this study, at the initial state the protein gel is not dry but has some water content so it is expected that the initial pressure difference between the gel and the bulk is zero. Figure 4.5 shows that Treloar model gives its highest pressure difference at initial state. Other three models, Kuhn-Wall-Flory, Ogden and Moonery, provide zero pressure difference at initial state. Therefore the pressure model can be chosen between Kuhn-Wall-Flory, Ogden and Mooney. Equation (4.5.7) of Kuhn-Wall-Flory will be used in the simulation.

4.6 Summary

At this point the mathematical model of the protein gel swelling is finally set up. Compared with previous models in literature, this model has many significant features. First of all the diffusion model is based on the GMS equations. Previous models either used Fickian diffusion (Hong et al., 2008) or the Nernst-Planck equation (Grimshaw et al., 1990; De and Aluru, 2004). It has been already discussed that with many limitations, Fick's law cannot provide a reliable solution in the case that involves multicomponents and the gel. The Nernst-Planck equation is valid for dilute electrolytes and is only a limiting case of the GMS equations (Taylor and Krishna, 1993). The model of Bisschops et al. (1998) was the only one that used the GMS

equations to describe diffusion. However, it only had two components and was not a multicomponent diffusion system.

Secondly it is the first known swelling model that includes thermodynamics. This was very challenging because it was very difficult to define the thermodynamics of a polyelectrolyte system. It was not clear how ionic and polymer effects should be combined to the solvent activity. The influence of the charge number of the gel on the activity of ions and solvent was not known. After lots of research, this problem was solved and the thermodynamics model in the thesis was achieved by combining thermodynamics of electrolytes and Manning condensation theory in polyelectrolytes. However, models found in literature (Hasa et al., 1975; Horkay et al., 2000; Grimshaw et al., 1990; De and Aluru, 2004; Bisschops et al., 1998) assumed that the aqueous solution was ideal.

Thirdly the pressure model is described by rubber elasticity theory. By using deformation free energy, the pressure is a function of the gel volume. However, the pressure term in previous models was obtained from the water equilibrium (Grimshaw et al., 1990; De and Aluru, 2004). This pressure was actually the osmotic pressure and not applicable for dynamic diffusion. Then the Hooke's law was used to describe the swelling structure displacements (Tanaka et al., 1973; Tanaka and Fillmore, 1979; Grimshaw et al., 1990; De and Aluru, 2004). This was also wrong because Hooke's law is only valid for small displacements. The swelling degree of a polyelectrolyte gel can be large. When immersed in a solvent, a polyelectrolyte network is able to absorb large amounts of solvent molecules up to several hundred times its dry mass (Mann et al., 2005).

The model includes the protein charge as a function of pH. Therefore, the model can be easily shifted from acid conditions to alkaline conditions. The gel swelling model of Tanaka et al. (1973) and Tanaka and Fillmore (1979) only had two components: water and a neutral gel. Although some models considered ionic species in gel

swelling (Grimshaw et al., 1990; De and Aluru, 2004), the gel charge density was considered constant and not a function of pH.

Finally mass balance equations are modified by eliminating the reaction terms to ensure stable solutions. The model can be easily extended to already systems with more ions.

5 Results and discussion

Chapter 4 has presented the complete mathematical equations of a polyelectrolyte gel system. In this section these equations are going to be solved using COMSOL Multiphysics general form. Firstly it is useful to check the non-ideal effect on the diffusion process.

5.1 Ideal vs. non-ideal

5.1.1 Ideal vs. non-ideal in electrolyte systems

In Section 3.3 the diffusion in an ideal mixture of NaCl and HCl ideal mixture was solved in COMSOL. Next the non-ideal mixture of NaCl and HCl with the same conditions were solved in COMSOL and then compared with the ideal solution presented in Section 3.3.

The calculation of thermodynamics is defined in Section 4.2:

$$Q = \frac{G^{DH}}{RT} = -\frac{4A_x I_x}{b_x} ln\left[\frac{1 + b_x I_x^{1/2}}{1 + b_x (I_x^0)^{1/2}}\right] + \sum_c \sum_a x_c x_a B_{ca} \mathrm{g}\left(\alpha I_x^{1/2}\right) \quad (5.1.1)$$

Followed by:

$$\Gamma_{ij} = \delta_{ij} + x_i \left\{ Q_{ij} - Q_{in} - \sum_{k=1}^{n} x_k \left(Q_{kj} - Q_{kn}\right) \right\} \quad (5.1.2)$$

with

$$Q_i = \left.\frac{\partial Q}{\partial x_i}\right|_{\Sigma} \quad (5.1.3)$$

and

$$Q_{ij} = \left.\frac{\partial Q_i}{\partial x_j}\right|_{\Sigma} \quad (5.1.4)$$

Modelling parameters:

$$A_x = 2.917 \quad b_x = 14 \quad \alpha_x = 13 \quad (5.1.5)$$

$$B_{NaCl} = 16.2622 \quad B_{HCl} = 20.009 \tag{5.1.6}$$

The governing equations for the GMS diffusion in NaCl and HCl mixture can be found in Appendix C.

The following figures show the comparisons between ideal and non-ideal solutions of generalised Maxwell-Stefan diffusion in NaCl and HCl mixture. It can be seen that the non-ideal matrix in the driving force does not influence the diffusion physics. It lowers the activity of each ion and, as a result the concentrations of all three ions were lower in the non-ideal case than in the ideal case. The non-ideal influence is more significant on hydrogen ion than other ions shown by Figure 5.1 to 5.4. From these comparisons we can draw the conclusion that the non-ideal influence on ion diffusion is small and that ideal solution behaviour is sufficient for the modelling.

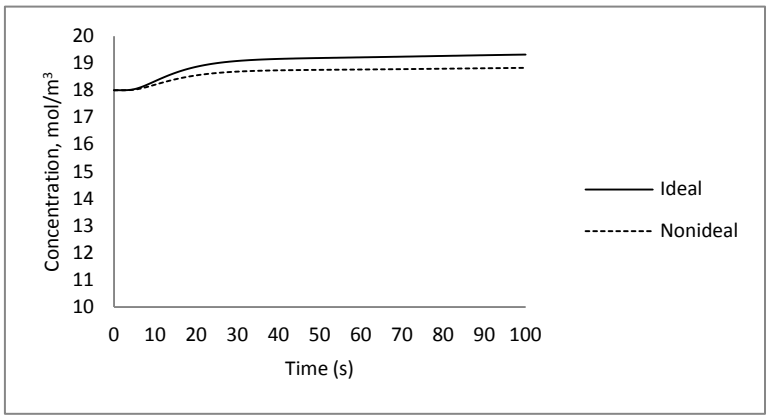

Figure 5.1 Concentration of H^+ in the centre versus time

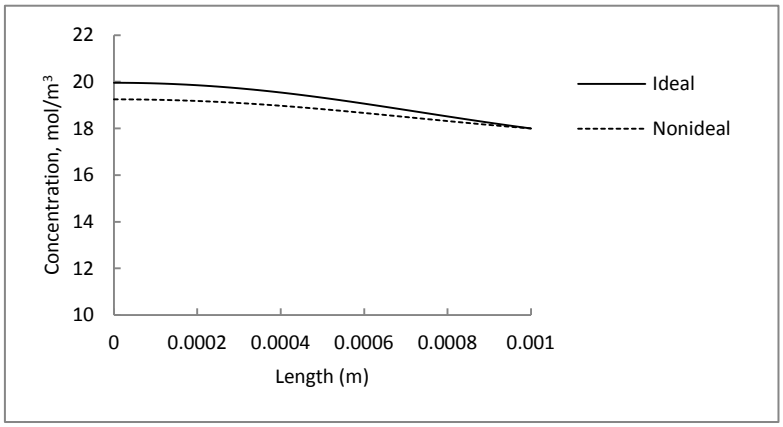

Figure 5.2 Concentration of H^+ along the membrane at 100 seconds

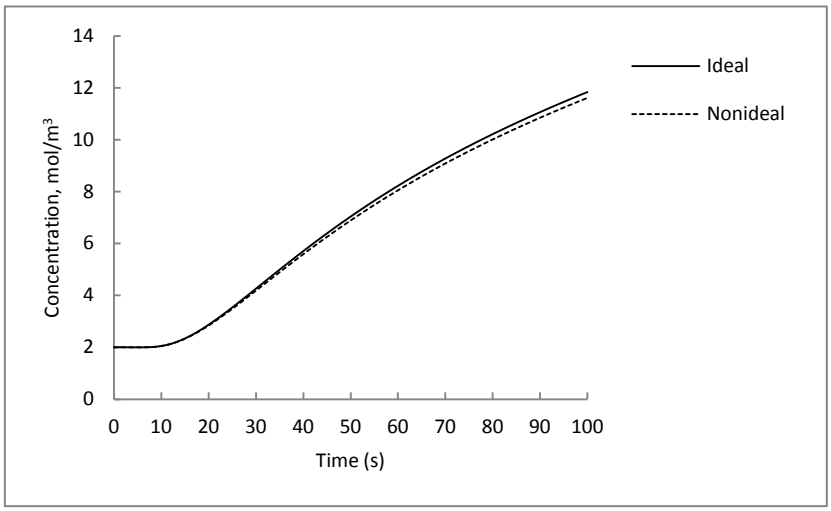

Figure 5.3 Concentration of Na^+ in the centre versus time

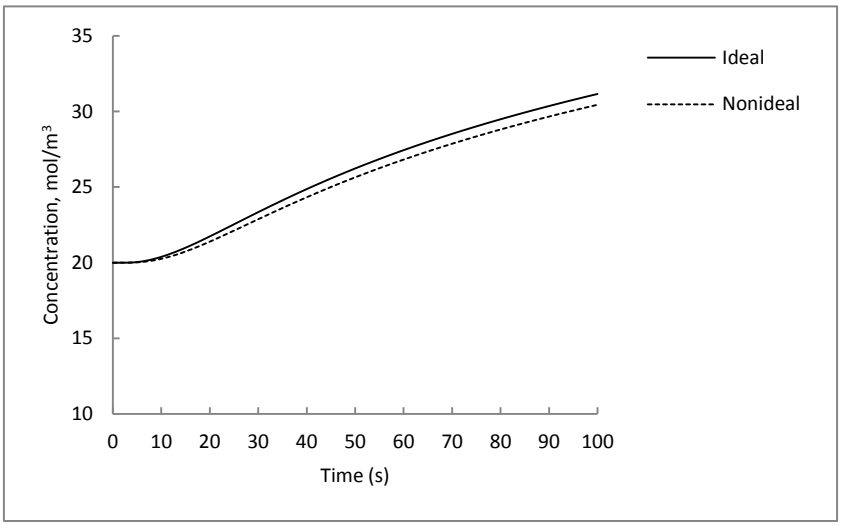

Figure 5.4 Concentration of Cl^- in the centre versus time

Figure 5.5 to 5.7 present the activity coefficient of each ion in the centre as a function of time.

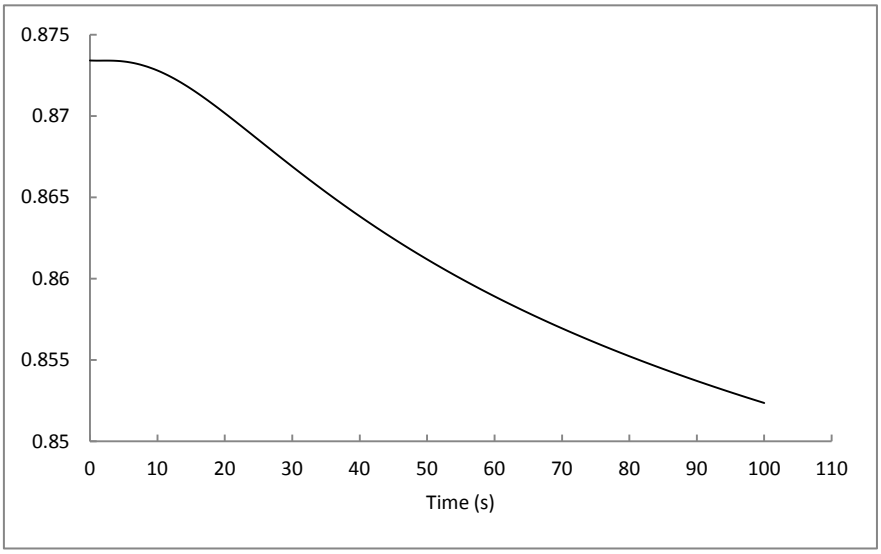

Figure 5.5 Activity coefficient of H^+ in the centre

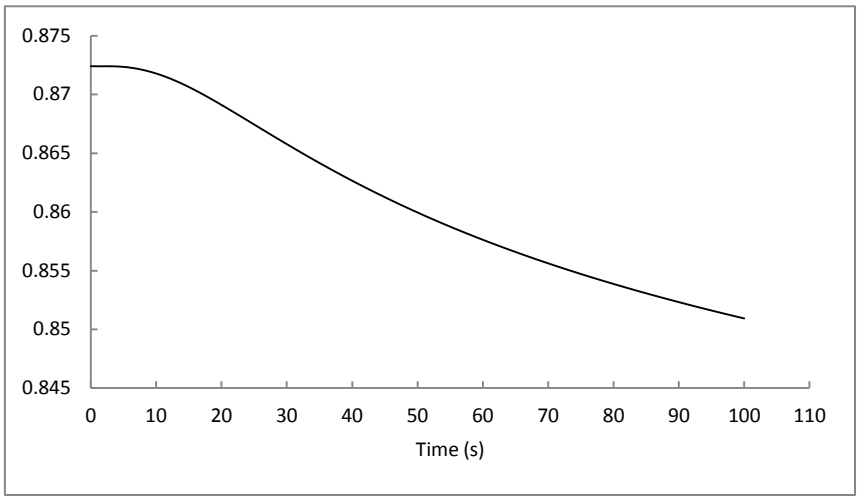

Figure 5.6 Activity coefficient of Na^+ in the centre

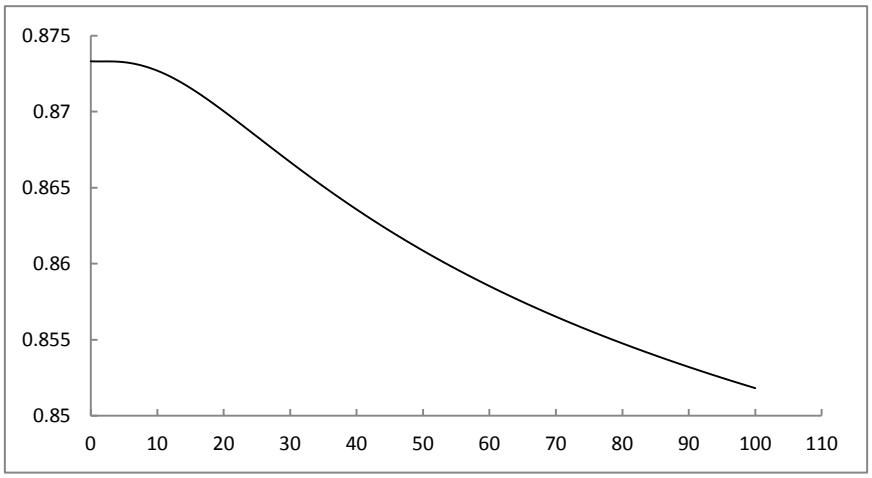

Figure 5.7 Activity coefficient of Cl^- in the centre

It can be seen from Figure 5.5 to 5.7 that the activity coefficients of all three ions are very similar with the range between 0.875 and 0.85 during the simulation time of 100 seconds. This is probably the reason that the non-ideal influence on ion diffusion is small. Figure 5.8 compares the activity coefficients of all three ions. It shows the similar activity coefficients during the simulation time especially for Cl^- and Na^+. The activity curve of H^+ slightly diverges from the other two and this may cause the more significant non-ideal effect on hydrogen ion than the others.

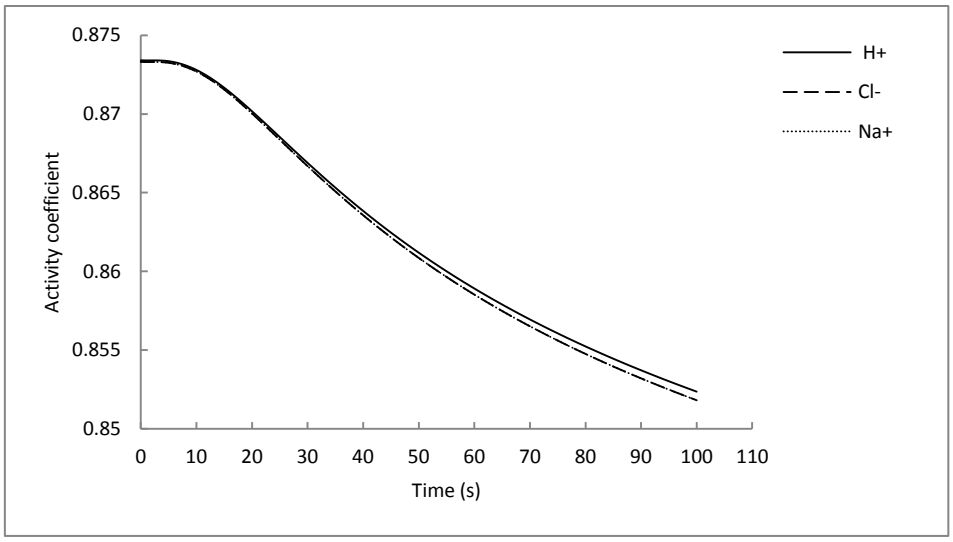

Figure 5.8 Activity coefficient comparisons of three ions (Cl^- and Na^+ curves overlap)

In conclusion the activity coefficients of H^+, Cl^- and Na^+ for diffusion in HCl and NaCl mixture are similar and thus thermodynamics does not influence the diffusion pattern. For the generalised Maxwell-Stefan diffusion in multielectrolyte systems with similar activity coefficients of all ions, the non-ideal effect is small, and it is sufficient to use ideal solution behaviour for the modelling. However, for systems with different activity coefficients there is no conclusive proof to support this argument.

5.1.2 Ideal vs. non-ideal in protein gel

In this section, the 1D protein gel swelling model was solved in COMSOL Multiphysics to investigate the ideal and non-ideal results. For simulation, the thickness of the gel was set to 1 mm. At initial state the volume fraction of the protein

gel was 10% and pH value inside the protein gel was set to 7. The pH of the bulk was 10. The initial and bulk concentrations of H^+ and OH^- were obtained by pH. The simulation time was 100 seconds. The details of modelling equations and COMSOL settings were presented in Appendix D.

Figure 5.9 and 5.10 show the concentration of Na^+ and water along the gel thickness after 100 seconds. The non-ideal influence is significant. The diffusion process of Na^+ and water of non-ideal case is slower than the ideal case.

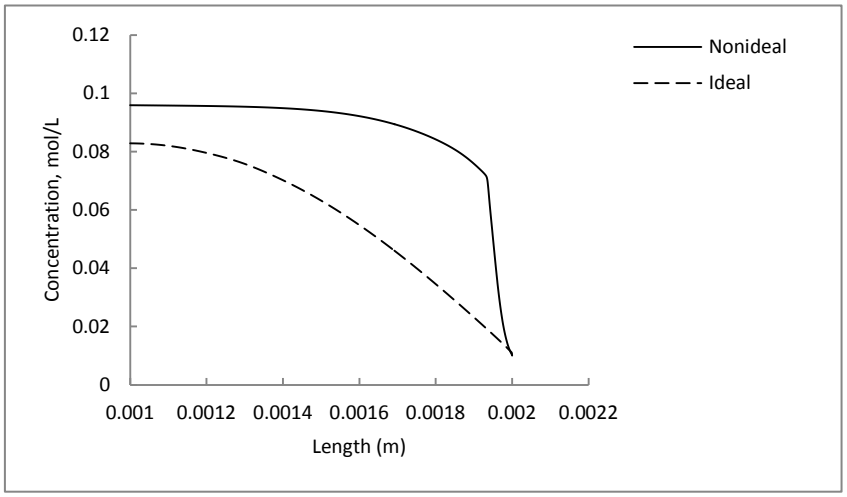

Figure 5.9 Concentration of Na^+ along the length at time =100s

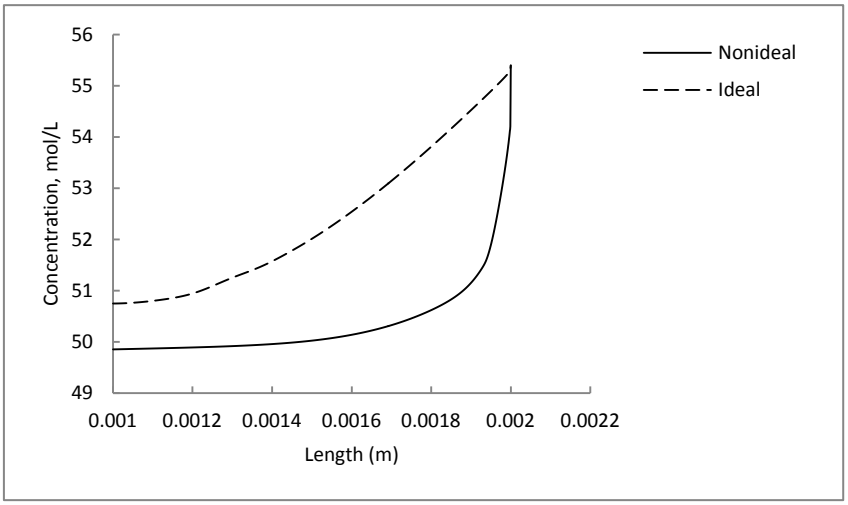

Figure 5.10 Concentration of water along the length at time =100s

The volume expansion at the centre of ideal is larger than that of non-ideal shown by Figure 5.11 and 5.12. The unexpected jump in Figure 5.12 at 10 seconds shows that

the COMSOL can produce some unrealistic solutions. There is no reason for non-idealities to cause the discontinuity seen in the graphs so it was concluded that there were numerical calculation errors. Some calculation problems are investigated later in Section 5.3.2. The slow transport process in the non-ideal case can be explained by the activity coefficients. Figure 5.13 and 5.14 present the activity coefficients of Na^+ in the centre of the protein gel with Manning condensation and without Manning condensation respectively. Manning condensation effect reduces the activity coefficient of Na^+ from about 0.8 to about 0.53 shown by Figure 5.15. Figure 5.16 shows that the overall activity coefficient of Cl^- is about 0.78 which is larger than that of Na^+. This is because the protein gel is negatively charged when the pH value is between 4 and 7. Na^+ is the counter-ion for the negatively charged protein and the Manning effect is more significant on the counter-ion (Na^+) than on the co-ion (Cl^-).

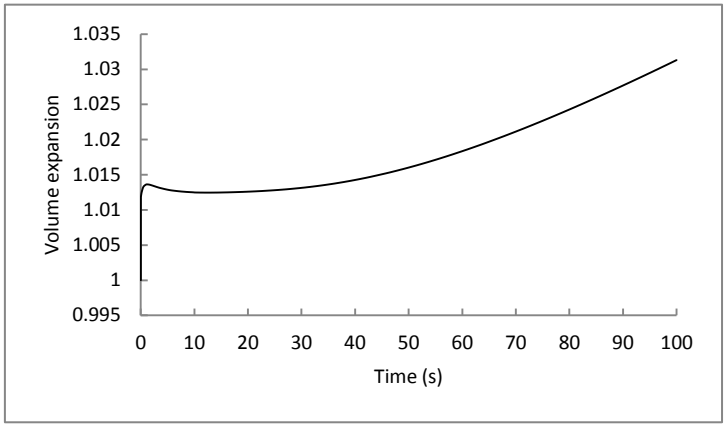

Figure 5.11 Volume Expansion at the centre (non-ideal)

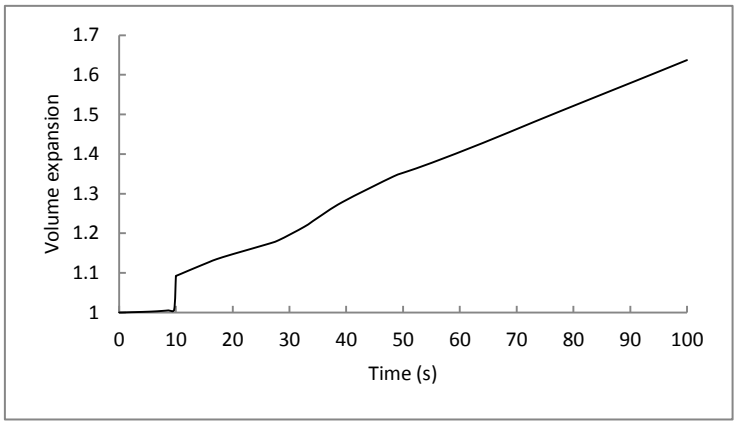

Figure 5.12 Volume Expansion at the centre (ideal)

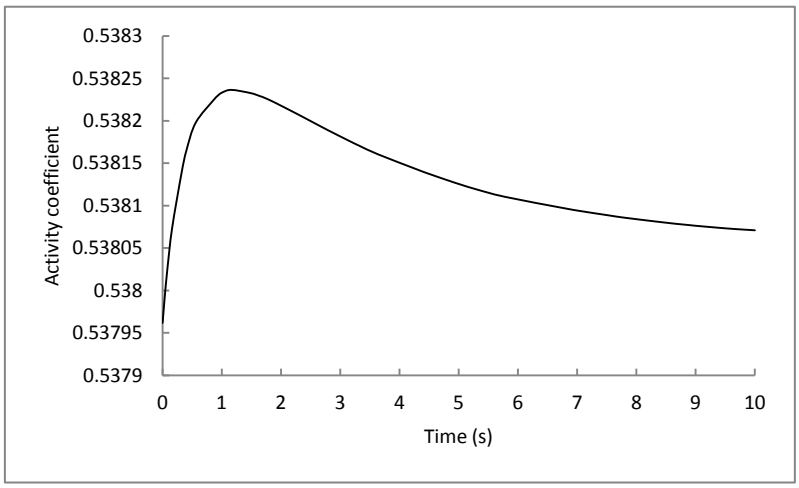

Figure 5.13 Overall activity coefficient of Na^+ (with Manning effect) at the centre over time

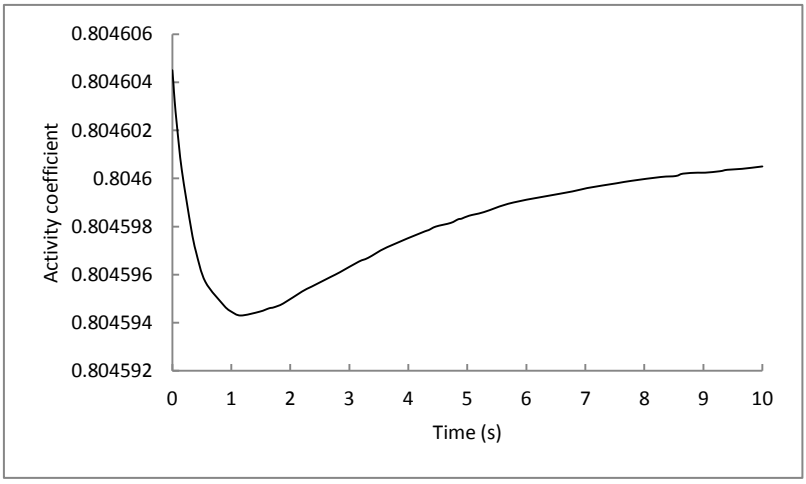

Figure 5.14 Activity coefficient of Na^+ without Manning effect at the centre over time

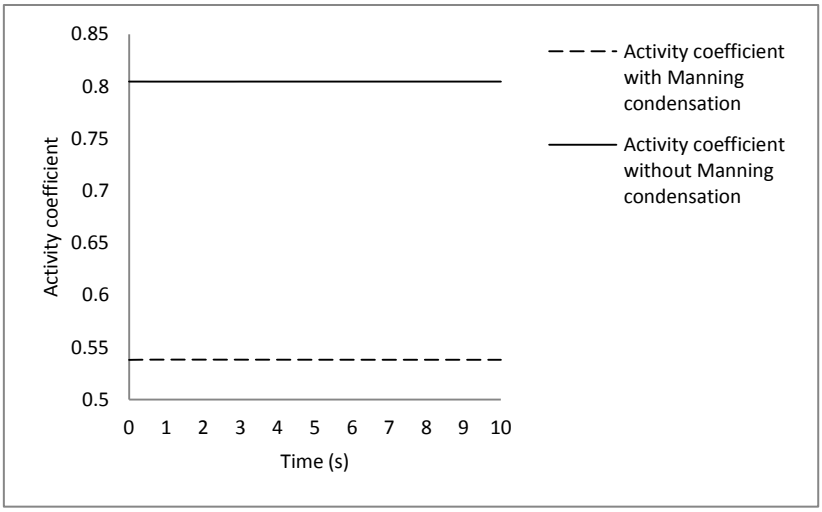

Figure 5.15 Activity coefficient of Na^+ at the centre over time

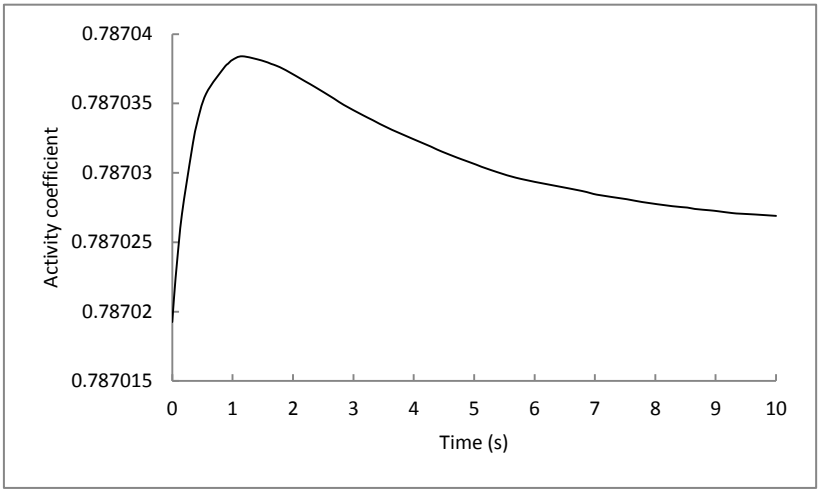

Figure 5.16 Overall activity coefficient of Cl^- at the centre over time

In conclusion the non-ideal effect is small in the multielectrolyte systems shown by Section 5.1.1 but the non-ideal effect is not small in the protein gel swelling case and should be considered. Therefore it is always a good idea to check the non-ideal effect in the simulation first. The ideal case was used in the following simulations to reduce the complexity of the problem in the hope that COMSOL would be able to find solutions. If ideal solutions could not be achieved there was little point in attempting non-ideal solutions.

5.2 The influence of pH and salt concentrations

The effect of pH on the swelling ratio for β-lactoglobulin (βLg) was reported by Mercadé-Prieto et al. (2007b) shown by Figure 5.17.

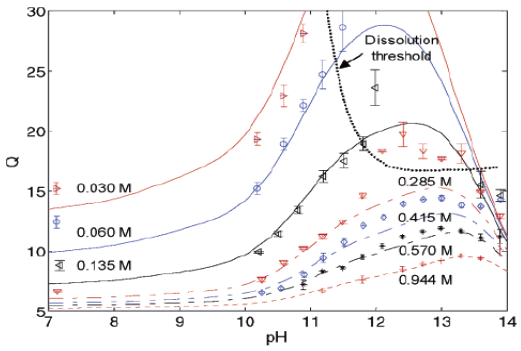

Figure 5.17 Effect of pH on the equilibrium swelling degree in βLg gels at different NaCl concentrations (Figure 4 in Mercadé-Prieto et al., 2007b)

The points in Figure 5.17 are the experimental values. These experimental values

suggest that high pH and high salt concentrations reduce the swelling. The purpose of the following simulation is to get numerical results that are in good agreement with these experimental results. However, problems were found during COMSOL simulation. For the simulation the gel thickness was 1 mm and the equilibrium shear modulus was 2×10^6 Pa. Initially the protein gel was set to be neutral.

Firstly the bulk conditions were: the concentration of NaCl was 0.01M and the pH was 4. It was found that COMSOL stopped at simulation time of around 200 seconds shown by Figure 5.18. Numerical calculation errors were also suspected as the cause.

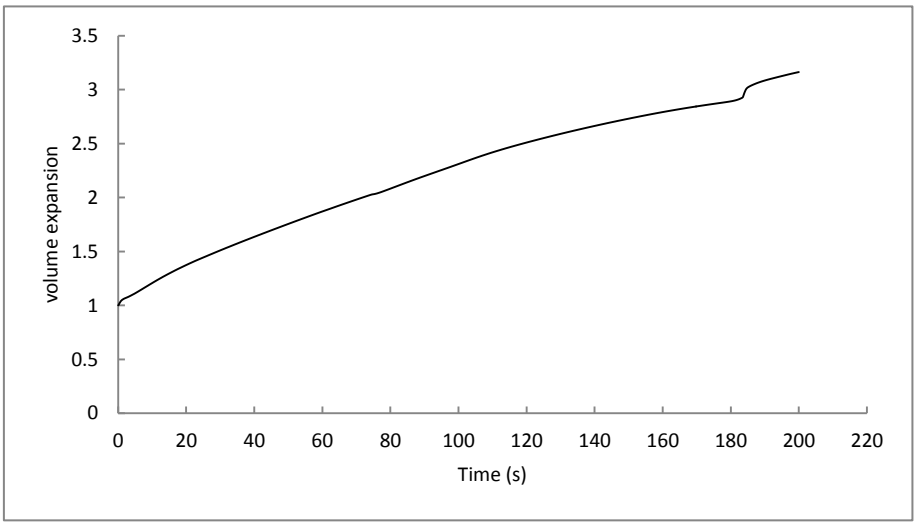

Figure 5.18 Volume expansion at centre with pH=4 and NaCl=0.01M

Then the bulk condition of pH was set to 11. The simulation was quite smooth. Therefore the calculation was carried out with two different salt concentrations in the bulk, 0.01M and 0.05M of NaCl, respectively. Figure 5.19 and 5.20 show that swelling equilibrium is reached after 800 seconds. The equilibrium volume expansion at the centre of the high salt concentration is less than that of the low salt concentration. This can be demonstrated by below the value of 3 in Figure 5.19 and above the value of 3 in Figure 5.20.

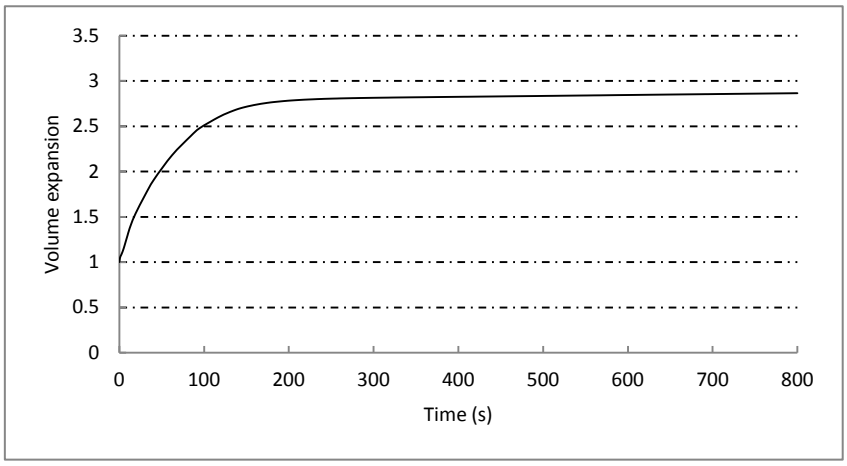

Figure 5.19 Volume expansion at the centre with pH=11 and NaCl=0.05M

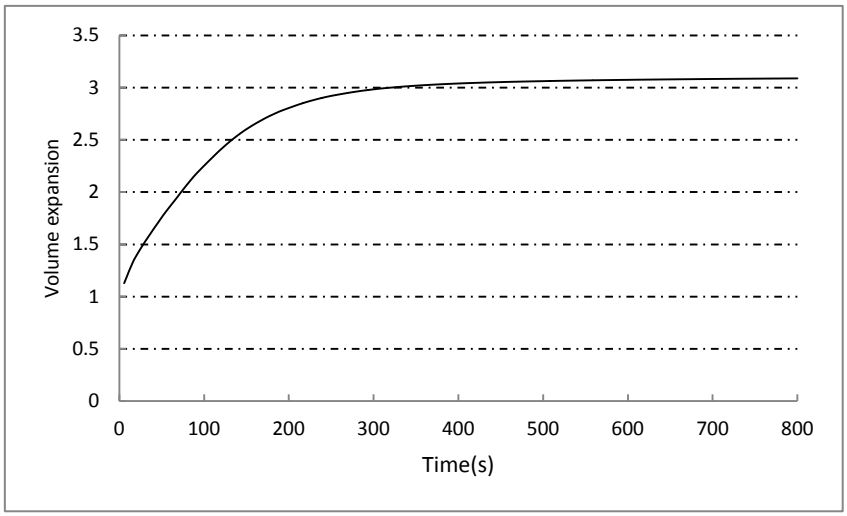

Figure 5.20 Volume expansion at the centre with pH=11 and NaCl=0.01M

When the pH of the bulk was above 12, COMSOL failed to find solutions. At this point it was urgent to identify the problems with simulation. After carefully checking the equations we realise that there are two obstacles for COMSOL to solve the equations. Firstly the modelling equations require a very strict local conservation of mass, but COMSOL Multiphysics is based on the Galerkin finite element method and it cannot ensure local conservativeness (Cockburn, et al., 2007; Kees, et al., 2008; Sochala, et al., 2009; Bevan et al., 2009). Secondly the gel geometry is moving with time due to swelling. All the above results were obtained without considering the moving geometry. Therefore the ability of COMSOL to solve mass balance equations with swelling geometry was in doubt.

5.3 COMSOL problems

During COMSOL trial simulations, it was found that there were problems with COMSOL calculation. In order to find the problems caused by mathematics in equations or caused by incapability of COMSOL a simple swelling problem was considered which involved only two components: water and a neutral protein. Firstly the moving mesh method (ALE) of COMSOL needs to be introduced.

5.3.1 Arbitrary Lagrangian-Eulerian (ALE) method

The gel geometry is not fixed in space but moving with time due to swelling, so we need to understand two coordinate systems: the spatial coordinate system with coordinate axes fixed in space and the material coordinate system with coordinate axes fixed in the material. The former is often called an Eulerian formulation and the latter is called Lagrangian as has been discussed in Section 2.7. The focus of this study is on simulating the physical state such as concentrations at fixed points in space, and it is unreasonable to follow the state of individual material particle. Therefore Eulerian formulation is used. An inherent problem with the Eulerian formulation is that it cannot handle moving domain boundaries, since physical quantities are referred to fixed points in space, but the set of spatial points currently inside the domain boundaries changes with time. To allow moving boundaries, an arbitrary Lagrangian-Eulerian (ALE) method in COMSOL Multiphysics was needed. For the details of mathematical description of this method readers can refer to COMSOL Multiphysics User's Guide (COMSOL Multiphysics 3.5, 2008).

After adding the ALE method to the governing equations, there are two frames existing in the system: the spatial frame and the material frame. The spatial frame is the fixed Euclidean coordinate system with spatial coordinates (x, y). The material frame is a coordinate system which identifies material points by their spatial coordinates (X, Y). Figures 5.21 and 5.22 show the relationship between the two

frames.

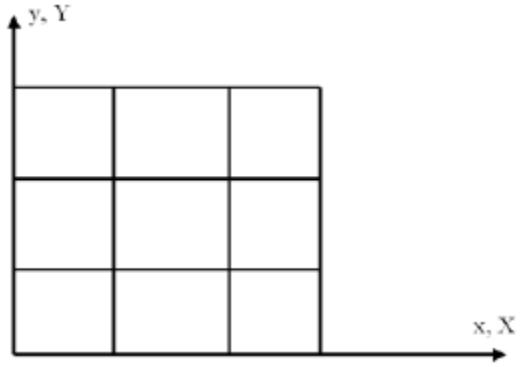

Figure 5.21 An undeformed geometry. The spatial frame (*x*, *y*) and the material frame (*X*, *Y*) coincide (COMSOL Multiphysics 3.5, 2008)

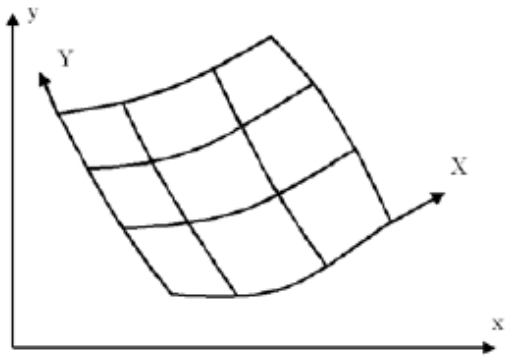

Figure 5.22 A deformed geometry. The spatial frame (*x*, *y*) remains the same but the material frame (*X*, *Y*) has moved (COMSOL Multiphysics 3.5, 2008)

Therefore the mathematical equations of protein gel swelling should be solved in the spatial frame, and the geometry of the gel should move with physically induced movement obtained by integration of the protein gel velocity over time. There the FEM nodes were moved with the displacement calculated by the velocity of the protein matrix at each node. However when the ALE method was added to the simulation, COMSOL failed to find solutions at any conditions.

5.3.2 Results of water and a neutral protein

Since COMSOL failed during trial simulations, suspicions arose that COMSOL may not handle situations with strict mass conservation conditions. The conservativeness of the FVM used in CFD software is fully discussed by Versteeg and Malalasekera

(2007). Therefore a simple swelling model was simulated to check the COMSOL ability in conservativeness and for comparison a MATLAB® program with forced mass conservation was written. In MATLAB programming finite volume segments were used and the swelling on each time step determined each segment boundary and position. This simple swelling model involves two components: a neutral protein with solvent (water). The model equations are the simplified version of the complete mathematical equations in the previous chapter.

The model equations are:

$$\frac{\partial c_w}{\partial t} = -\nabla \cdot \left(\boldsymbol{J}_w + c_w \boldsymbol{u}_p \right) \tag{5.3.1}$$

with $\boldsymbol{J}_w$ defined by the GMS equations:

$$\boldsymbol{J}_w = -\mathcal{D}_{w,p} \left(\frac{x_p}{c_t} \right)^{-1} \nabla x_w \tag{5.3.2}$$

where c_w represents the water concentration, $\boldsymbol{J}_w$ denotes the diffusion flux of water, x_p denotes the mole fraction of the neutral protein, x_w is the mole fraction of water, c_t is the total concentration, $\mathcal{D}_{w,p}$ is the Maxwell-Stefan diffusion coefficient of water in the gel and $\boldsymbol{u}_p$ is the moving velocity of the protein.

The concentration of the protein, c_p, is calculated by:

$$c_w \bar{V}_w + c_p \bar{V}_p = 1 \tag{5.3.3}$$

with $\bar{V}_w$ the molar volume of water and $\bar{V}_p$ the molar volume of the protein.

$\boldsymbol{u}_p$ is defined by:

$$\nabla \cdot \left(\boldsymbol{J}_w \bar{V}_w + \boldsymbol{u}_p \right) = 0 \tag{5.3.4}$$

For COMSOL simulation, two domains were set up shown by Figure 5.23.

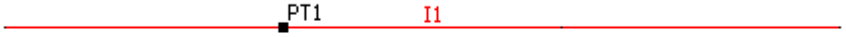

Figure 5.23 Two domains in COMSOL with PT1 the interface of the left and right domain
The length of the left domain is 0.001 m and the length of the right is 0.002 m

Ideally the left domain is the protein gel domain with 10% protein content at the initial state and the right domain is the bulk with no protein content. However, there must be some protein in the right domain to get COMSOL simulation results. COMSOL can find solutions with at least 0.3% protein in the right domain. When the protein in the right was set to 0.2% COMSOL failed.

Figure 5.24 shows the concentration of the protein gel solved by COMSOL and MATLAB. The simulation is carried out with 8% protein in the right domain. It can be seen that COMSOL solution matches with the MATLAB solution.

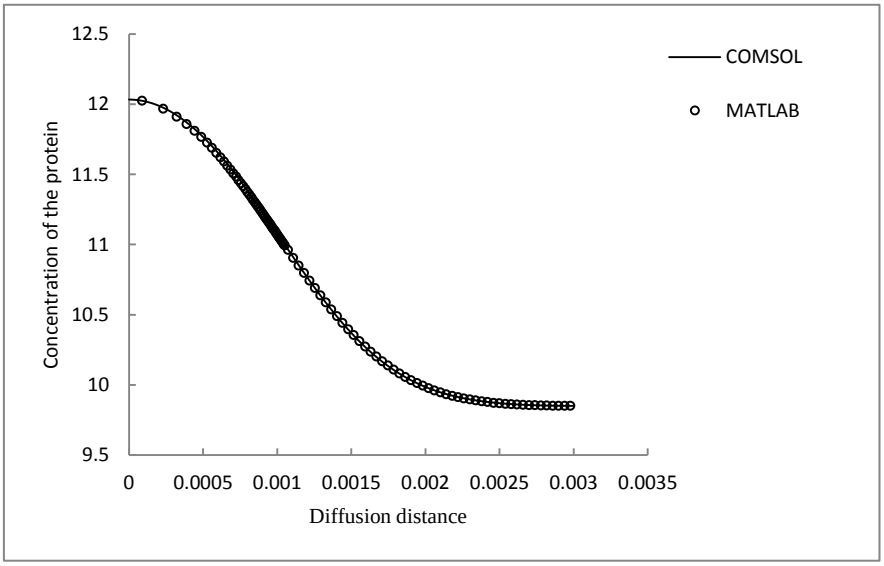

Figure 5.24 Concentration of the protein along the distance after 200 seconds (8% protein in the right)

Then the percentage of the protein in the right domain is reduced to 1% and the COMSOL result was still in agreement with the result of MATLAB shown by Figure 5.25.

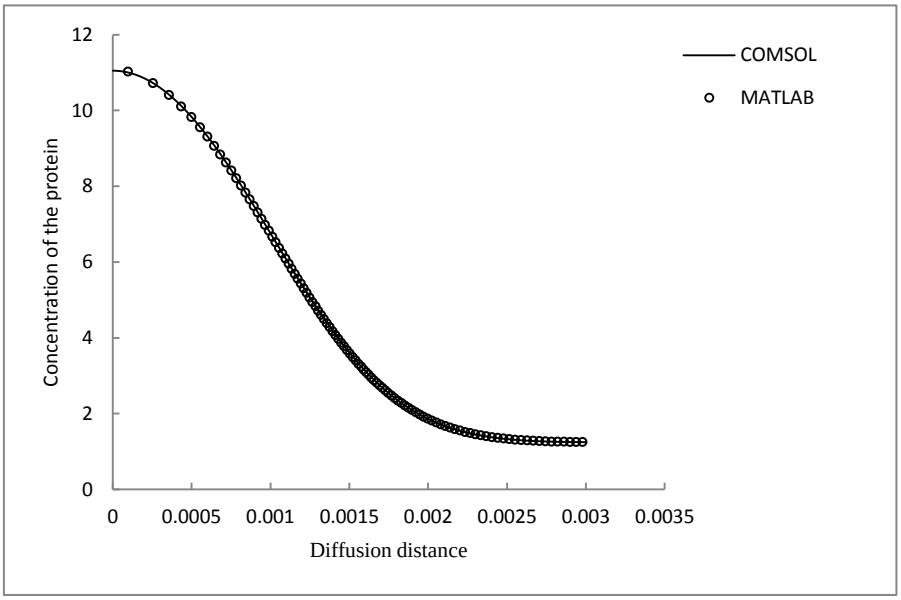

Figure 5.25 Concentration of the protein along the distance after 200 seconds (1% protein in the right)

The percentage of the protein in the right department is further reduced to 0.3% and Figures 5.26 and 5.27 show the concentrations of water and the protein obtained by COMSOL and MATLAB. They are still matched with each other. However when the volume fraction of the gel in the right is set to 0.2%, COMSOL cannot solve this problem but MATLAB still get good solutions shown by Figure 5.28. Figure 5.29 shows the concentration of the protein solved by MATLAB when there is no protein in the right domain.

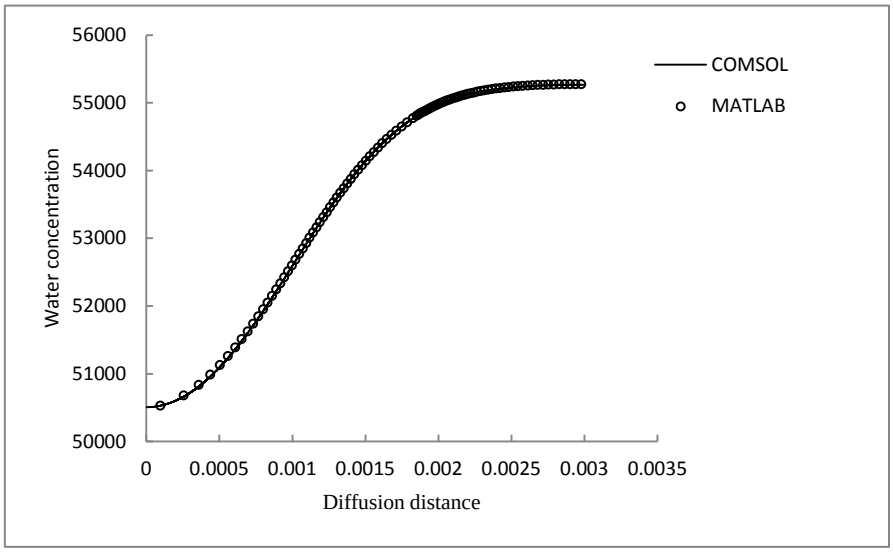

Figure 5.26 Concentration of water along the distance after 200 seconds (0.3% protein in the right)

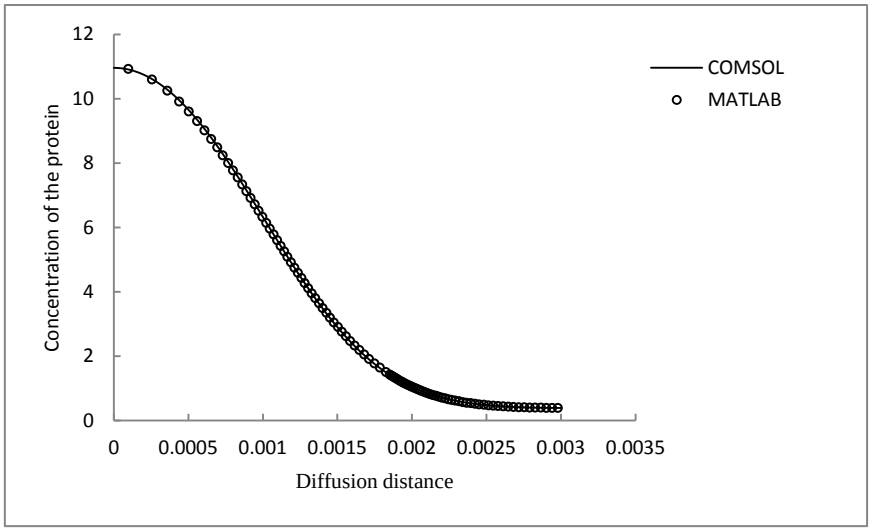

Figure 5.27 Concentration of the protein along the distance after 200 seconds (0.3% protein in the right)

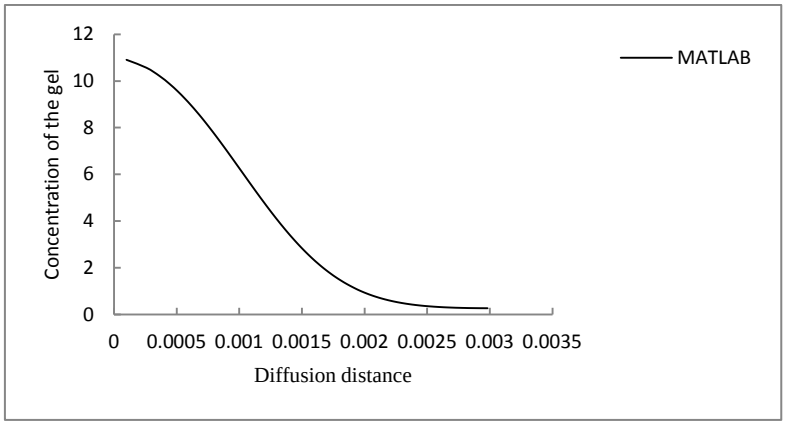

Figure 5.28 Concentration of the protein along the distance after 200 seconds solved by MATLAB (0.2% protein in the right)

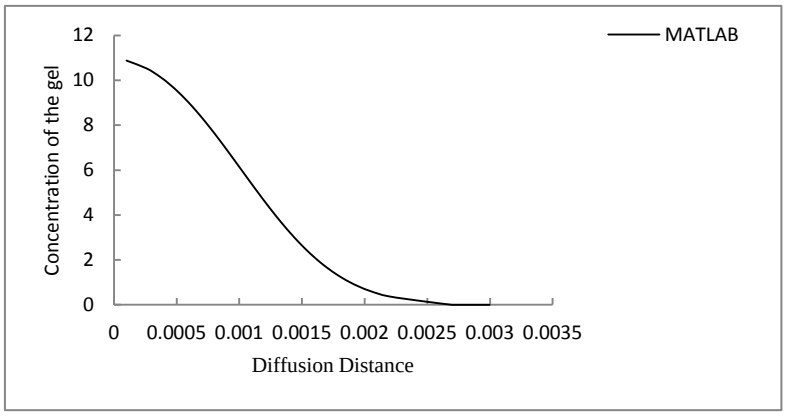

Figure 5.29 Concentration of the protein along the distance after 200 seconds solved by MATLAB (0.0% protein in the right)

Since the same equations can be solved by the MATLAB programming method, the mathematical problems of the equations can be ruled out. The mass conservation

check was then carried out. For the whole system including the left and the right domains, there was no water and protein produced so the mass of water and the protein should be conserved. Table 5.1 and Table 5.2 show the total molar mass comparison between initial state and after some simulation time.

Table 5.1 Mass conservation comparison of COMSOL and MATLAB (1% protein in the right)

Total moles	Time=0	Time=200s (COMSOL)	Error% of COMSOL	Time=200s (MATLAB)	Error% of MATLAB
Protein	0.01476923077	0.01476923710	4.28641E-07	0.01476923077	0
Water	159.68	159.6799971	1.78622E-08	159.68	0

Table 5.2 Mass conservation comparison of COMSOL and MATLAB (0.3% protein in the right)

Total moles	Time=0	Time=200s (COMSOL)	Error% of COMSOL	Time=200s (MATLAB)	Error% of MATLAB
Protein	0.01304615385	0.01304616067	5.2275943E-07	0.01304615385	0
Water	160.4562222	160.4562191	1.9158359E-08	160.4562222	0

It can be seen from Table 5.1 and Table 5.2 that the mass was perfectly conserved in MATLAB. This was no surprise because the mass was forced to be conserved. In the MATLAB programming, flux leaving a face of one finite volume exactly equalled the flux entering the neighbouring volume through the same face. However, there were some mass variations in COMSOL solutions. The percent errors increased when the protein content in the right department is reduced. This was probably the reason why COMSOL fails when the volume fraction of the protein in the right domain is 0.2%. The percent errors are estimated with the order of magnitude around 10^{-7} and this may seem small in the simple gel swelling. However, for the protein gel swelling system the concentration of hydrogen atoms in H^+ and OH^- is of the order of magnitude around 10^{-7} mol/L while the concentration of hydrogen atoms in water is about 110 mol/L so the required errors are extremely small. The hydrogen (H) and oxygen (O) balance equations outlined in Section 4.4 in the thesis model cannot be satisfied in

COMSOL calculation. The alternative of using fast acid/base reactions was rejected in Section 2.7.1.

In conclusion, COMSOL could solve multicomponent diffusion in multielectrolytes as shown in section 3.3 and 5.1. In this case the mass of each component was of the same order and therefore the requirement of conservativeness was not strict. However, COMSOL was not suitable for even simple swelling problems. It can be seen from Table 5.1 and 5.2 that the mass was not conserved in the swelling of water and a neutral protein. For the protein gel swelling system, the hydrogen concentration is the summation of H^+ concentration, water concentration and undissociated hydrogen in protein. The H^+ concentration was much smaller than water concentration and therefore the hydrogen balance requirement is very strict. However, in COMSOL the concentration of H^+ was of the same order of magnitude as the percent errors in the simple swelling model. The strict mass balance of hydrogen (H) could not be achieved. The same situation applied to the oxygen balance. Therefore, another numerical method needs to be considered for the protein gel swelling model.

6 Overall discussion, conclusions and future work

A complete mathematical model of protein gel swelling was set up. Compared with previous models found in literature there are many contributions made by the thesis model.

6.1 Overall discussion

One of the contributions is that the dynamics of diffusion of electrolytes in a protein gel was described by the GMS equation not the Fickian diffusion in this thesis. This was thought to be the first time that the GMS equation has been used in a protein gel swelling system. Most previous models either used Fickian diffusion such as Hong et al. (2008; 2010) or used the Nernst-Planck diffusion such as Grimshaw et al. (1990) and De and Aluru (2004). Although Bisschops et al. (1998) used the GMS equation in their model, the model had two components only and it was not a multicomponent diffusion model. Fickian diffusion failed to include different driving forces in cases that involve multicomponents. Wesselingh and Krishna (2000) observed that in a solution of sodium chloride and hydrogen chloride, sodium diffused against its gradient, in the direction opposite to what we expected from Fickian diffusion. A numerical example of diffusion in the mixture of HCl and NaCl was done in Section 3.3. In this example the concentration of H^+ inside and outside a membrane was deliberately set equal. By Fickian diffusion, H^+ did not move because there was no concentration gradient for H^+ across the region. However the GMS diffusion predicted the diffusion of H^+ into the membrane caused by the diffusion potential. Fickian diffusion cannot provide a reliable solution for multicomponent diffusion systems, let alone the diffusion of multielectrolytes into a gel. The Nernst-Planck equation is valid for dilute electrolytes and is only a limiting case of the GMS equation (Taylor and Krishna, 1993).

Second contribution of this model is that the pressure term was considered to be a

driving force in the GMS equation and was described by rubber elasticity theory. A lot of effort was put into this part of the research. Because the most important physical characteristic of a rubber-like material is the degree of deformability exhibited under the action of stresses, plenty of force-extension experiments have been carried out. Rubber elasticity theories have been provided to match those experimental results (Treloar, 2005). At the start it was not clear if rubber elasticity theory could be used in a protein gel swelling system. In previous models the pressure term was obtained from the water equilibrium (Grimshaw et al., 1990; De and Aluru, 2004). Then the Hooke's law was used to describe the swelling structure displacements (Tanaka et al., 1973; Tanaka and Fillmore, 1979; Grimshaw et al., 1990; De and Aluru, 2004). This kind of approach is unlikely to be accurate. Firstly the pressure used was the osmotic pressure and is applicable for equilibrium states only. Secondly Hooke's law of elasticity describes the linear relationship between a material body deformed (the strain) and the force causing the deformation (the stress). The modulus was assumed to be constant during swelling.

However, rubber-like materials such as protein gels are nonlinear. The modulus of a swollen rubber decreases as the rubber swelling ratio increases as demonstrated by equation (2.5.71) in Section 2.5.1. Then the paper of Ogden (1972) was found and it considered the inflation of a circular membrane into a spherical shape by using rubber elasticity theory. The general form of the pressure-extension ratio relation for the inflation of a spherical membrane was given by Hart-Smith (1966). The swelling of a gel is similar to the inflation of a spherical membrane and therefore it was decided to use rubber elasticity theory to describe the pressure term in the GMS equation.

As the research continued, the Maurer and Prausnitz (1996) equation to describe the pressure difference between the gel and its surroundings was found and is given by equation (2.5.17). In this thesis, by using equation (2.5.17), the pressure is a function of the gel volume. In Section 2.5.1, several pressure models were obtained from different deformation free energy equations. However they were not very satisfactory.

When those models were compared with experimental results of the inflation of a spherical rubber balloon of Hart-Smith (1966), divergence was found in regions with large swelling ratios as suggested in Figure 2.12 and 2.13. However, there was no evidence that the pressure models could be improved without a significant amount of new research.

The third contribution was the inclusion of thermodynamic non-ideality. The difficulty in this part was to define the thermodynamics with the influence of a charged gel. It was not clear how ionic and polymer effects should be combined to the solvent activity. The influence of the charge number of the gel on the activity of ions and solvent was not known. Previous models found in literature (Hasa et al., 1975; Horkay et al., 2000; Grimshaw et al., 1990; De and Aluru, 2004; Bisschops et al., 1998) assumed that the aqueous solution was ideal because they believed that ideal solution modelling could get diffusion behaviours in good agreement with experiments. However, this assumption needs to be justified. One advantage of the Maxwell-Stefan equation is its ability to deal with thermodynamic non-idealities with the matrix Γ. Therefore making the assumption of ideal behaviour was avoided as doing so would defeat the purpose of using the Maxwell-Stefan equations. To include non-ideal behaviour in the GMS equation the activity coefficients of all components in a charged gel system must be determined. The presence of a polyelectrolyte is likely to lower the activity of the surrounding ions and it is possible that counter-ion condensation will occur (Manning, 1969a; 1969b). After lots of research, the influence of protein charged number on activity coefficients was modelled using Manning's condensation theory as discussed in Section 2.4.3. Finally it was decided that the calculation of thermodynamics of ions in a polyelectrolyte gel was divided into two parts. Pitzer's method was used to get activity coefficients of ions in electrolytes and equations (2.4.38) to (2.4.47) were presented in Section 2.4.2. Manning condensation theory (equations (2.4.60) and (2.4.61)) was used to determine activity coefficients of ions with protein gel influence. The overall activity coefficients were obtained by equation (2.4.68). The osmotic coefficient in

electrolytes was obtained by equation (2.4.40). The osmotic coefficient with the influence of a protein gel was obtained by equation (2.4.62). The overall osmotic coefficient was then obtained by equation (2.4.69). Water activity coefficient in the protein gel was calculated from the overall osmotic coefficient using equation (2.4.48). Finally equation (4.2.1) was used to calculate the thermodynamic factor in the GMS equations. Pitzer's method to describe the activity coefficients in multielectrolytes is well studied and only a few parameters in Pitzer's method have not been found. Pitzer's method can accurately predict the activities of ions in multielectrolytes and this can be proved by Figure 2.6 and 2.7 in Section 2.4.2. On the other hand, the accuracy of Manning's condensation theory is not clear. Experiments have been carried out for systems in which the polyelectrolyte and the added simple salt had a common counter ion. It was found that the theory was in excellent agreement with the value of experiments in the more dilute region. In less dilute regions the Manning condensation theory did not perform well because the short range interactions between polyelectrolyte ion and counter-ions were ignored. Therefore, the Manning theory may not necessarily be accurate in condensed polyelectrolyte solutions. For real polyelectrolyte solutions, Manning's condensation theory needs to be improved to include short range interaction. The overall framework used for non-ideality should remain satisfactory even if other component non-ideal equations are used.

This was the first model known to include pH as a variable. Therefore, the model can be easily shifted from acid conditions to alkaline conditions. Most previous models treated gels as neutral such as Tanaka et al. (1973) and Tanaka and Fillmore (1979). Although some models considered ionic species in gel swelling (Grimshaw et al., 1990; De and Aluru, 2004), the gel charge density was considered constant. In the thesis model, the protein charge number was a function of pH. To do this, research on protein chemistry was applied to obtain equations in a suitable form for the model. For a normal acid or base, such as HCl or NaOH, the dissociation equilibrium can be described by the Henderson-Hasselbach equation, equation (2.6.7) presented in Section 2.6. However, things are more complicated for proteins. Proteins are natural

polymer molecules consisting of amino acid units. Each amino acid has at least one basic amine group $–NH_2$ and one acidic functional group –COOH shown in Figure 2.14. There is an internal transfer of a hydrogen ion from the –COOH group to the $–NH_2$ group to form a zwitterion. When an amino acid dissolves in water, the zwitterion interacts with water molecules acting as both an acid and a base. Therefore, in an aqueous solution of an amino acid the two acid-base dissociation equilibria take place simultaneously. The pH dependent dissociation equilibrium of alanine was studied first. Each protein molecule has different amino acid residues with potential hydrogen ion equilibria. At any given pH, these residues will be in various protonation states depending on their individual hydrogen ion dissociation constant *i.e.* pK_as. With knowledge of this and parameters of amino acids found in β-lactoglobulin protein, Table 2.3 in Section 2.6, the net charge of a protein was then calculated by equation (2.6.45) and the concentration of undissociated hydrogen in β-lactoglobulin protein was calculated by equation (2.6.46). Experiments suggest that the swelling degree deceases as pH increases and deswelling may occur at high pH (Mercadé-Prieto et al., 2007b). The relationship between the swelling ratio and the pH can be investigated only if the pH is included in the swelling model.

General material balance equations are normally applied to a fixed control volume. Previously derived proof was given in the thesis that they can also be applied to a swelling geometry. Three different control volumes, namely material control volume, fixed control volume and moving control volume, were studied. The general form for a balance principle in a material control volume was first derived. By applying the Reynolds theorem along with the divergence theorem, the point equation for balance principle was obtained by equation (2.7.12). Then the material balance equations were derived in a moving control volume. It showed that the point equation describing the mass balance was independent of the choice of a control volume. The same result, comparing equation (2.7.16) with equation (2.7.27), was obtained whether a moving control volume or a material control volume was used. After this proof, the general balance principle can be used in the case of swelling with confidence.

Finally, the model was developed to handle to the mass balance terms from both diffusion and fast acid-base reactions. Two reactions, protein dissociation and water dissociation, happened spontaneously in the dynamical swelling. Therefore in the original equations, reaction terms were involved in mass balance equations. The problem with solving these equations is that the reaction rates for each reaction are sometimes high leading to stiffness of the equations. The model of Di Toro (1976) was studied to find out how to use equilibrium equations instead of reaction terms to ensure stability solutions. The example of Di Toro was carbon dioxide dissolved in water equilibrium. Three dissociation constants were associated with three reactions. Species involved in the carbon dioxide dissolution were identified as CO_2, HCO_3^-, CO_3^{2-}, H^+, H_2O and OH^-. Then components were chosen as CO_2, H^+ and H_2O. The species matrix was formulated by multiplication a formula matrix with the component matrix. The transformation matrix was obtained by the transpose of the formula matrix. Different component choices resulted in different formula matrix and hence different transformation matrix. With a chosen component matrix multiplying both sides of the original equations with its transformation matrix the reaction terms were eliminated. For components chosen as CO_2, H^+ and H_2O, the formula matrix was defined by equation (2.7.51). The transformation matrix was defined by equation (2.7.57). It was then found that reaction rates were cancelled out in the new equations (2.7.60). It was shown that the choice of components was not limited to get the alternative equations with zero reaction rates. Practically atoms were often used as components. In the protein gel swelling, atoms, H and O, were used as components. By using Di Toro's method, mass balance equations of the thesis model were solved without the presence of reaction terms. Interestingly Di Toro's approach seems to have been lost and was "re-invented" by Moe et al. (1995) and Kakhu and Pantelides (2003).

After each piece of the gel swelling model was finally put together, great efforts were put into COMSOL in the hope that COMSOL could solve the model equations.

With the examples in Section 3.2 and 3.3, the steps involved in COMSOL simulation were understood and successfully used. After the equation coefficients, constants and variables were all set in COMSOL, there were two important steps to be done before COMSOL simulation.

Firstly it was necessary for COMSOL to have well defined initial conditions. The given initial values were the volume fraction of the total protein, 10% and the pH inside the protein, 7. The initial concentration of H^+ was defined by the given pH and hence the initial concentration of OH^-. The initial concentrations of the total protein and water were defined by the volume fraction. The initial concentration of undissociated H in the protein was obtained by the total protein concentration. The initial concentration of Cl^- was set to be an arbitrary value and finally the initial concentration of Na^+ was calculated by electroneutrality. After the initial concentration of each component was well defined, the initial concentrations of H and O were defined. Unless the initial values were set up rigorously, COMSOL was unable to proceed.

Secondly it was very important to set good boundary conditions for COMSOL. There were two considerations for the boundary setting. Firstly, it was considered that there was no external resistance between the gel and the bulk. Further, the concentrations in the protein gel could be set equal to those in the bulk at the boundary; the protein gel could be treated as a porous model. Therefore, the concentrations in the protein gel pores were equal to those in the bulk at the boundary. A relationship between the pore concentrations with the total protein concentration was needed. It was similar to the partition coefficient in dialysis models. Alternatively, the concentrations in the gel at the boundary could be defined as a function of the bulk concentrations via some form of equilibrium, such as the Donnan equilibrium. Secondly, an external resistance between the gel and the bulk was considered. In other words, there was a liquid boundary layer between the gel and the bulk. This was the same as the first one

because boundary concentrations for the gel and liquid boundary layer interface were still needed. Therefore the boundary conditions used in COMSOL were that the concentrations in the protein gel equal to those in the bulk.

Then several trial runs were carried out by COMSOL and problems occurred in converging the solution. The first problem encountered was that COMSOL failed to find consistent initial values. Checking the model, it was found that there were sharp increases or decreases in the concentrations at the boundary shown by Figure 6.1. Strong transient signals in the boundary were introduced. It was very difficult for the time-stepping algorithm to resolve the transient. The time step could be very small, and the solution time might be very long, or the solution process might even stop. For most parameters tested, the solution process stopped. To ensure that the boundary conditions were consistent with the initial conditions, they were ramped up over a finite time from equilibrium initial conditions to the desired boundary conditions. Doing this would avoid the discontinuity when concentrations at the boundary changed instantaneously. There are several smoothed functions available in COMSOL, such as flc1hs, a smoothed Heaviside function with a continuous first derivative without overshoot, and flc2hs, a smoothed Heaviside function with a continuous second derivative without overshoot. The second one, flc2hs, was used in the modelling. The smooth transition at the boundary is shown by Figure 6.2. The inconsistent initial problem was finally solved.

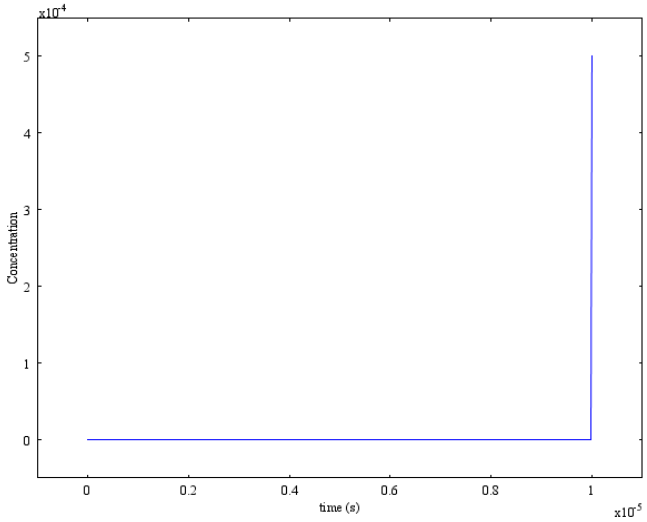

Figure 6.1 The concentration of OH^- at boundary at a small time step of 10^{-5} s with pH=11

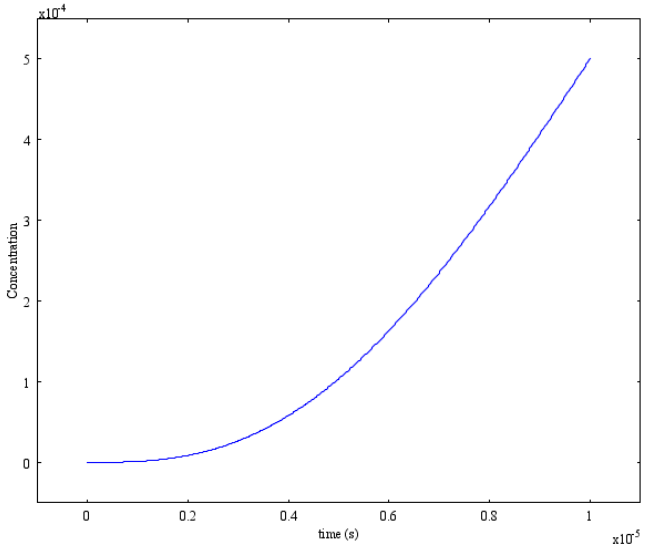

Figure 6.2 The concentration of OH^- at boundary at a small time step of 10^{-5} s with pH=11 after applying flc2hs

The second problem was negative concentrations of H^+ and OH^- which were found during the post-processing. To solve this problem a very small absolute tolerance of 10^{-12} was used since the concentration of H^+ was around 10^{-11} when pH was 11. This did not help. Reducing the absolute tolerance did not solve the problem because the absolute and relative tolerances controlled the error in each integration time step. H^+ was used in the algebraic equation to calculate H and it was the derivative of H that was controlled by the absolute tolerance. A new concentration, which was 10^6 times the concentration of H^+, was introduced. It failed as well. The concentrations of H^+

and OH^- were defined as global expressions in COMSOL instead of calculating in the equation system. This forced explicit calculation of these concentrations rather than solution by Newton's method. This solved the problem.

Then it was found that COMSOL solutions were not satisfactory as shown by the unexpected jumps in Figure 5.12 and 5.18. It was realised that there were two possible frames of reference in the swelling model. The fluxes relative to the protein gel matrix should be solved in the material frame. The point equations should be solved in the spatial frame. It was wrong to use one frame in the simulations. However, COMSOL failed in solving the model equations when two frames were used in the simulation. This made us suspicious about the ability of COMSOL to handle situations with a very strict conservativeness requirement. Given the sensitivity of the model to H^+ concentration, mass conservation is an absolute requirement. Therefore, a simple swelling model was solved by both COMSOL and MATLAB to check the mass conservation. It was found that mass was not conserved in COMSOL calculation shown by Table 5.1 and 5.2. Therefore, COMSOL was not a good choice to solve the swelling model of this thesis.

6.2 Conclusions

Although it was found that COMSOL could not be used as a numerical method to solve the model equations, some conclusions can be made as follows:

1) The model was able to describe the dynamic behaviour of diffusion in polyelectrolytes and it predicted that the equilibrium swelling degree of the gel was decreased with high concentration of salts in the bulk solution.

2) The model included thermodynamic factors in the GMS equations and it was found that the non-ideal effect was not always small and it depended on the activity coefficients of the species.

3) It is not limited to protein gels with electrolytes. The model is also applicable to drug delivery system provided that the diffusion coefficients are available.

4) In contrast to earlier models, like Fickian diffusion model, the GMS model can be easily extended.

5) It was found that COMSOL Multiphysics failed to solve the model equations because the Galerkin finite element method within COMSOL did not conserve mass.

6.3 Future work

A complete mathematical model of protein gel swelling has been established. Satisfactory solutions could not be obtained by using the COMSOL Multiphysics method. There is no software available to solve the gel swelling problem. CFD software such as CFX is based on the finite volume method which can ensure conservativeness in the control volume but it is not flexible enough to use user-defined equations. Therefore, the most important future work should be focus on writing the programming code for a finite volume method to solve the system in three dimensions. After successfully programming it would be good to investigate the swelling of the gel with the influence of the pH and the salt concentration in the bulk.

There are also several improvements that could be made to this model. Firstly, the pressure model could be improved. However there is little hope that a more accurate pressure model could be obtained by using rubber elasticity theory. A large amount of new research possibly in a different field could be required to obtain a better pressure model for swelling gels. Secondly, the Manning condensation theory in the thermodynamic non-ideality needs to be investigated further. Manning condensation theory used in the thesis was set up for the system of a gel and a simple salt such as

NaCl. Only one counter-ion and co-ion were in the polyelectrolyte system. For the system of a gel with multiple ions, the accuracy of the Manning's model needs to be studied. A modified Manning condensation theory could be needed. Manning condensation theory was accurate for very dilute polyelectrolyte solutions. Future research could focus on how to include the short range interaction in the Manning's original theory and hence the performance of the Manning theory in concentrated regions could be improved. Possibly studies of ions around individual proteins could be extended to yield ion activities in polyelectrolyte studies. Experiments would be needed to validate the accuracy of the modified Manning's model.

References

Achilleous, E. C., Prudhomme, R. K. and Kevrekidis, I. G. (2000) Quantifying deformation in gel swelling: experiments and simulations, *Fluid Mechanics and Transport Phenomena*, 46(11), 2128-2139.

Achilleous, E. C., Christodoulou, K. N. and Kevrekidis, I. G. (2001) A transport model for swelling of polyelectrolyte gels in simple and complex geometries, *Computational and Theoretical Polymer Science*, 11, 63-80.

Allen, G., Aggarwal, S. L. and Russo, S. (1996) *Comprehensive Polymer Science Second Supplement*, Pergamon, Oxford.

Bansal, B. and Chen, X.D. (2006) A critical review of milk fouling in heat exchangers, *Comprehensive Reviews in Food Science and Food Safety*, 5, 27-33.

Bas, D. C., Rogers, D. M. and Jensen, J. H. (2008) Very fast prediction and rationalisation of pKa values for protein-ligand complexes, *Proteins*, 73, 765-783.

Berkenblit, S. I., Quinn, T. M. and Grodzinsky, A. J. (1995) Molecular electromechanics of cartilaginous tissues and polyelectrolyte gels, *Journal of Electrostatics*, 34, 307-330.

Bevan, R. L. T., Raoul vanLoon and Nithiarasu, P. (2009) The locally conservative Galerkin (LGG) method—a discontinuous methodology applied to a continuous framework, *Advances in Applied Mathematics and Mechanics*, 1, 319-340.

Bisschops, M.A.T., Luyben, K.Ch.A.M., and van der Wielen, L.A.M. (1998) Generalised Maxwell-Stefan approach for swelling kinetics of Dextran gels, *Industrial & Engineering Chemistry Research*, 37, 3312-3322.

Buchholz, F. L. and Peppas, N. A. (1994) Superabsorbent polymers: science and technology, *ACS symposium Series*, 573, 121-124.

Burden, R. L. and Faires, J. D. (2005) *Numerical Analysis*, 8thed, Thomson Brooks/Cole, United States.

Carty, R. and Schrode, T. (1975) Concentration profiles in ternary gaseous diffusion, *Industrial & Engineering Chemistry Fundamentals*, 14, 276-278.

Caykara, T., Dogmus, M. and Kantoglu, O. (2004) Network structure and swelling-shrinking behaviours of pH-sensitive poly hydrogels, *Journal of Polymer Science Part B: Polymer Physics*, 42, 2586-2594.

Cockburn, B., Gopalakrishnan, J. and Wang, H. Y. (2007) Locally conservative fluxes for the continuous Galerkin method, *SIAM Journal on Numerical Analysis*, 45, 1742-1776.

COMSOL Multiphysics 3.5 (2008) http://www.comsol.com/support/knowledgebase

Denbigh, K. (1981) *The Principles of Chemical Equilibrium*, 3rd, Cambridge University Press, Cambridge.

De Rossi, D., Chiarelli, P., Buzzigoli, G., Domenici, C. and Lazzeri, L. (1986) Contractile behaviour of electrically activated mechanochemical polymer actuators, *Transactions of the American Society of Artificial Organs*, XXXII, 157-162.

De, S. K. and Aluru, N. R. (2004) A chemo-electro-mechanical mathematical model for simulation of pH sensitive hydrogels, *Mechanics of Materials*, *36*, 395-410.

Debye, P. and Hückel, E. (1923) The theory of electrolytes I. The lowering of the freezing point and related occurrences, *Physikalische Zeitschrift*, 24, 185-206.

Di Toro, D. M. (1976) Combining chemical equilibrium and phytoplankton models-a general methodology, *Modelling Biochemical Processes in Aquatic Ecosystems*, edited by Canale, R. P., Ann Arbor Science, 233-255.

Falciola, L., Mussini, P. R., Mussini, T., Pozzi, S. and Rondinini, S. (2003) A thermodynamic study of the aqueous (sodium chloride + sodium hydroxide) electrolyte using sodium amalgam and thallous chloride electrode cells, *The Journal of Chemical Thermodynamics*, 35, 3, 405-416.

Fessenden, R. J. and Fessenden, J. S. (1986) *Organic Chemistry*, 3rd Edition, Brooks, California.

Fick, A. (1855) On liquid diffusion, *The London, Edinburgh and Dublin Philosophical Magazine and Journal of Science*, 10, 30-39.

Flory, P. J. (1953) *Principles of Polymer Chemistry*, Cornell University Press, New York.

Flory, P. J. (1969) *Statistical Mechanics of Chain Molecules*, Interscience Publishers, New York.

Flory, P. J. and Rehner, R. (1943) Statistical mechanics of crosslinked polymer networks. I. Rubber elasticity, *The Journal of Chemical Physics*, *11*, 521-527.

Green, A. E. and Adkins, J. E. (1960) *Large Elastic Deformations* Oxford University Press, Oxford.

Grimshaw, P. E., Nussbaus, J. H. and Grodzinsky, A. J. (1990) Kinetics of electrically and chemically induced swelling in polyelectrolyte gels, *The Journal of Chemical Physics*, 93 (6), 4462-4472.

Gunasekaran, S., Ko, S. and Xiao, L. (2007) Use of whey proteins for encapsulation and controlled delivery applications, *Journal of Food Engineering*, 83, 31-40.

Hart-Smith, L. J. (1966) Elasticity parameters for finite deformations of rubber-like materials, *Zeitschrift fur angewandte Mathematik und Physik*, 17, 608-626.

Hasa, J., IIavsky, M. and Dusek, K. (1975) Deformational, swelling and potentiometric behaviour of ionised poly (methacrylic acid) gels. I. Theory, *Journal of Polymer Science Polymer Physics Edition*, 13 (2), 253-262.

Higgins, B. G. (2004) *Balance equations and conservation of mass*, http://www.ekayasolutions.com/ech256/ECH256ClassNotes/BalanceLaws.pdf

Hill, T. R. (1986) *An introduction to Statistical Thermodynamics*, Dover Publications, New York.

Hofmann, A. F., Meysman, F. J. R., Soetaert, K. and Middelburg, J. J. (2008) A step-by-step procedure for pH model construction in aquatic systems, *Biogeosciences*, 5, 227-251.

Horkay, F., Tasaki, I. and Basser, P. J. (2000) Osmotic swelling of polyacrylate hydrogels in physiological salt solutions, *Biomacromolecules*, 1, 84-90.

Hong, W., Zhao, X. H., Zhou, J. X. and Suo, Zh. G. (2008) A theory of coupled diffusion and large deformation in polymeric gels, *Journal of the Mechanics and Physics of Solids*, 56, 1779-1793.

Hong, W., Zhao, X. H. and Suo, Zh. G. (2010) Large deformation and electrochemistry of polyelectrolyte gels, *Journal of the Mechanics and Physics of Solids*, 58, 558-577.

Iwasa, K. and Kwak, J. C. T. (1977) The contribution of higher order cluster terms to the activity coefficients of the small ions in polyelectrolyte solutions, *The Journal of Physical Chemistry*, 81, 408-412.

Iwasa, K., McQuarrie, D. A. and Kwak, J. C. T. (1978) High-order limiting laws of polyelectrolyte solutions, *The Journal of Physical Chemistry*, 82, 1979-1985.

James, H. M. and Guth, E. (1943) Theory of the elastic properties of rubber, *The Journal of Chemical Physics*, 11, 455-481.

Kakhu, A. I. and Pantelides, C. C. (2003) Dynamic modelling of aqueous electrolyte systems, *Computers and Chemical Engineering*, 27, 869-882.

Katchalsky, A. (1949) Rapid swelling and de-swelling of reversible gels of polymeric acids by ionisation, *Experientia*, 5, 319-320.

Katchalsky, A. and Lifson, S. (1953) The electrostatic free energy of polyelectrolyte solutions. I. Randomly kinked macromolecules, *Journal of Polymer Science*, 11 (5), 409-423.

Kees, C. E., Farthing, M. W. and Dawson, C. N. (2008) Locally conservative, stabilised finite element methods for variably saturated flow, *Computer Methods in Applied Mechanics and Engineering*, 197, 4610-4625.

Kenkare, N. R., Hall, C. K. and Khan, S. A. (2000) Theory and simulation of the swelling of polymer gels, *The Journal of Chemical Physics*, 113(1), 404-418.

Komori, T. and Sakamoto, R. (1989) On Tanaka-Fillmore's kinetics swelling of gels, *Colloid Polymer Science*, 267, 179-183.

Kowblansky, M., Tomasula, M. and Ander, P. (1978) Mean and single ion activity coefficients of sodium halides in aqueous sodium polyphosphate and sodium carrageenan solutions, *The Journal of Physical Chemistry*, 82, 1491-1496.

Kraaijeveld, G., Sumberova, V., Kuindersma, S. and Wesselingh, H. (1995) Modelling electrodialysis using the Maxwell-Stefan description, *Chemical Engineering Journal*, 57, 163-176.

Krishna, R. (1987) Diffusion in multicomponent electrolyte systems, *Chemical Engineering Journal*, 35, 19-24.

Krishna, R. and Wesselingh, J. A. (1997) The Maxwell-Stefan approach to mass transfer, *Chemical Engineering Science*, 52(6), 861-911.

Kuhn, W. (1936) Beziehungen zwischen Molekühlgrösse, statistischer Molekülgestalt und elastischen Eigenschaften hochpolymerer Stoffe, *Kolloid Zeitschrift*, 76, 258–271.

Kuhn, W. (1949) Reversible dehung and contraction bei anderung der ionization lines netweks plyvalenter fadenmolekulionen, *Experientia*, 5, 318-319.

Kuhn, W., Hargitary, B., Katchalsky, A. and Eisenberg, H. (1950) Reversible dilation and contraction by changing the state of ionization of high-polymer acid network, *Nature*, 165, 514-516.

Kwak, J. C. T., O'Brien, M. C. and MacLean, D. A. (1975) Mean activity coefficients for the simple electrolyte in aqueous mixtures of polyelectrolyte and simple electrolyte, *The Journal of Physical Chemistry*, 79, 2381-2386.

Lee, W. J. (1996) *Polymer Gel Based Actuator: Dynamic Model of Gel for A Real Time Control*, PhD Thesis, Massachusetts Institute of Technology, Massachusetts U.S.A.

Lee, K. Y. and Mooney, D. J. (2001) Hydrogels for tissue engineering, *Chemical Reviews*, 101, 7, 1869-1880.

Li, Y. and Tanaka, T. (1990) Kinetics of swelling and shrinking of gels, *The Journal of Chemical Physics*, 92(2), 1365-1371.

Li, Y. and Tanaka, T. (1992) Phase transitions of gels, *Annual Review of Materials Science*, 22, 243-277.

Lin, C. C. and Metters, A. T. (2006) Hydrogels in controlled release formulations: Network design and mathematical modelling, *Advanced Drug Delivery Reviews*, 58, 1379-1408.

Loeb, J. (1921) Donnan equilibrium and the physical properties of proteins. I. Membrane potentials, *Journal of General Physiology*, 1920-1921, 667-690.

Lowman, A. M. and Peppas, N. A. (2000) Molecular analysis of interpolymer complexation in graft copolymer networks, *Polymer*, 41, 73-80.

Lu, K. (2007) *The Application of Generalised Maxwell-Stefan Equations to Protein Gels*, ME Thesis, University of Canterbury, Christchurch, NZ.

Mann, B. A., Holm, C. and Kremer, K. (2005) Swelling of polyelectrolyte networks, *The Journal of Chemical Physics*, 122, 154903 (1-14).

Manning, G. S. (1969a) Limiting laws and counterion condensation in polyelectrolyte solutions. I. Colligative properties, *The Journal of Chemical Physics*, 51, 924-933.

Manning, G. S. (1969b) Limiting laws and counterion condensation in polyelectrolyte solutions. II. Self-diffusion of the small ions, *The Journal of Chemical Physics*, 51, 934-938.

Manning, G. S. (1979) Counterion binding in polyelectrolyte theory, *Accounts of Chemical Research*, 12, 443-449.

Maurer, G. and Prausnitz, J. M. (1996) Thermodynamics of phase equilibrium for systems containing gels, *Fluid Phase Equilibria*, 115, 113-133.

Maxwell, J. C. (1867) On the dynamical theory of gases, *Philosophical Transactions of the Royal Society of London*, 157, 49-88.

Mercadé-Prieto, R. and Chen, X. D. (2006) Dissolution of whey protein concentrate gels in alkali, *American Institute of Chemical Engineers Journal*, 52, 792-803.

Mercadé-Prieto, R., Falconer, R. J., Paterson, W. R. and Wilson, D. I. (2006a) Probing the mechanisms limiting dissolution of whey protein gels during cleaning, *Fouling, Cleaning and Disinfection in Food Processing 2006*.

Mercadé-Prieto, R., Falconer, R. J., Paterson, W. R. and Wilson, D. I. (2006b) Effect of gel structure on the dissolution of heat-induced β-Lactoglobulin gels in alkali, *Journal of Agricultural and Food Chemistry*, 54, 5437-5444.

Mercadé-Prieto, R., Sahoo, P. K., Falconer, R. J., Paterson, W. R. and Wilson, D. I. (2007a) Polyelectrolyte screening effects on the dissolution of whey protein gels at high pH conditions, *Food Hydrocolloids*, 21, 1275-1284.

Mercadé-Prieto, R., Falconer, R. J., Paterson, W. R. and Wilson, D. I. (2007b) Swelling and dissolution of β-Lactoglobulin gels in alkali, *Biomacromolecules*, 8, 469-476.

Mercadé-Prieto, R., Paterson, W. R. and Wilson, D. I. (2007c) The pH threshold in the dissolution of β-Lactoglobulin gels and aggregates in alkali, *Biomacromolecules*, 8, 1162-1170.

Moe, H. I., Hauan, S., Lien, K. M. and Hertzberg, T. (1995) Dynamic model of a system with phase and reaction equilibrium, *Computers and Chemical Engineering*, 19, Supplement, S513-S518.

Mooney, M. (1940) A theory of large elastic deformation, *Journal of Applied Physics*, 11, 582-592.

Ogden, R. W. (1972) Large deformation isotropic elasticity – on the correlation of theory and experiment for incompressible rubberlike solids, *Proceedings of the Royal Society of London, Series A, Mathematical and Physical Sciences*, 326, 565-584.

Osada, Y. Okuzaki, H. and Hori, H. (1992) A polymer gel with electrically driven motility, *Nature*, 355, 242-244.

Osada, Y. and Khokhlov, A. R. (2002) *Polymer Gels and Networks*, Marcel Dekker, New York.

Pitzer, K. S. and Simonson, J. M. (1986) Thermodynamics of multicomponent, miscible, ionic systems: theory and equations, *The Journal of Physical Chemistry*, 90, 3005-3009.

Pitzer, K. S. (1991) *Activity Coefficients in Electrolyte Solutions*, 2nd edition, CRC Press, Boston.

Rivlin, R. S. (1948) Large elastic deformations of isotropic material. IV. Further developments of the general theory, *Philosophical Transactions of the Royal Society of London. Series A, Mathematical and Physical Science*, 241, 379-397.

Robinson, R. A. and Stokes, R. H. (1959) *Electrolyte Solutions*, Butterworths Scientific Publications, London.

Sassi, A. P., Blanch, H. W. and Prausnitz, J. M. (1996) Phase equilibria for aqueous protein/polyelectrolyte gel systems, *AIChE Journal*, 42, 2335-2353.

Segel, I. H. (1968) *Biochemical Calculations: How to Solve Mathematical Problems in General Biochemistry*, Wiley, New York.

Shahinpoor, M. (1993) Nonhomogeneous large deformation theory of ionic polymeric gels in electric and pH fields, *Proceedings of the 1993 SPIE Conference on smart structures and materials*, Albuquerque, 1916, 40-50.

Siegel, R. A. (1990) A pH sensitive gels: swelling equilibria, kinetics and applications for drug delivery, *Pulse and Self-Regulated Drug Delivery*, CRC Press, 129-155.

Smith, K. J., Ciferri, A. and Hermans, J. J. (1964) Anisotropic elasticity of composite molecular networks formed from non-Gaussian chains, *Journal of Polymer Science*, 2(3), 1025-1535.

Sochala, P., Ern, S. and Piperno, S. (2009) Mass conservative BDF-discontinuous Galerkin/explicit finite volume schemes for coupling subsurface and overland flows, *Computer Methods in Applied Mechanics and Engineering*, 198, 2122-2136.

Stefan, J. (1871) Über das gleichgewicht und die bewegung, insbesondere die diffusion von gemischen, *Sitzungsberichte der Kaiserlichen Akademie der Wissenschaften in Wien*, **63**, 63-124.

Tanaka, T., Hocker, L. and Benedek, G. (1973) Spectrum of light scattered from a viscoelastic gel, *The Journal of Chemical Physics*, 59, 5151-5159.

Tanaka, T. and Fillmore, D. J. (1979) Kinetics of swelling of gels, *The Journal of Chemical Physics*, 70, 1214-1218.

Tanaka, T., Nishio, I., Sun, S. T. and Ueno-Nishio, S. (1982) Collapse of gels in an electric field, *Science*, 218, 467-469.

Taylor, R. and Krishna, R. (1993) *Multicomponent Mass Transfer*, John Wiley & Sons, New York.

Treloar, L. R. G. (1943) The elasticity of a network of longchain molecules II, *Transactions of the Faraday Society*, 39, 241-246.

Treloar, L. R. G. (1944) Stress-strain data for vulcanised rubber under various types of deformation, *Transactions of the Faraday Society*, 40, 59-70.

Treloar, L. R. G. (1975) *The Physics of Rubber Elasticity*, Clarendon Press, Oxford.

Treloar, L. R. G. (2005) *The Physics of Rubber Elasticity*, Oxford University Press, Oxford.

Uhrich, K., Cannizzaro, S. and Langer, R. (1999) Polymeric systems for controlled drug release, *Chemical Reviews*, 99, 3181-3189.

Vasheghani-Farahani, E., Vera, J. H., Cooper, D. G. and Weber, M. E. (1990) Swelling of ionic gels in electrolyte solutions, *Industrial & Engineering Chemistry Research*, 29 (4), 554-560.

Versteeg, H. K. and Malalasekera, W. (2007) *An Introduction to Computational Fluid Dynamics*, 2nded, Pearson Education Limited, England.

Wall, F. T. (1942a) Statistical thermodynamics of rubber, *The Journal of Chemical Physics*, 10, 132-134.

Wall, F. T. (1942b) Statistical thermodynamics of rubber II, *The Journal of Chemical Physics*, 10,485-488.

Wallmersperger, T., Keller, K., Kröplin, B., Günther, M. and Gerlach, G. (2011) Modelling and simulation of pH-sensitive hydrogels, *Colloid Polymer Science*, 289, 535-544.

Wells, J. D. (1973) Salt activity and osmotic pressure in connective tissue I. A study of solutions of dextran sulphate as a model system, *Proceedings of the Royal Society B: Biological Sciences*, 183, 399-419.

Wesselingh, J.A., Vonk, P. and Kraaijeveld, G. (1995) Exploring the Maxwell-Stefan description of ion exchange, *Chemical Engineering Journal.* 57, 75-89.

Wesselingh, J. A. and Krishna, R. (2000) *Mass Transfer in Multicomponent Mixtures*, VSSD, Delft, Netherlands.

White, F. M. (1998) *Fluid Mechanics*, 5th Edition, Mcgraw-Hill College, Columbus.

Xin, H., Chen, X.D. and Ozkan, N. (2004) Removal of a model protein foulant from metal surfaces, *American Institute of Chemical Engineers Journal*, 50, 1961-1973.

Zemaitis, J. F., Clark, D. M., Rafal, M. and Scrivner, N. C. (1986) *Handbook of Aqueous Electrolyte Thermodynamics: Theory & Application*, American Institute of Chemical Engineers, New York.

Zhang, J. P., Zhao, X. H., Suo, Zh. G. and Jiang, H. Q. (2009) A finite element method for transient analysis of concurrent large deformation and mass transport in gels, *Journal of Applied Physics*, 105, 093522.

Appendix A

Ternary gaseous diffusion in a Stefan tube

In 1975, Carty and Schrodt presented an experimental study in which a gas mixture of acetone and methanol was diffusing in a Stefan tube through stagnant air. This study has been already used for the validation of methods for the numerical resolution of the MS equations. Here, it was used as an example for the numerical approach presented in the Section 3.2. In the following, the subscripts 1, 2 and 3 indicate acetone, methanol, and air, respectively. In the study of Carty and Schrodt, air was considered as a pure component since the diffusivities of acetone and methanol in oxygen and nitrogen are very similar. In the experimental setup, at the bottom of the tube, a film of a liquid mixture of acetone and methanol continuously flowed, so that the gas-phase concentrations close to the liquid-gas interface were considered constant. In one of their experiments the composition of the vapour at the liquid surface was x_1= 0.319 and x_2=0.528. At the top of the tube, a stream of dried air swept away the vapours of acetone and methanol, so that x_1=0, x_2=0 and x_3=1. The temperature was 328.5 K and the pressure was 99.4 kPa, and along the tube (0.238 m long), air was stagnant. For the simulation, the experimental value of the MS diffusivities at constant temperature (328 K) and pressure (1 atm) of acetone and of methanol in air were 13.72×10^{-6} m^2s^{-1} and 19.91×10^{-6} m^2s^{-1} respectively. The diffusivity of acetone in methanol was not experimentally available and was estimated to be 8.48×10^{-6} m^2s^{-1}. This problem is depicted schematically in Figure A.1. Taylor and Krishna (1993) reported the following exact values of fluxes of acetone and methanol which they calculated numerically using a fourth-order Runge-Kutta method: $N_1=1.783\times10^{-3}$ mol/m^2s and $N_2=1.783\times10^{-3}$ mol/m^2s which were in excellent agreement with the values determined experimentally by Carty and Schrodt (1975): $N_1=1.779\times10^{-3}$ mol/m^2s and $N_2=3.121\times10^{-3}$ mol/m^2s. The flux of air was kept at zero.

The Maxwell-Stefan flux equations for an ideal ternary mixture of neutral species, when written in terms of the molar fluxes $\boldsymbol{N}_i$ and with concentration gradients as the only driving force, are

$$\nabla x_i = \sum_{j=1}^{3} \frac{x_i \boldsymbol{N}_j - x_j \boldsymbol{N}_i}{c_t \mathcal{D}_{ij}} \tag{A.1}$$

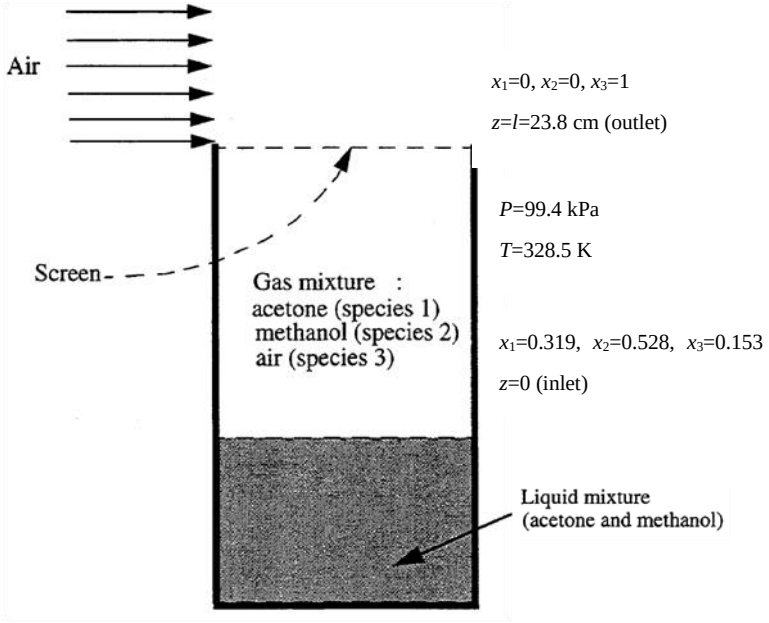

Figure A.1 Schematic diagram of ternary gaseous diffusion in a Stefan tube (Taylor and Krishna, 1993)

Appendix B

Diffusion of HCl as two ions (Lu, 2007)

This system consists of three components: hydrogen ion (component 1), chloride ion (2) and water (3). Water is chosen to be the reference component. The diffusion distance was set to 1 mm.

The GMS equation:

Since water is the reference frame and diffusion is only one dimension *z*, the resulting GMS equation for hydrogen and chloride ion in matrix form is:

$$\begin{bmatrix} \boldsymbol{J}_1 \\ \boldsymbol{J}_2 \end{bmatrix} = -c_t \begin{bmatrix} \frac{x_2}{\not{D}_{12}} + \frac{x_3}{\not{D}_{13}} & -\frac{x_1}{\not{D}_{12}} \\ -\frac{x_2}{\not{D}_{12}} & \frac{x_1}{\not{D}_{12}} + \frac{x_3}{\not{D}_{23}} \end{bmatrix}^{-1} \begin{bmatrix} \frac{\Delta x_1}{\Delta z} + x_1 z_1 \frac{\Im}{RT} \frac{\Delta \phi}{\Delta z} \\ \frac{\Delta x_2}{\Delta z} + x_2 z_2 \frac{\Im}{RT} \frac{\Delta \phi}{\Delta z} \end{bmatrix} \tag{B.1}$$

Transport equation:

The mass balance equation used here is:

$$\begin{aligned} \frac{\partial c_1}{\partial t} &= -\nabla \cdot \boldsymbol{J}_1 \\ \frac{\partial c_2}{\partial t} &= -\nabla \cdot \boldsymbol{J}_2 \end{aligned} \tag{B.2}$$

No net flux condition:

$$\boldsymbol{J}_1 z_1 + \boldsymbol{J}_2 z_2 = 0 \tag{B.3}$$

Boundary conditions:

It is found that it is more reasonable to set one side as zero diffusion potential with $\frac{\partial \phi}{\partial z} = 0$ on the same side. The concentration of HCl on the left side was set to 0.018 mol/L, the right was set to 0.

Diffusion coefficients:

The diffusion coefficients in this model are:

$$\begin{aligned} \overline{\overline{D}}_{H^+,water} &= 9.3 \times 10^{-9}\ \mathrm{m^2/s} \\ \overline{\overline{D}}_{Cl^-,water} &= 2.0 \times 10^{-9}\ \mathrm{m^2/s} \end{aligned} \tag{B.4}$$

Initial conditions:

Initially, zero concentration is inside gel and the solution should be electrically neutral everywhere as described by:

$$x_1 z_1 + x_2 z_2 = 0 \tag{B.5}$$

Appendix C

Diffusion of HCl and NaCl (Lu, 2007)

The case considers diffusion in a multi-electrolyte system. The difference between this case and the previous one is that there is an additional ion, Na^+, in the system. According to Wesselingh and Krishna (2000), hydrogen chloride in water diffuses down its concentration gradient. So does sodium chloride. However, in the mixture of hydrochloric acid and sodium chloride, sodium might diffuse against its gradient, in the direction opposite to what we expect from Fick's law. This is caused by the electrical field generated by the H^+ ions of the HCl, which diffuse more rapidly than the others.

System model:

This system consists of four components: hydrogen ion (component 1), chloride ion (2), sodium ion (3) and water (4). Water is chosen to be the reference component.

The GMS equation:

Since water is the reference frame and diffusion is only one dimension *z*, the resulting GMS equation for the three components except water in matrix form is:

$$\begin{bmatrix} J_1 \\ J_2 \\ J_3 \end{bmatrix} = -c_t \begin{bmatrix} \frac{x_2}{\mathcal{D}_{12}} + \frac{x_3}{\mathcal{D}_{13}} + \frac{x_4}{\mathcal{D}_{14}} & -\frac{x_1}{\mathcal{D}_{12}} & -\frac{x_1}{\mathcal{D}_{13}} \\ -\frac{x_2}{\mathcal{D}_{12}} & \frac{x_1}{\mathcal{D}_{12}} + \frac{x_3}{\mathcal{D}_{23}} + \frac{x_4}{\mathcal{D}_{24}} & -\frac{x_2}{\mathcal{D}_{23}} \\ -\frac{x_3}{\mathcal{D}_{13}} & -\frac{x_3}{\mathcal{D}_{23}} & \frac{x_1}{\mathcal{D}_{13}} + \frac{x_2}{\mathcal{D}_{23}} + \frac{x_4}{\mathcal{D}_{34}} \end{bmatrix}^{-1} \quad \text{(C.1)}$$

$$\begin{bmatrix} \frac{\Delta x_1}{\Delta z} + x_1 z_1 \frac{\Im}{RT} \frac{\Delta \phi}{\Delta z} \\ \frac{\Delta x_2}{\Delta z} + x_2 z_2 \frac{\Im}{RT} \frac{\Delta \phi}{\Delta z} \\ \frac{\Delta x_3}{\Delta z} + x_3 z_3 \frac{\Im}{RT} \frac{\Delta \phi}{\Delta z} \end{bmatrix}$$

Transport equation:

The mass balance equation used here has the same form as previously:

$$\begin{aligned} \frac{\partial c_1}{\partial t} &= -\nabla \cdot \boldsymbol{J}_1 \\ \frac{\partial c_2}{\partial t} &= -\nabla \cdot \boldsymbol{J}_2 \\ \frac{\partial c_3}{\partial t} &= -\nabla \cdot \boldsymbol{J}_3 \end{aligned} \tag{C.2}$$

No net flux condition:

$$\boldsymbol{J}_1 z_1 + \boldsymbol{J}_2 z_2 + \boldsymbol{J}_3 z_3 = 0 \tag{C.3}$$

Diffusion coefficients:

The diffusion coefficients in this model are chosen from Table 3.1.1 (Lu, 2007):

$$\begin{aligned} \not{D}_{14} &= 9.3 \times 10^{-9} \\ \not{D}_{24} &= 2.0 \times 10^{-9} \\ \not{D}_{34} &= 1.3 \times 10^{-9} \end{aligned} \tag{C.4}$$

The diffusion coefficient of ion and ion pairs can be calculated by:

$$\begin{aligned} \not{D}_{12} &= \frac{\not{D}_{14} + \not{D}_{24}}{2} \frac{i^{0.55}}{|z_1 z_2|^{2.3}} \\ \not{D}_{23} &= \frac{\not{D}_{24} + \not{D}_{34}}{2} \frac{i^{0.55}}{|z_2 z_3|^{2.3}} \end{aligned} \tag{C.5}$$

where

$$i = \frac{1}{2}(z_1^2 x_1 + z_2^2 x_2 + z_3^2 x_3) \tag{C.6}$$

$\not{D}_{13}$ can also be calculated with the same equation but with a negative sign.

Initial conditions:

Initially, the solution should be electrically neutral everywhere as described by:

$$x_1 z_1 + x_2 z_2 + x_3 z_3 = 0 \tag{C.7}$$

There were 0.018 mol/L of HCl and 0.002 mol/L of NaCl inside an open matrix.

Boundary conditions:

There were 0.018 mol/L of HCl and 0.03 mol/L of NaCl in the right boundary. The right side diffusion potential was set to be zero.

Appendix D

The complete equations of protein gel swelling

In this section the complete set of mdelling equations are presented as follows:

Mass balance equations:

$$\begin{aligned} \frac{\partial c_H}{\partial t} + \nabla \cdot \boldsymbol{N}_H &= 0 \\ \frac{\partial c_O}{\partial t} + \nabla \cdot \boldsymbol{N}_O &= 0 \\ \frac{\partial c_4}{\partial t} + \nabla \cdot \boldsymbol{N}_4 &= 0 \end{aligned} \tag{D.1}$$

with c_H and c_O defined by:

$$\begin{aligned} c_H &= c_1 + c_2 + 2c_3 + c_7 \\ c_O &= c_2 + c_3 \end{aligned} \tag{D.2}$$

and $\boldsymbol{N}_H$ and $\boldsymbol{N}_O$ defined by:

$$\begin{aligned} \boldsymbol{N}_H &= \boldsymbol{N}_1 + \boldsymbol{N}_2 + 2\boldsymbol{N}_3 + \boldsymbol{N}_7 \\ \boldsymbol{N}_O &= \boldsymbol{N}_2 + \boldsymbol{N}_3 \end{aligned} \tag{D.3}$$

with $\boldsymbol{N}_i$:

$$\boldsymbol{N}_i = \boldsymbol{J}_i^n + c_i \boldsymbol{u}_p \tag{D.4}$$

The concentration of Na^+, c_5, is calculated by electrical neutrality:

$$c_1 - c_2 - c_4 + c_5 + z_p c_6 = 0 \tag{D.5}$$

with c_1 and c_2 defined by:

$$\begin{aligned} c_1 &= 10^{-pH} \\ c_2 &= 10^{pH-14} \end{aligned} \tag{D.6}$$

Equations (D.2) and (D.6) form four equations with variables c_1, c_2, c_3 and pH.

Protein charge z_p is obtained by:

$$z_p = \sum_{j=amino\ acids} N_{k,j} z_j \frac{10^{z_j(pK_{aj}-pH)}}{10^{z_j(pK_{aj}-pH)} + 1} \tag{D.7}$$

The total protein, c_6, is calculated by:

$$c_6 \bar{V}_p + c_3 \bar{V}_3 = 1 \tag{D.8}$$

c_7 and $\boldsymbol{u}_p$ are calculated by:

$$c_7 = c_6 \sum_{j=amino\ acids} N_{k,j} \frac{1}{10^{(pH-pK_{aj})} + 1} \tag{D.9}$$

$$\nabla \cdot \left(\boldsymbol{J}_3^n \bar{V}_3 + \boldsymbol{u}_p \right) = 0 \tag{D.10}$$

The diffusion fluxes, $\boldsymbol{J}_i^n$, are determined by the GMS equations:

$$\begin{bmatrix} -c_t \left(\Gamma \nabla \mathrm{x} + \dfrac{(\mathrm{c} \cdot \bar{\nabla} - \omega)}{c_t RT} \nabla P \right) \\ \cdots\cdots\cdots\cdots\cdots\cdots\cdots\cdots\cdots\cdots\cdots\cdots \\ 0 \end{bmatrix} = \begin{bmatrix} [\mathrm{B}] & \vdots & [\mathrm{c} \cdot \mathrm{z}] \\ \cdots\cdots\cdots & \vdots & \cdots\cdots\cdots \\ [\mathrm{z}] & \vdots & 0 \end{bmatrix} \begin{bmatrix} [\mathbf{J}^n] \\ \cdots\cdots \\ \dfrac{\Im}{RT} \nabla \varphi \end{bmatrix} \tag{D.11}$$

B is an *n*-1 square matrix with elements:

$$\begin{aligned} B_{ii} &= \sum_{j \neq i} \frac{x_j}{\mathcal{D}_{ij}} \quad i = 1, \ldots, n-1 \\ B_{ij} &= -\frac{x_i}{\mathcal{D}_{ij}} \quad i \neq j \end{aligned} \tag{D.12}$$

Pressure term is calculated by:

$$P = \frac{NkT}{V} \left[\left(\frac{V}{V_0} \right)^{\frac{2}{3}} - 1 \right] \tag{D.13}$$

Thermodynamics:

$$\Gamma_{ij} = \delta_{ij} + x_i \left. \frac{\partial \ln \gamma_i}{\partial x_j} \right|_{T,P,\Sigma} \tag{D.14}$$

Calculation of activity coefficients in multielectrolytes (*M* for a cation and *X* for an anion):

$$\begin{aligned} ln(\gamma_M^m) = z_M^2 F &+ \sum_a m_a (2B_{Ma} + ZC_{Ma}) \\ &+ \sum_c m_c \left(2\Phi_{Mc} + \sum_a m_a \psi_{Mca} \right) \\ &+ \sum_a \sum_{a'} m_a m_{a'} \psi_{Maa'} + z_M \sum_c \sum_a m_c m_a C_{ca} \end{aligned} \tag{D.15}$$

$$ln(\gamma_X^m) = z_X^2 F + \sum_c m_c(2B_{cX} + ZC_{cX}) + \sum_a m_a\left(2\Phi_{Xa} + \sum_c m_c\psi_{cXa}\right) + \sum_c\sum_{c'} m_c m_{c'}\psi_{cc'X} + |z_X|\sum_c\sum_a m_c m_a C_{ca} \quad \text{(D.16)}$$

The above activity coefficients are converted from a molal basis to a mole fraction basis:

$$\gamma_\pm = (1 + M_s\nu m_\pm)\gamma_\pm^m \quad \text{(D.17)}$$

Osmotic coefficient:

$$\phi - 1 = \frac{2}{\sum_i m_i}\left[\frac{-A_\phi I^{\frac{3}{2}}}{\left(1 + bI^{\frac{1}{2}}\right)} + \sum_c\sum_a m_c m_a\left(B_{ca}^\phi + ZC_{ca}\right) + \sum_c\sum_{c'} m_c m_{c'}\left(\Phi_{cc'}^\phi + \sum_a m_a\psi_{cc'a}\right) + \sum_a\sum_{a'} m_a m_{a'}\left(\Phi_{aa'}^\phi + \sum_c m_c\psi_{caa'}\right)\right] \quad \text{(D.18)}$$

Manning's condensation effect on activity coefficients:

$$y_{counter} = \frac{(\xi^{-1}X + 1)}{X + 1}\exp\left(\frac{-\frac{1}{2}\xi^{-1}X}{\xi^{-1}X + 2}\right) \quad \text{(D.19)}$$

$$y_{co} = \exp\left(\frac{-\frac{1}{2}\xi^{-1}X}{\xi^{-1}X + 2}\right) \quad \text{(D.20)}$$

$$\phi = \frac{-\frac{1}{2}\xi^{-1}X + 2}{X + 2} \quad \text{(D.21)}$$

where $y_{counter}$ and y_{co} are the activity coefficients of counter-ion and co-ion calculated by Manning's condensation theory.

with

$$X = \frac{n_e}{n_s} \tag{D.22}$$

Overall:

$$\gamma_{\pm} = y_{\pm}^{p.m} \gamma_{\pm}^{m.m} \tag{D.23}$$

where $\gamma_{\pm}^{m.m}$ is $\gamma_{\pm}$ in equation (D.16).

$$\phi = \phi^{p.m} + \phi^{m.m} - 1 \approx \phi^{p.m} \phi^{m.m} \tag{D.24}$$

Where $\phi^{p.m}$ is the ϕ in equation (D.21) and $\phi^{m.m}$ is the ϕ in equation (D.18)

Water activity:

$$\ln a_w = -\frac{M_w \sum_i v_i m_i}{1000} \phi \tag{D.25}$$

For the non-ideal effect calculation initial conditions and boundary conditions in COMSOL are tabulated in Table D.1.

Table D.1 Initial conditions and boundary conditions (concentrations in mol/L)

	Initial conditions	Boundary conditions
pH	7	10
c_1	10^{-7}	10^{-10}
c_2	10^{-7}	10^{-4}
c_3	49.8561043	55.3956715
c_4	0.001	0.01
c_5	0.094901	0.0101
c_6	0.008743	0
c_H	100.03698	110.791443
c_O	49.8561044	55.3957715

The equilibrium shear modulus used was 2×10^6 Pa in non-ideal calculation. Volume expansion in COMSOL is determined by:

$$\frac{V}{V_0} = \frac{c_{60}}{c_6} \tag{D.26}$$